POLITEHNICA UNIVERSITY TIMIŞOARA
Civil Engineering Faculty
Department of Steel Structures and Structural Mechanics

FEM MODELLING OF BOLTED BEAM TO COLUMN JOINTS WITH HAUNCHES

Author: Abdul Siddik Hossain, Civ. Eng.

Supervisor: Assoc. Professor Aurel Stratan, Ph.D.

Acknowledgment

First of all the author wishes to express his gratitude to almighty Allah for giving him this opportunity and for enabling him to perform this thesis work.

I would like to express my heartiest gratitude and profound indebtedness to my supervisor Assoc.Prof.dr.ing. Aurel Stratan, for his continuous guidance, invaluable suggestions and affectionate encouragement at every stage of this study. Thanks to Ing. Ionel Marginean and Mihai Cristian Vulcu, Ph.D for their help with the numerical modelling. Thanks also to ing. MARIŞ Cosmin-Ilie for providing the design of joints.

Finally I would like to acknowledge here my parents, who have always encouraged me for learning and studying.

Abstract

The aim of this dissertation work is to investigate the behaviour of bolted beam to column joints with haunches under monotonic and cyclic load. To attain this purpose, a finite element solver named ABAQUS has been used. In the beginning of this paper is presented seismic performance of moment resisting frame. After that calibration of a numerical model of a T-stub is performed. The reference structures from which joints have been extracted for numerical analysis are briefly described in frame and joints design. Then a parametric study has been performed to assess the influence of different parameters on joints behaviour. These parameters are verification of design procedure, influence of member size, influence of haunch geometry, influence of panel zone strength, influence of beam clear span to depth ratio, influence of lateral restraints and influence of cyclic loading. At the end of this paper is presented conclusion where the important outcomes of this numerical analysis have been presented concisely.

Table of contents

List of figures

List of tables

European Erasmus Mundus Master
Sustainable Constructions under natural hazards and catastrophic events
520121-1-2011-1-CZ-ERA MUNDUS-EMMC

ГUГCOГ

1   Introduction

This dissertation work includes an in depth analysis on haunched beam to column connections under monotonic and cyclic load. It is a small part of European pre-QUALified steel JOINTS (EQUALJOINTS).

EQUALJOINTS is concerned with the pre-qualification of all-steel Beam-to-Column joints in steel structures and it is aimed at introducing a codified practice currently missing in Europe. At the present time, there are no reliable design tools able to predict the seismic performance of dissipative Beam-to-Column connections in order to meet code requirements. The use of prequalified joints is a common practice in US and Japan. Nevertheless, the standard joints prequalified according to codified procedures in US and Japan cannot be extended to Europe. This project is planned and finalized as a pre-normative research aiming to propose relevant criteria for the next version of EN 1998-1. The partners who will carry out the tests of the selected joint typologies are as follows:

1).UNIVERSITY OF NAPLES FEDERICO II (Coordinator) 2).ARCELORMITTAL BELVAL & DIFFERDANGE SA 3).UNIVERSITE DE LIEGE 4).UNIVERSITATEA POLITEHNICA DIN TIMISOARA 5).IMPERIAL COLLEGE OF SCIENCE, TECHNOLOGY AND MEDICINE 6).UNIVERSIDADE DE COIMBRA 7).EUROPEAN CONVENTION FOR CONSTRUCTIONAL STEELWORK VERENIGING 8.CORDIOLI & C. S.P.A.

Three types of bolted beam-to-column joints will be considered for EU pre-qualification (see Figure 1). The haunched stiffened joints are assigned to Universitatea Politehnica Din Timisoara to develop analytical and numerical models predicting the behaviour of beam to column joints under cyclic loading. My dissertation work is related with this numerical modelling of these Haunched beam to column joints under monotonic and cyclic loading. In order to extend experimental results, these models have been used to perform parametric study
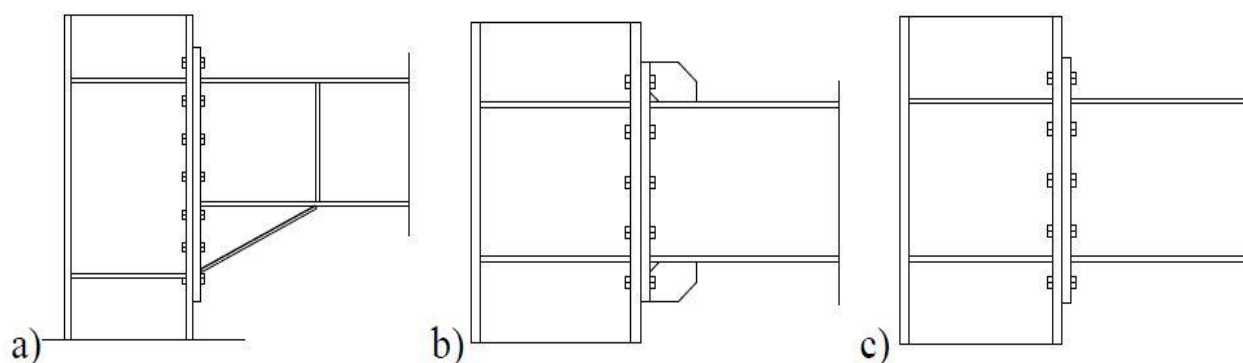
Figure 1.Types of joints considered for EU pre-qualification.

2   Design criteria for steel moment-resisting joints

2.1   Seismic performance of moment-resisting frames

The horizontal forces are mainly resisted by members acting in essentially flexural manner. Energy is thus dissipated by means of cyclic bending.
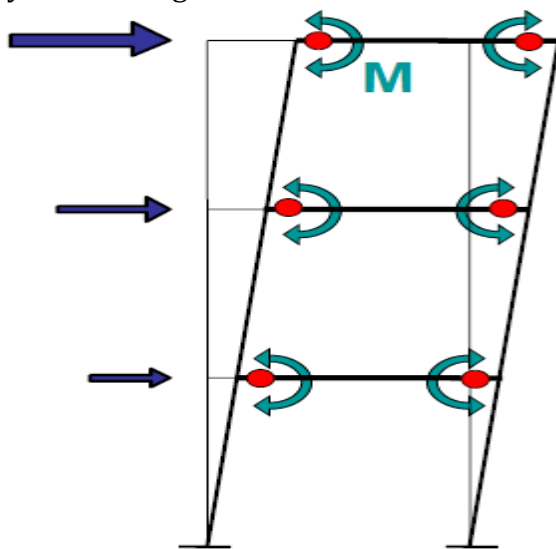
Figure 2.1.1. Global mechanism in moment resisting frame.

Plastic hinges in beams not in columns. The dissipative zones should be mainly located in plastic hinges in the beams or in the beams-to-columns joints. Dissipative zone in columns may be located: at the base of the frame; at the top of the column in the upper story of multi storey building

If the structure is designed to dissipate energy in the beams, the beam to column connections of the whole frame must provide adequate overstrength to permit the formation of the plastic hinges at the ends of the beams. So the following relationship must be achieved: $M_{j,Rd} => 1.1 * \gamma_{ov} * M_{b,pl,Rd}$.

where: $M_{j,Rd}$ is the bending moment resistance of the connection, $M_{b,pl,Rd}$ is the bending moment resistance of the connected beam γ_{ov} is the overstrength factor

Non-dissipative systems are designed to remain in the elastic range, not only during frequent seismic events, having a return period comparable with the service life of the structure, but also in the case of destructive earthquakes, having a low probability of occurrence. This design strategy is usually adopted for strategical buildings, in which the damage of both structural and non-structural elements (which derives from the

development of dissipative mechanisms) is not accepted. The resistance of structural elements is the only parameter to be controlled.

Dissipative structures are systems in which some structural elements or special devices are able to absorb a significant amount of the seismic input energy, thus reducing the damage on the structural system. Supplemental energy dissipation devices may take many forms and dissipate energy through a variety of mechanisms (yielding, viscoelastic actions, sliding friction). In ordinary dissipative structures the energy input is dissipated trough the hysteretic plasticization of some structural elements. In the structure are preliminary detected some parts addressed to the plasticization (ductile elements or dissipative zones) and the rest (non-dissipative zones) are considered as brittle elements, addressed to be in elastic range. This strategy results in the controlled damaging of structural elements, avoiding brittle fracture or non-global plastic mechanisms.

Non dissipative members have to be overstrength with respect to dissipative zones, to allow the cyclic plasticization of them

Ductile elements: Plastic hinges at the beam ends

Brittle elements: Overstrength beams and columns
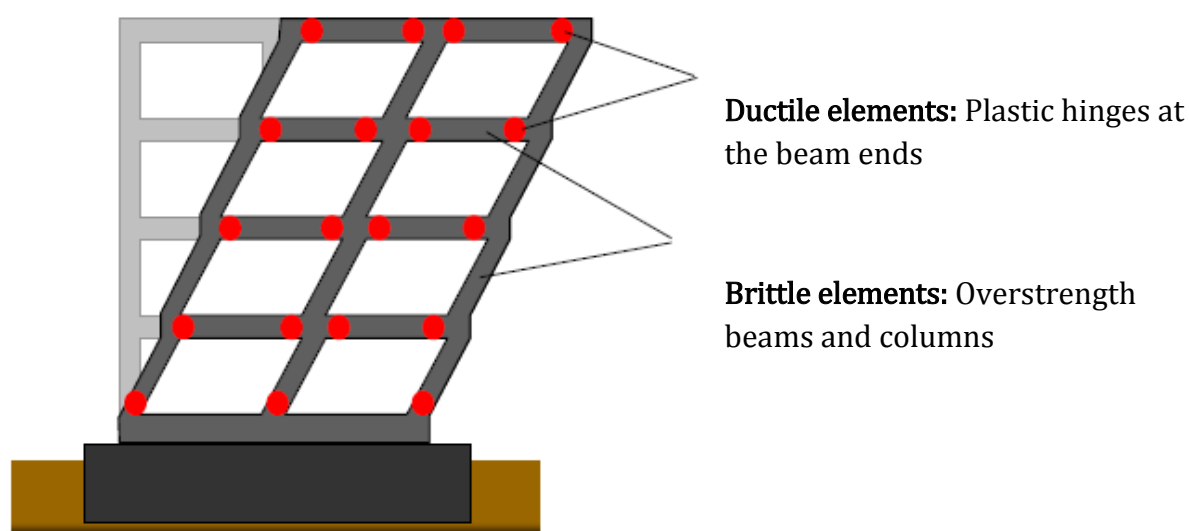
Figure 2.1.2. Design concept in moment resisting frame.

The analysis of post-earthquake scenarios reveals that steel structures most likely will provide high performances even in case of strong ground motions, most likely suffering for negligible earthquake induced damage if compared with traditional masonry and reinforced concrete buildings.

"*Buildings of structural steel have performed excellently and better than any other type of substantial construction in protecting life safety, limiting economic loss, and minimizing business interruption due to earthquake-induced damage.*"

Yanev, P.I., Gillengerten, J.D., and Hamburger, R.O. (1991). *The Performance of Steel Buildings in Past Earthquakes.* The American Iron and Steel Institute.

2.2   Moment resisting beam to column joints

For capacity design it is important to consider ductile elements in dissipative zones and brittle elements in non-dissipative zones. Ductility is a fundamental requirement for dissipative structure design. Ductility is the capability of material to perform plastic deformations without failure.
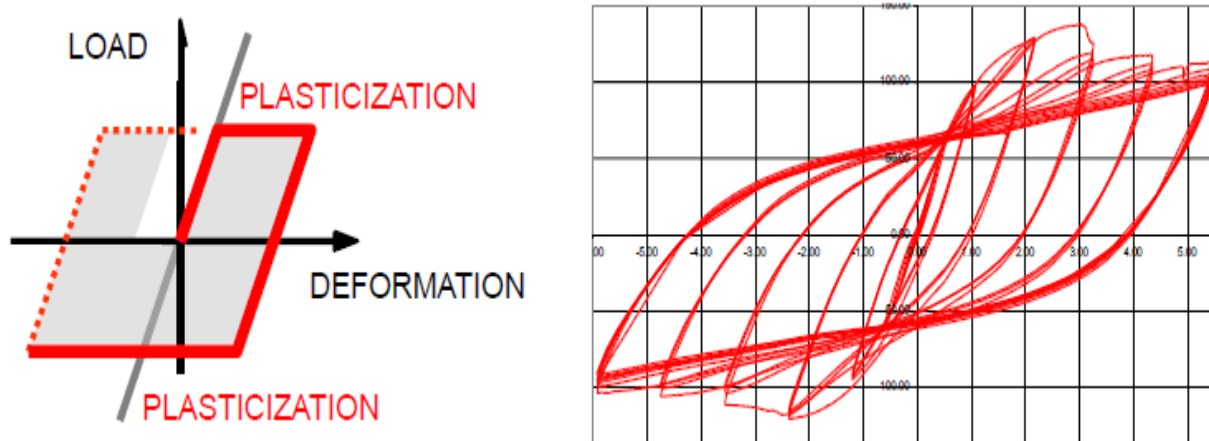
Figure 2.1.3. Dissipation of energy is introduced into the structure by plastic cyclic behaviour.

The quantitative measure of global ductility is represented by the behaviour factor "q",that is used for the reduction of seismic forces . This parameter is influenced by:

- Construction system
- Structural typology
- Ductility classes

Some design criteria for dissipative structures are as follows:

• Structures with dissipative zones shall be designed such that yielding or local buckling or other phenomena due to hysteretic behaviour do not affect the overall stability of the structure

• Dissipative zones shall have adequate ductility and resistance. The resistance shall be verified in accordance with EN 1993

• Dissipative zones may be located in the structural members or in the connections

• If dissipative zones are located in the structural members, the non-dissipative parts and the connections of the dissipative parts to the rest of the structure shall have sufficient overstrength to allow the development of cyclic yielding in the dissipative parts

• When dissipative zones are located in the connections, the connected members shall have sufficient overstrength to allow the development of cyclic yielding in the connections.

There are many types and varieties of connections, and each has different rotational characteristics that affect the frame behaviour. Butt welding, fillet welding, bolting, and riveting may be employed for aseismic connections, either individually or in combination. As fully bolted or riveted connections tend to be large and expensive, fully welded connections or a combination of welding and bolting are the most frequently used. Bolts have the advantage of providing more damping to frames than welds. Connections should be designed to make fabrication and erection of the framework as simple and rapid as possible. Conclusive design criteria for beam-to-column joints are not yet available for seismic conditions. Until the recent past relatively few cyclic load tests had been performed on joints commonly used in Europe. At present many experimental investigations are in progress in different European laboratories. They deal with cyclic behaviour of rigid and semi-rigid joints, both for bare steel and composite constructions. Preliminary research to investigate the influence of detailing of the joint was performed by Ballio, Mazzolani et al on fourteen specimens [4, 5]. The connection types were in compliance with the technology commonly used in Europe for rigid and semi-rigid joints. The experiments followed the ECCS recommended testing procedure for short tests [1]. The specimens were grouped into four main categories (Figure 11):
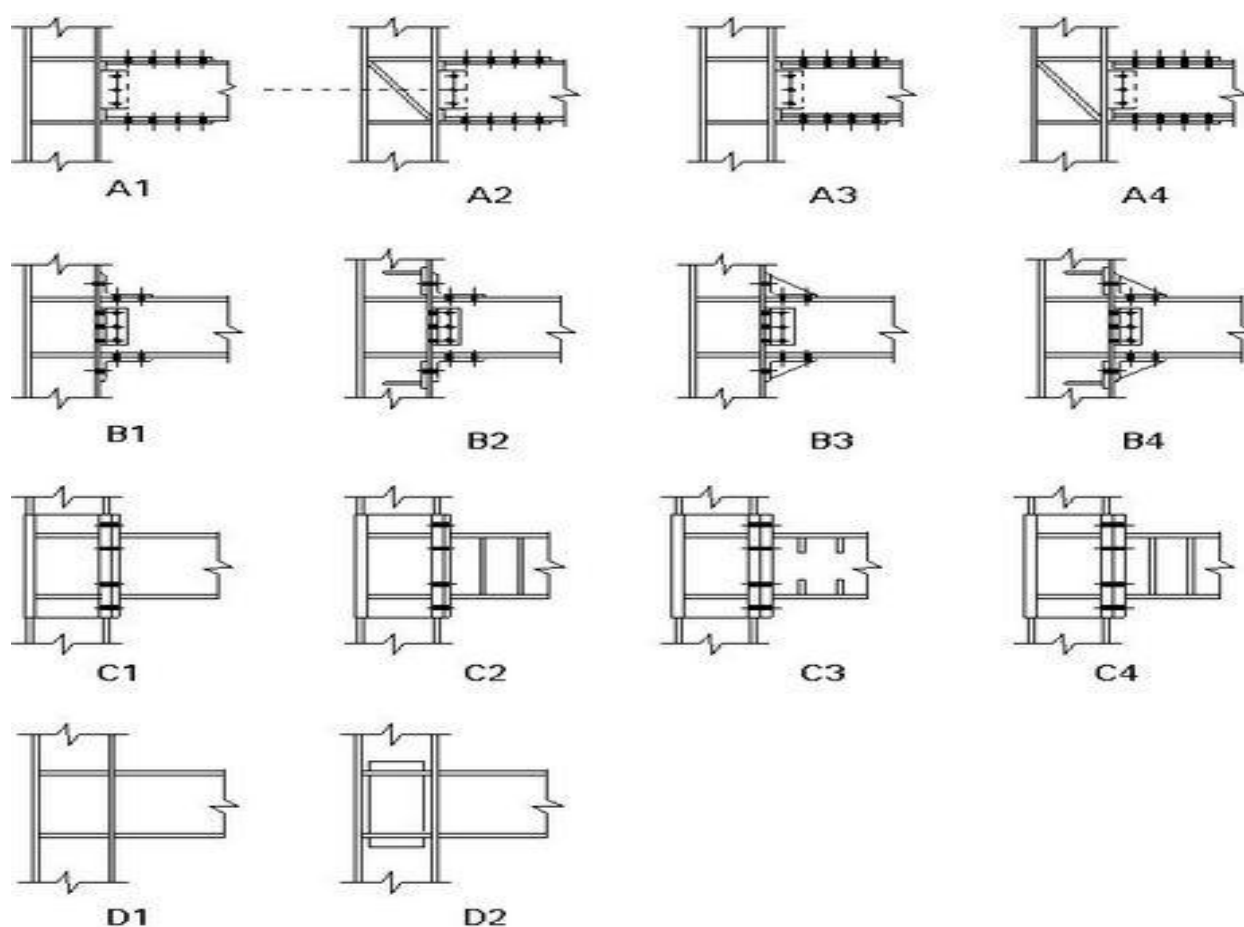
Figure 11   Types of beam-to-column connections tested by Ballio, Mazzolani et al.

3   Calibration of a numerical model of a T-stub

3.1   Description of the model

A finite element model of bolted T-stub connection which has characteristic of nonlinear behaviour that idealized the tension zone of bolted joints. Existing experimental results (Girão Coelho 2004) were used to calibrate the numerical model. For welded T-stubs, the differences are greater between the numerical model and experimental tests due to the effect of residual stresses and modified mechanical properties close to the weld toe, which are not easy to quantify.

The rotational behaviour of bolted end plate beam to column joint is inherently nonlinear. This behaviour may results from different mechanisms which include, 1) web panel zone deformation; 2) column flange and end plate bending deformations; 3) combined tension/bending bolt elongation; 4) beam deformations within the connecting zone; and 5) weld deformations. Generally bolted T-stub connection behaviour is three dimensional which is highly nonlinear having complex phenomena such as material plasticity, second order effects and unilateral contact boundary conditions. In this chapter ABAQUS (6.11) dynamic analysis explicit solver was used for the implementation of a FE model. The nonlinear analysis was needed to investigate the post plastic behaviour with large deformations. The geometrical characteristics of the specimens are depicted in Figure 3.1.1 and specified in Table 3.1.1 for two types of specimens.
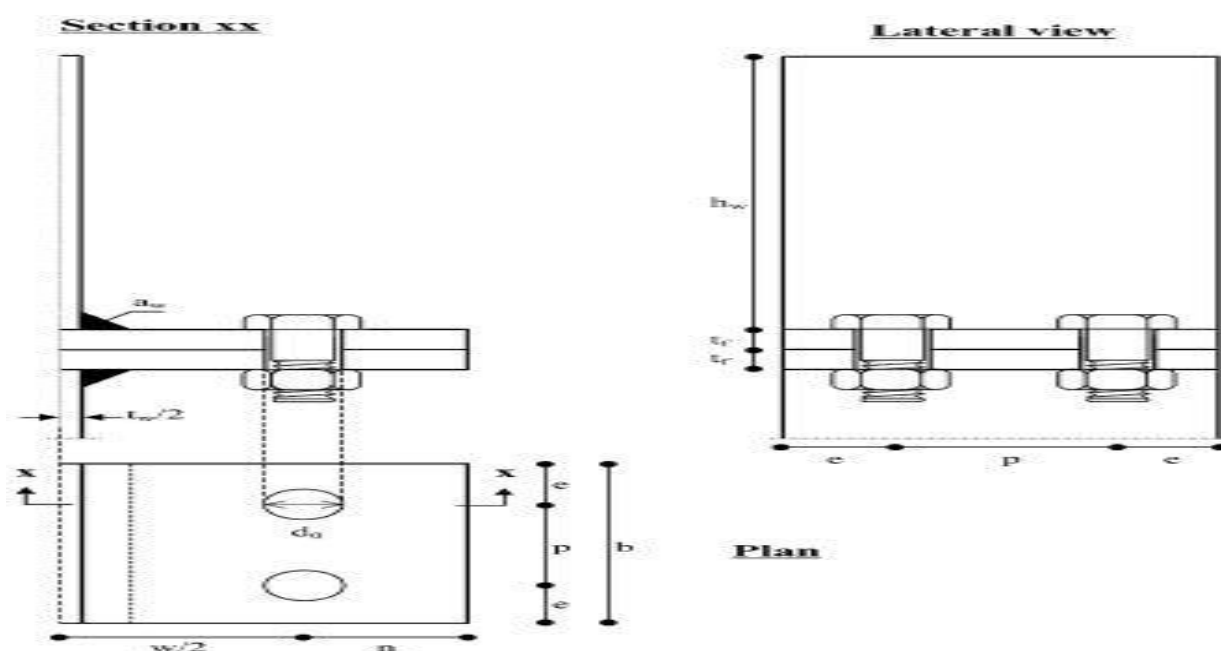
Figure 3.1.1.T-stub specimen general characteristics.

Table 3.1.1 Nominal Geometrical Properties of Various Specimens.

Test	Assembly	T-elements geometry									Bolt characteristics		
		h	t_f	t_w	w	n	p/2	e	r/a_w	d_0	φ	Washer	Number
ID	Type	mm	mm	(mm)	(mm)	(mm)	(mm)	(mm)	(mm)	(mm)	(mm)	(mm)	(mm)
T1	Rolled	150	10.7	7.1	90	30	20	20	15	14	12	Yes	4
WT1	Welded	200	10	10	90	30	25	20	5	14	12	No	4

The specimen WT1 is selected for calibration of the numerical procedure

For good correlation with experimental results, the full actual stress-strain relationship of the materials was adopted in the numerical simulation.
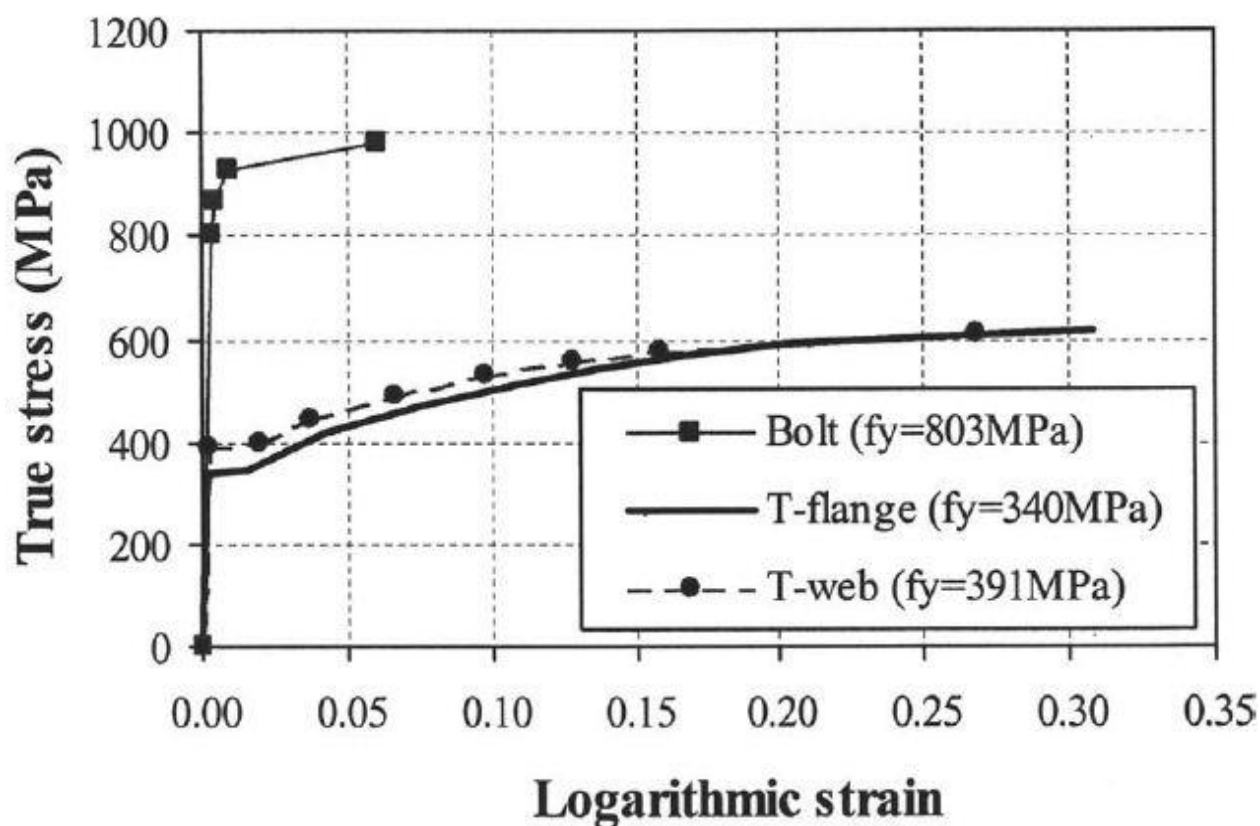
Figure 3.1.2. True stress-logarithmic strain material laws: WP-T-stub specimens (Girão Coelho 2004)

3.2 Modelling approaches

The T-stub connection was created with solid three-dimensional hexahedral element, the elements type is C3D8R (continuum, 8-node). The material properties for bolt, flange and web were taken from the Figure 3.1.2. To make failure in the numerical model, two types of material properties were used between bolt head and thread. In bolt thread, drop down failure was made in plastic strain region (see

Figure 3.2.1). The model was coupled at both ends with reference points which act as supports. Figure 3.2.2 shows the mesh of the model in parts and globally. The bottom reference point was fixed as boundary condition and 20 mm displacement was applied at top reference point. Regarding the interface boundary conditions, a friction coefficient μ of 0.25 was adopted. For the interaction of the model, general contact (explicit) type was defined during the step of apply load.
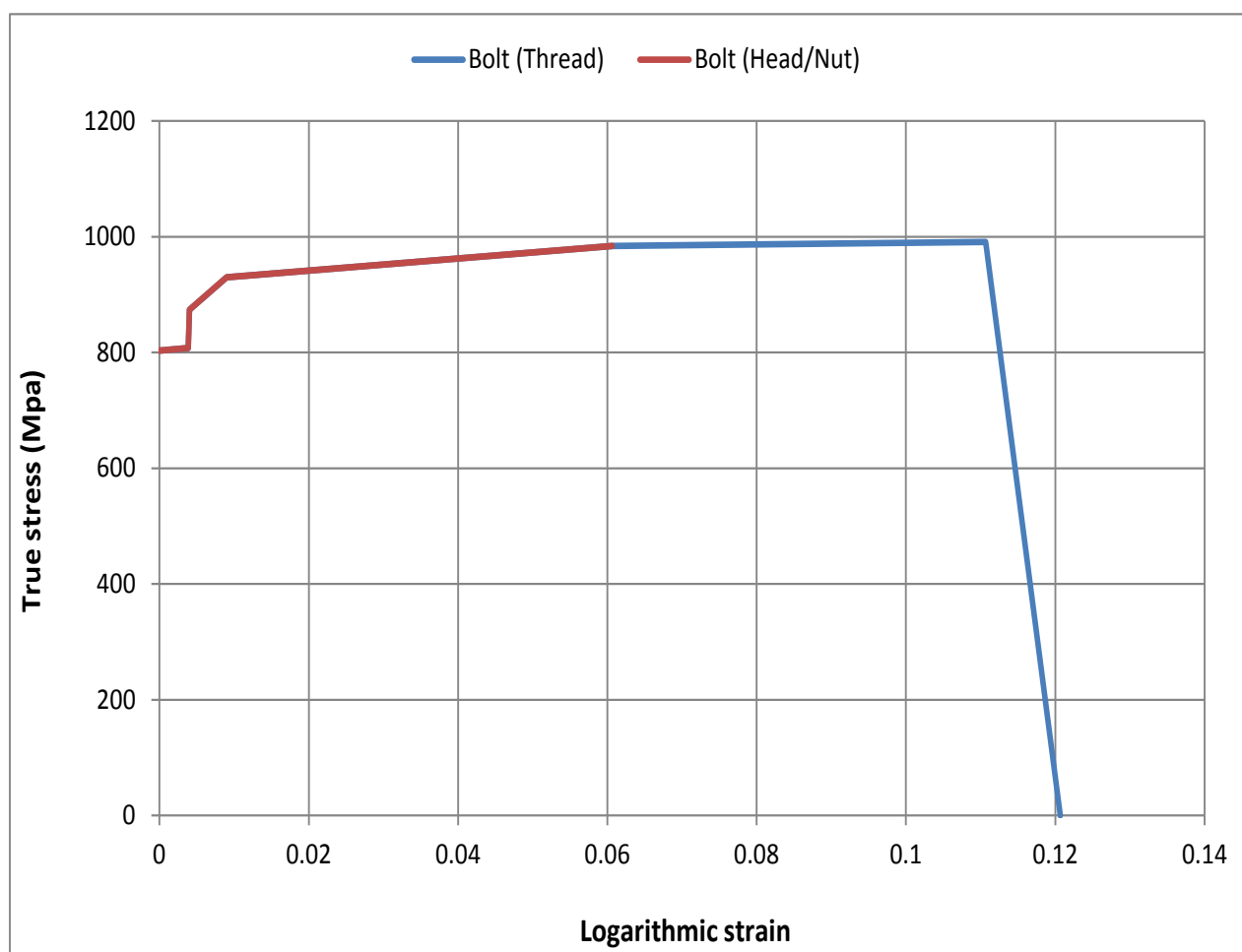
Figure 3.2.1. True stress-logarithmic strain material laws for bolts.

(a)

(b)   (c)
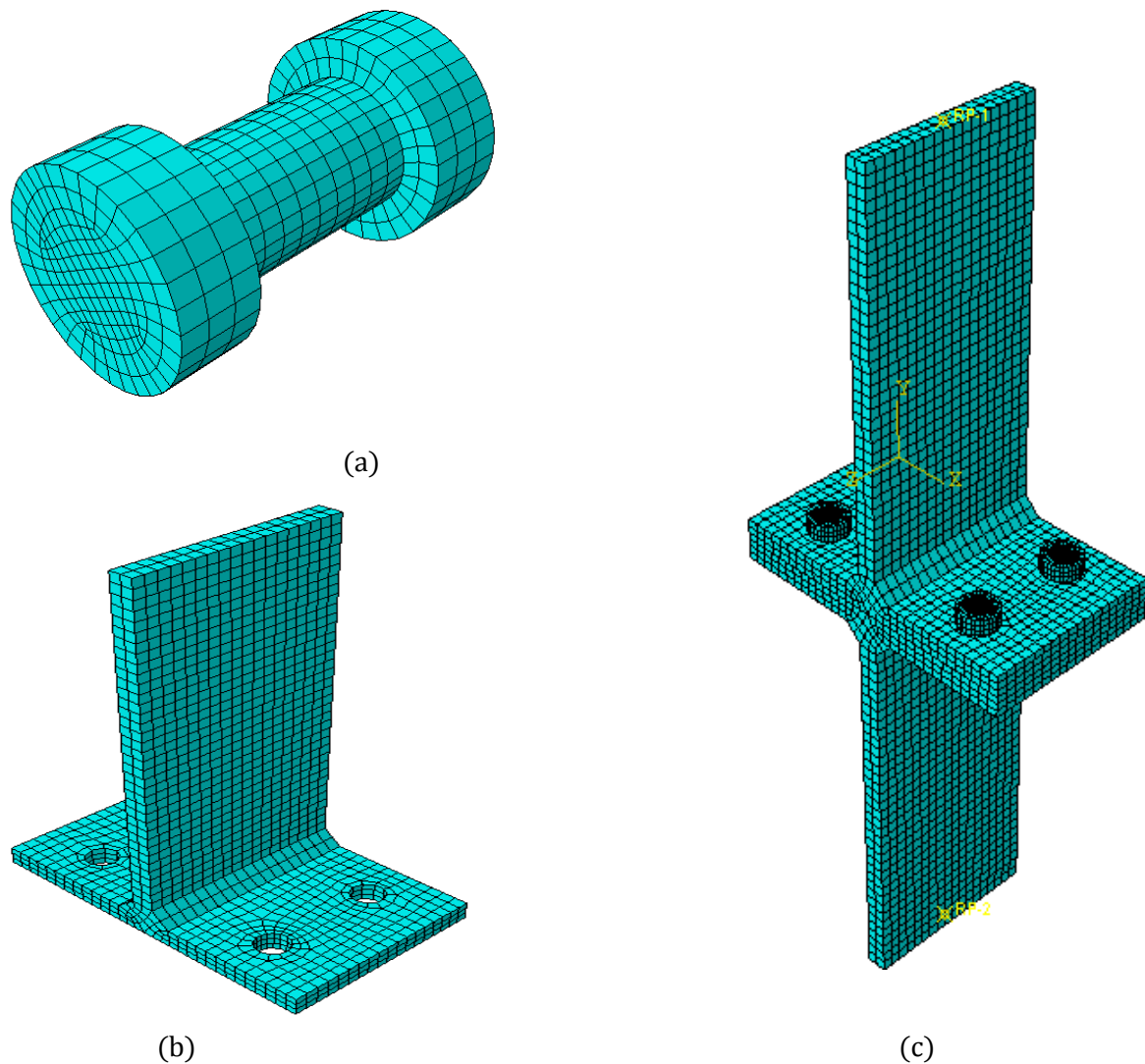
Figure 3.2.2. Finite element mesh: a) bolt model, b) T-stub C), Global model.

3.3 Results

The specimen WT1 (WT1g/h) were selected for the calibration of the FE model. (Girão Coelho et al. 2004) implemented a FE model using the commercial FE package LUSAS (2000) for the numerical analysis**.**

Figure 3.3.1. Shows the comparison of the experimental results with FE package LUSAS (2000) and ABAQUS (6.11). From the experimental tests both for specimens WT1g/h, bolt fracture determines the failure mode. From Figure 3.2.4, we can see that ABAQUS model gives us the similar type of failure mode for the model. Figure 3.2.2. and Figure

3.2.3 present von Mises stresses and equivalent plastic strain in the models a) and b). Figure 3.2.4. Shows von Mises stresses and equivalent plastic strain in bolts.
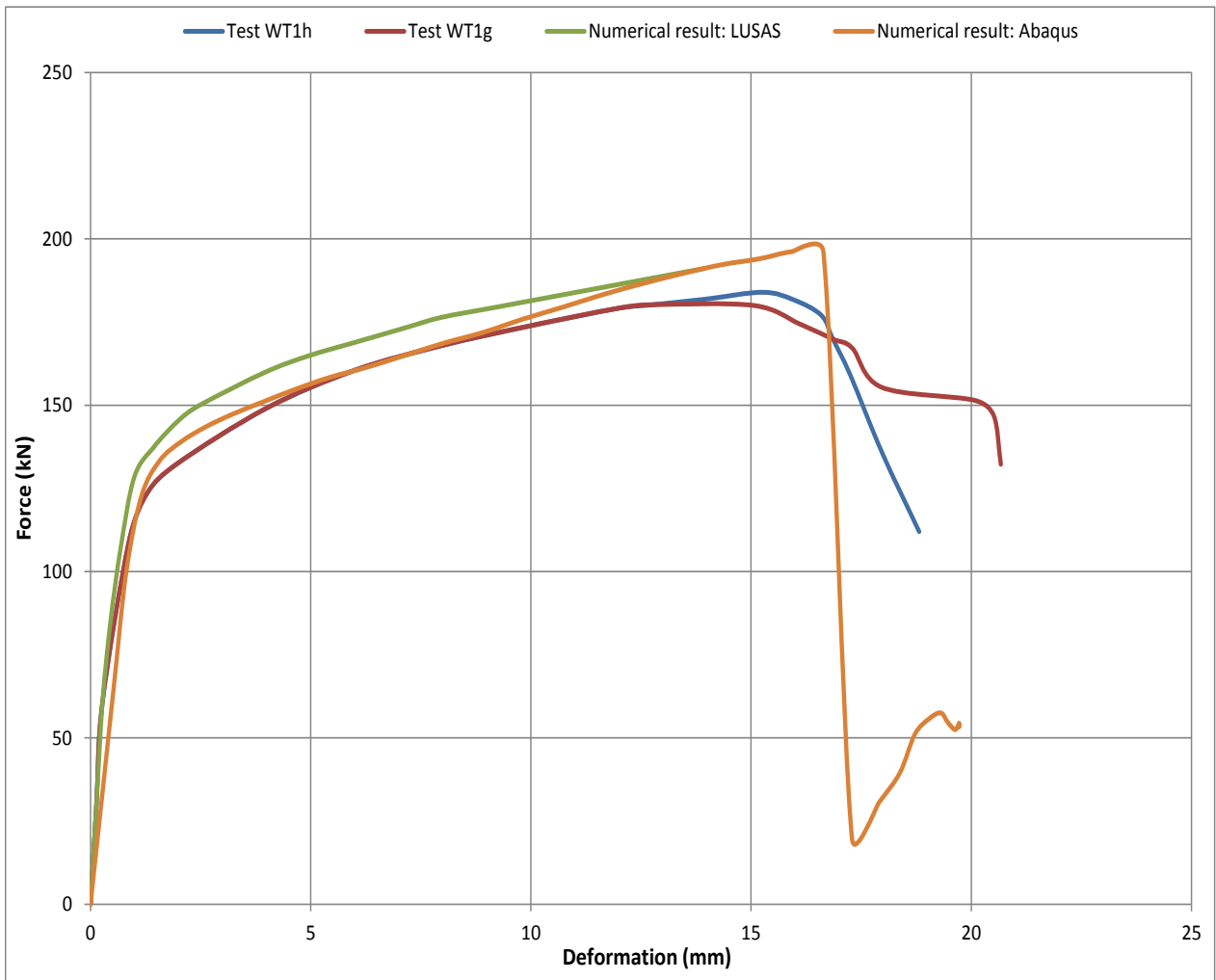
Figure 3.3.1. Global response of specimen WT1: numerical and experimental results.

(a)   (b)
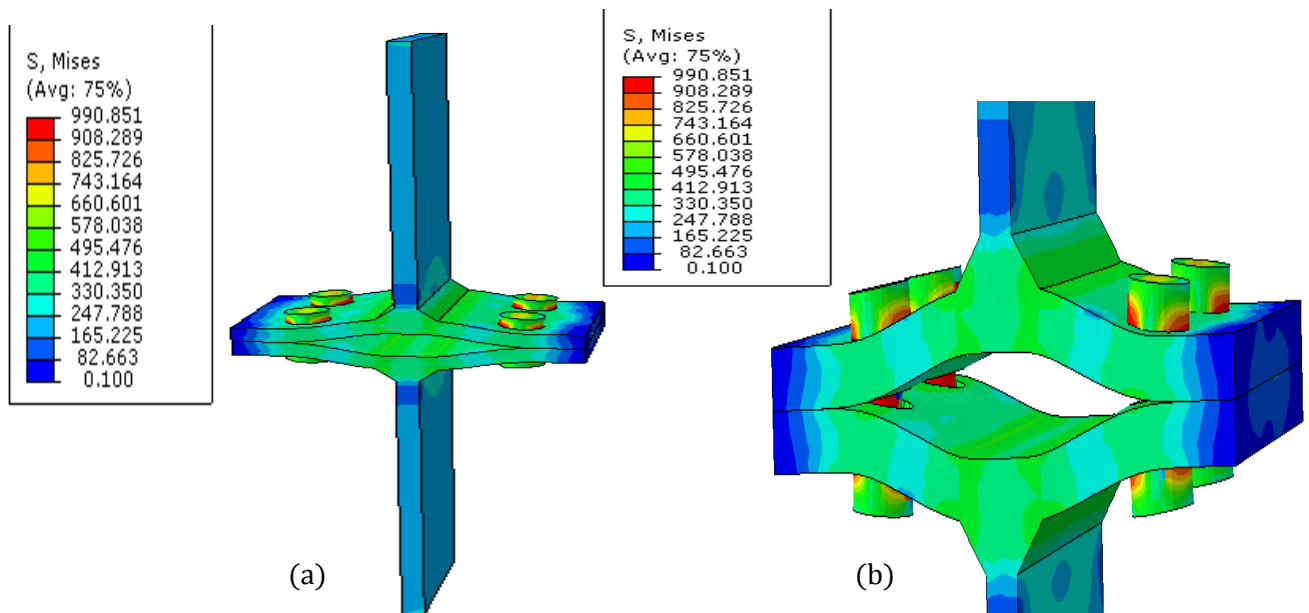
Figure 3.2.2. von Mises stresses in models a) and b).

(a)   (b)
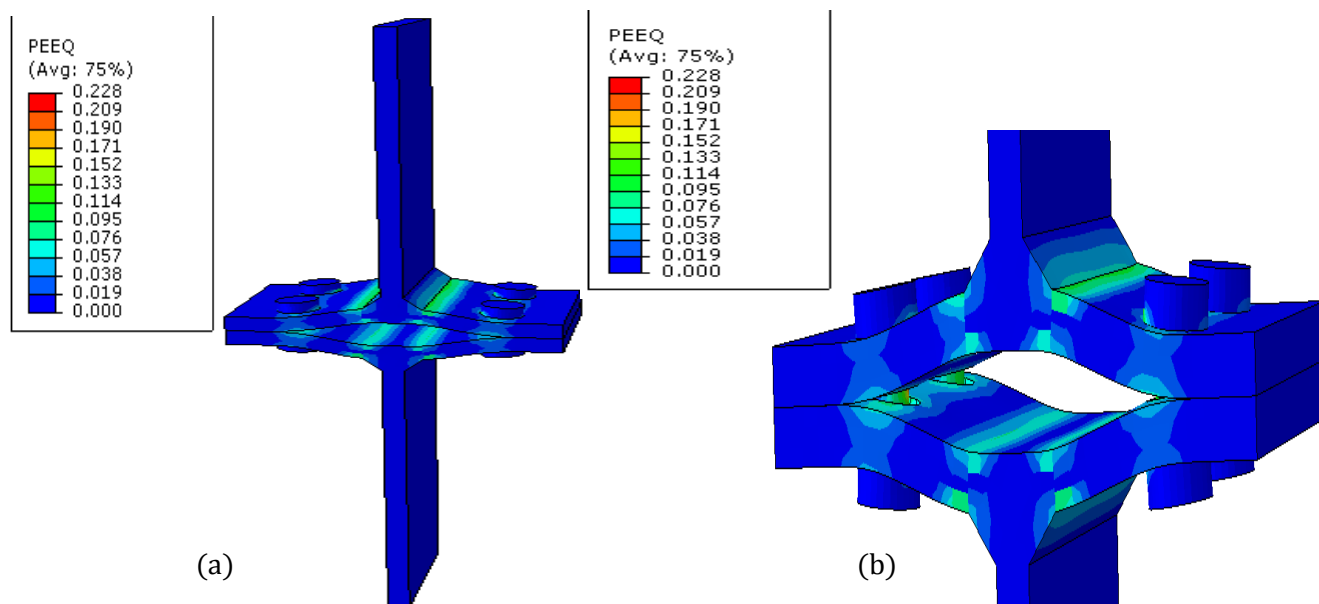
Figure 3.2.3. Equivalent plastic strain in models a) and b).

(a)   (b)
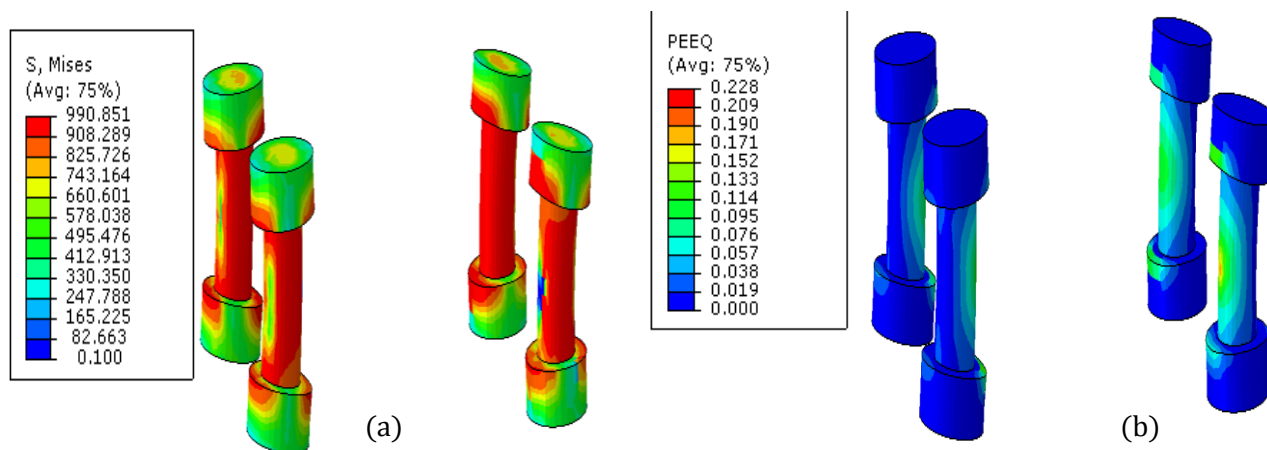
Figure 3.2.4. von Mises stresses and equivalent plastic strain in bolts a) and b).

4   Frame and joints design

4.1   Design of moment resisting frame

This section summarizes the design of 9 reference structures from which beam to column joint specimens could be extracted. The varied parameters for the structures were the system for resisting lateral loads (Figure 4.1.1), the number of storeys above ground (3 and 6) and the level of seismic hazard (high and medium). All structures were considered to have one underground level. The parameters of the designed systems are summarised in Table 4.1.1. The reference structures are designed according to standard code procedures, using provisions given by EN 1993-1-1, EN 1998-1 and EN 1994-1-1. The joints were considered to be full strength and full rigid, and their finite dimensions were not considered in frame design.
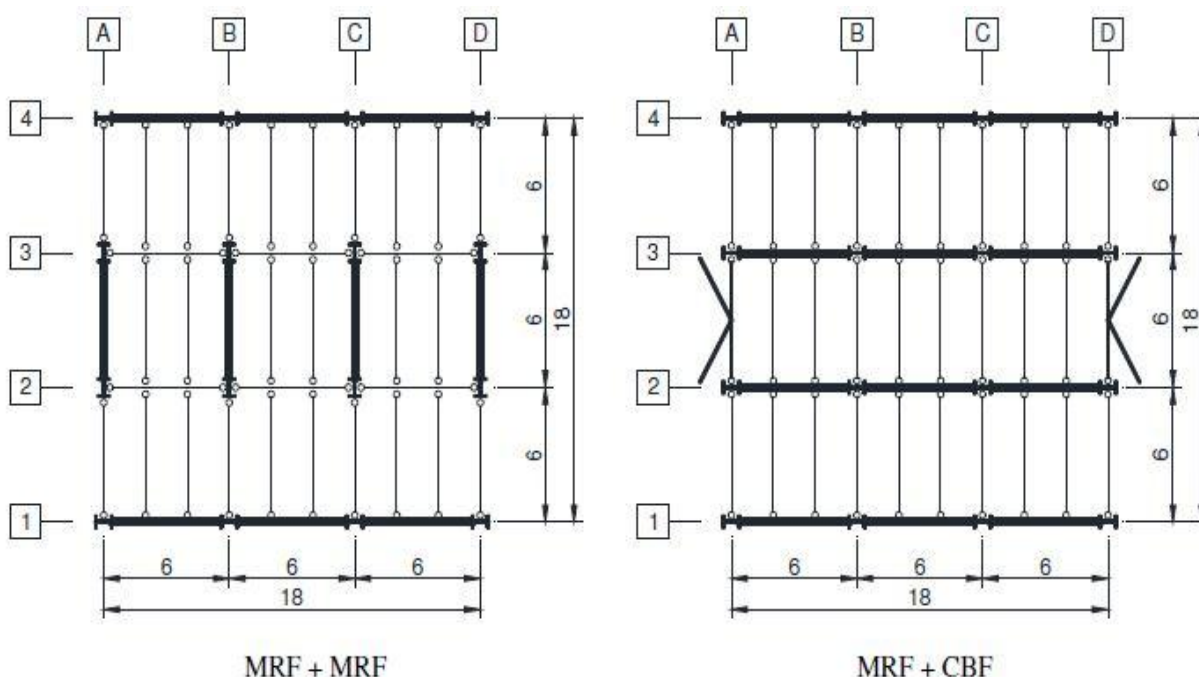
Figure 4.1.1. Plan views of buildings.

European Erasmus Mundus Master
Sustainable Constructions under natural hazards and catastrophic events
520121-1-2011-1-CZ-ERA MUNDUS-EMMC

SUSCOS
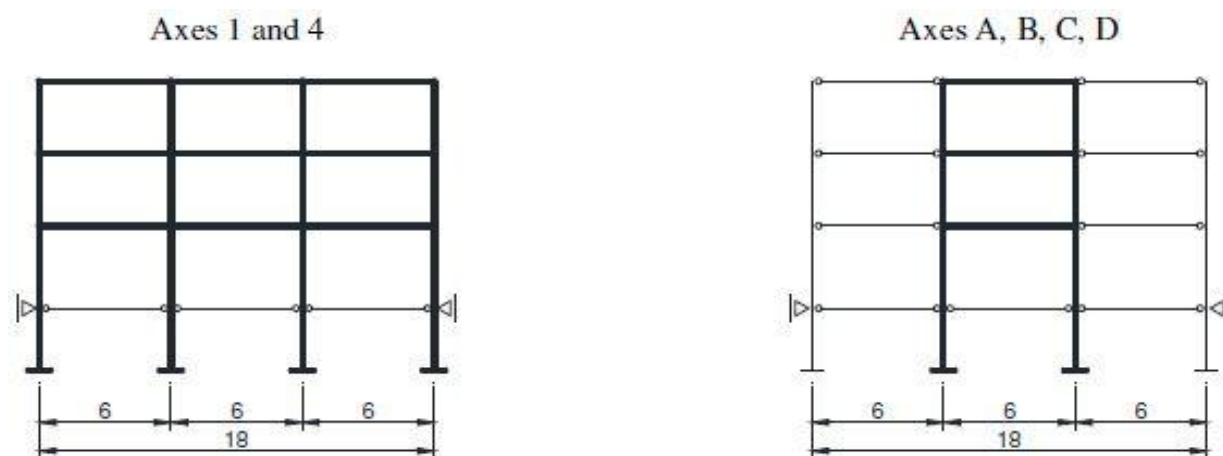
Figure 4.1.2. Vertical sections (MRF + MRF).
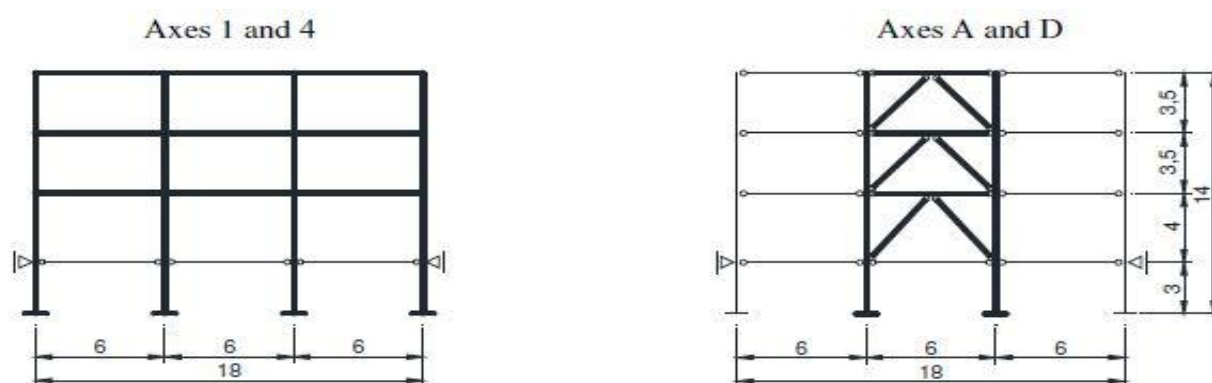
Figure 4.1.3. Vertical sections (MRF + CBF).

Table 4.1.1. Overview of designed frames.

Seismic level, a_g	Structural configuration			
	MRF+MRF		MRF+CBF	
	3 storeys	6 storeys	3 storeys	6 storeys
High (a_g=0.35 g)	MM63H	MM66H	MC63H	MC66H/MC86H
Medium (a_g=0.25 g)	MM63M	MM66M	MC63M	MC66M

Note: MM63H refers to structural configuration MRF+MRF with bays of 6 meters and having 3 storeys that is designed for high level of seismic hazard.

Table 4.1.2. Size of members for experimental program.

	Beam/column depth		
	1	2	3
Beam	IPE360	IPE450	IPE600
Column for exterior (T) joints	HEB280	HEB340	HEB500
Column for interior (X) joints	HEB340	HEB500	HEB650
Span in frame	6m	6m	8m

4.2   Joint detailing and design procedure

DESIGN PROCEDURE OF HAUNCHED BEAM TO COLUMN JOINTS.

Design assumption: plastic hinge forms at the end of the haunch.	
Connection designed according to EN 1993-1-8 for the expected maximum moment at the plastic hinge, projected at the column face $M_{j,Ed}=1.1\gamma_{ov}M_{pl,Rd}+V_{Ed,e}*s_h$ The following components were not considered when computing connection strength: • Column web panel in shear • Beam flange and web (and haunch) in compression	
The beam end including the haunch checked according to EN 1993-1-1 for the expected maximum moment at the plastic hinge, projected at the column face $M_{j,Ed}=1.1\gamma_{ov}M_{pl,Rd}+V_{Ed,e}*s_h$	
The column web panel was designed according to EN 1998-1 and EN 1993-1-8 for the shear forces corresponding to the plastic moment at the plastic hinge location, projected at the column face $M_{cwp,Ed}=M_{pl,Rd}+V_{Ed}*s_h$ When calculating the strength and stiffness of column web panel, its shear area was determined as the sum of (1) column shear area, (2) contribution of transverse stiffeners and column flanges, and (3) *full* area of additional web plates. That is, the following provision in EN 1993-1-8 was disregarded: Where a column web is reinforced by adding a supplementary web plate, see Figure 6.5, the shear area A_{vc} may be increased by $b_s t_{wc}$. If a further supplementary web plate is added on the other side of the web, no further increase of the shear area should be made. It's background is unclear and against evidence from some past tests at UPT.	

5   Numerical simulations

5.1   Overview of the numerical study
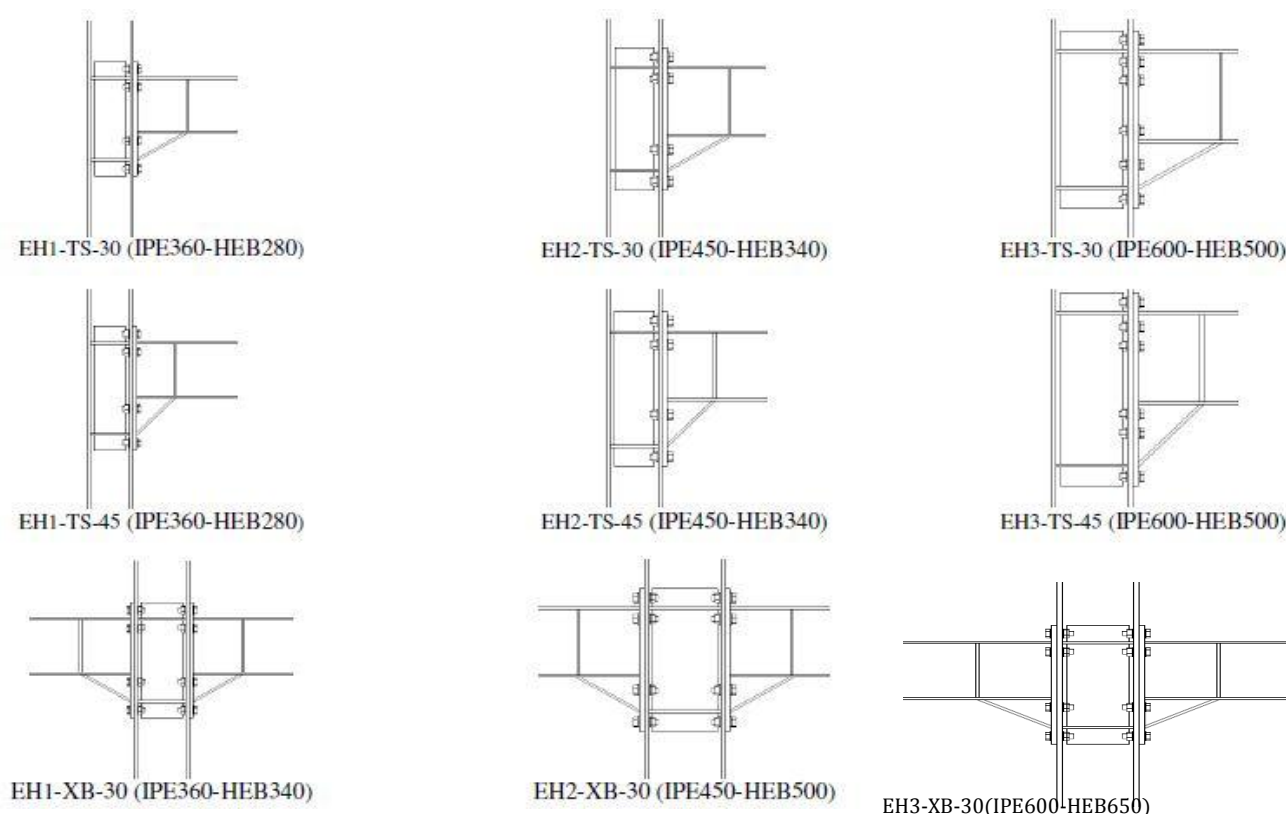
Figure 5.1.1. Configuration of haunched beam to column joints.

For the numerical analysis, total 9 joints have been selected (see **Figure 5.1.1**) from 3 groups. **Table 5.1.1** and **Table 5.1.2** present detailts about all the models.

Table 5.1.1. Size of members for numerical model.

	Beam/column depth		
	1	2	3
Beam	IPE360	IPE450	IPE600
Column for exterior (T) joints	HEB280	HEB340	HEB500
Column for interior (X) joints	HEB340	HEB500	HEB650
Span in frame	6m	6m	8m

Table 5.1.2.Model parameters and designations for haunched beam to column connections

Connection type	Joint configuration (interior / exterior)	Haunch geometry	Loading protocol	Beam/column depth			Key specimen and test characteristics
				1	2	3	
EH	TS	30	M		EH2-TS-30-M		Exterior (T) joint, full-strength & rigid conn., shallow haunch, strong web panel. 1 monotonic test; 6 cyclic tests (2 per beam size); 3 cyclic tests with alternative protocol; 2 cyclic tests with strong beam
EH	TS	30	C1	EH1-TS-30-C1	EH2-TS-30-C1	EH3-TS-30-C1	
EH	TS	30	C2	EH1-TS-30-C2	EH2-TS-30-C2	EH3-TS-30-C2	
EH	TS	30	CA	EH1-TS-30-CA	EH2-TS-30-CA	EH3-TS-30-CA	
EH	TSO	30	C	EH1-TSO-30-C		EH3-TSO-30-C	
EH	TS	45	M		EH2-TS-45-M		Exterior (T) joint, full-strength & rigid conn., steep haunch, strong web panel. 1 monotonic test; 6 cyclic tests (2 per beam size)
EH	TS	45	C1	EH1-TS-45-C1	EH2-TS-45-C1	EH3-TS-45-C1	
EH	TS	45	C2	EH1-TS-45-C2	EH2-TS-45-C2	EH3-TS-45-C2	
EH	XB	30	M		EH2-XB-30-M|		Interior (X) joint, full-strength & semi-rigid conn., shallow haunch, balanced web panel. 1 monotonic test; 4 cyclic tests (2 per beam size). Joints with IPE600 beams not possible due to actuator capacity limitation.
EH	XB	30	C1	EH1-XB-30-C1	EH2-XB-30-C1		
EH	XB	30	C2	EH1-XB-30-C2	EH2-XB-30-C2		

Groups 1 and 2 serve for qualifying two alternative haunch geometries (lower and upper limit of reasonable haunch angle), for the considered range of beam sizes. Due to stiffness requirements, the panel zone is much stronger than EN 1998-1 requirements for T joints in groups 1 and 2. Group 3 investigates joints with balanced panel zone strength, but which are semi-rigid. Additionally, larger column depth increases the range of prequalified column sizes.

Table 5.1.3 Grouping of the members for numerical model.

Group 1	EH1-TS-30(IPE360-HEB280)	EH2-TS-30(IPE450-HEB340)	EH3-TS-30(IPE600-HEB500)
Group 2	EH1-TS-45(IPE360-HEB280)	EH2-TS-45(IPE450-HEB340)	EH3-TS-45(IPE600-HEB500)
Group 3	EH1-XB-30(IPE360-HEB340)	EH2-XB-30(IPE450-HEB500)	EH3-XB-30(IPE600-HEB650)

For all members in the groups, monotonic analysis was performed. Only for member EH3-TS-30 (IPE600-HEB500) cyclic analysis was carried out using an alternative loading protocol (ECCS Vs. AISC) in order to investigate the influence of the loading history on the deformation capacity of joints.

5.2 Finite element method (FEM)

Finite Element Method (FEM) is a numerical technique that concerned with all aspects of the numerical solution of a problem, from the theoretical development and understanding of numerical methods to their practical implementation as reliable and efficient computer programs. Most numerical analysts specialize in small sub-areas, but they share some common concerns, perspectives, and mathematical methods of analysis. These include the following:

- When presented with a problem that cannot be solved directly, then replace
  it with a "nearby problem" which can be solved more easily. Examples are
  the use of interpolation in developing numerical integration methods and
  root finding methods;
- There is widespread use of the language and results of linear algebra, real
  analysis, and functional analysis.
- There is a fundamental concern with error, its size, and its analytic form.
  When approximating a problem, as above in item 1, it is prudent to
  understand the nature of the error in the computed solution. Moreover,
  understanding the form of the error allows creation of extrapolation
  processes to improve the convergence behaviour of the numerical
  method.
- Stability is a concept referring to the sensitivity of the solution of a
  problem to small changes in the data or the parameters of the problem.
- accurate representation of complex geometry with including dissimilar
  material properties;

Finite Element Analysis (FEA) is the modelling of products and systems in a virtual environment that is used in engineering applications. FEA is the practical application of the finite element method (FEM), which uses the mesh generation techniques for dividing a complex problem into small elements. For the analysis of bolted beam to column joints with haunches, the Finite Element Analysis (FEA) software ABAQUS (6.11) have been selected within this thesis paper. The analysis package used here is ABAQUS (Dynamic Explicit) uses the central-difference operator. In an explicit dynamic analysis displacements and velocities are calculated in terms of quantities that are known at the beginning of an increment.

The explicit dynamics procedure performs a large number of small time increments efficiently. An explicit central-difference time integration rule is used; each increment is relatively inexpensive (compared to the direct-integration dynamic analysis procedure available in Abaqus/Standard) because there is no solution for a set of simultaneous equations. The explicit central-difference operator satisfies the dynamic equilibrium

equations at the beginning of the increment, t; the accelerations calculated at time t are used to advance the velocity solution to time t+Δt/2 and the displacement solution to time .the displacement solution to time t+Δt. Abaqus/Explicit provides the following advantages:

- is computationally efficient for the analysis of large models with relatively short dynamic response times and for the analysis of extremely discontinuous events or processes;
- allows for the definition of very general contact conditions;
- uses a consistent, large-deformation theory—models can undergo large rotations and large deformation;
- can use a geometrically linear deformation theory—strains and rotations are assumed to be small;
- can be used to perform an adiabatic stress analysis if inelastic dissipation is expected to generate heat in the material;
- can be used to perform quasi-static analyses with complicated contact conditions;
- allows for either automatic or fixed time incrementation to be used—by default, Abaqus/Explicit uses automatic time incrementation with the global time estimator.

Analysis procedure

In quasi-static tests, loads and/or displacements are applied at slow rates. Such type of tests are carried out to study structural performance of structures and members such as the rate of propagation of cracks, hierarchy of collapse and associated level of damage, etc. Quasi-static tests are performed by imposing predefined displacement or force histories on the testing specimen. Different type of displacement histories are shown below (**Figure 5.2.1**):
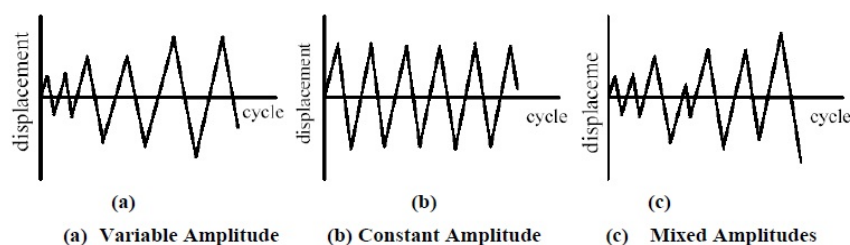
Figure 5.2.1. Various types of loading histories in quasi-static cyclic tests

The slow loading rate during the test has the advantage of providing an insight regarding the behaviour of structure/structural member in the post-yielding regime. However, the associated disadvantage is that the effects of acceleration-dependent inertial forces and velocity-dependent damping forces are neglected, which can be significant for some structural types.

For the loading of the system, the method of displacement was used. A displacement in the vertical direction was applied at the top plate of the missing column using smooth step data for defining the amplitude curve of the loading (displacement). This method is used to define the amplitude between two points, *a*, between two consecutive data points (t_i, A_i) and (t_{i+1}, A_{i+1}) (**Figure 5.2.2**).

$$t_0 = 0.0 \quad A_0 = 0.0 \quad t_1 = 0.1 \quad A_1 = 1.0$$

$$a = A_0 \text{ for } t \leq t_0$$

$$= A_0 + (A_1 - A_0)\, \xi^3\, (10 - 15\, \xi + 6\, \xi^2) \text{ for } t_0 < t < t_1$$

$$= A_1 \text{ for } t \geq t_1$$

$$\text{where } \xi = \frac{t - t_0}{t_1 - t_0}$$
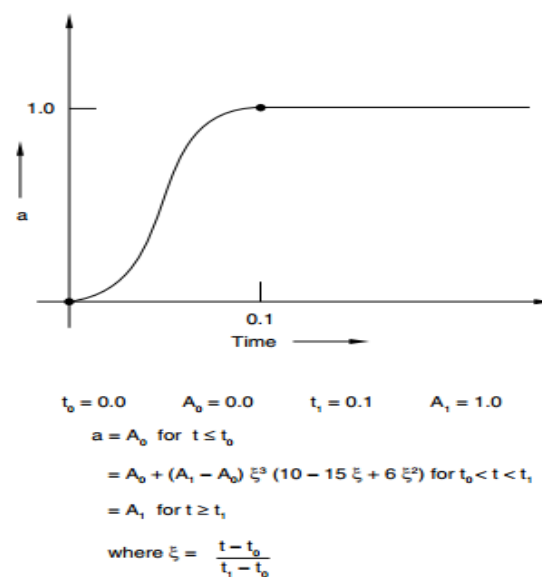
Figure 5.2.2. Smooth step amplitude definition example with two data points

This type of definition is intended to ramp up or down smoothly from one amplitude value to another. In this manner the displacement is applied in low increments, from zero to the final values. The analysis is considered to be completed structure collapses or after the full apply of the displacement. After each analysis, a displacement-force curve is requested from the software as output in order to evaluate the behaviour of the system.

Abaqus/Explicit offers fewer element types than Abaqus/Standard. For example, only first-order, displacement method elements (4-node quadrilaterals, 8-node bricks, etc.) and modified second-order elements are used.

Element name convention: Generally the element name convention depends on the element dimensions (see Figure 5.2.3)
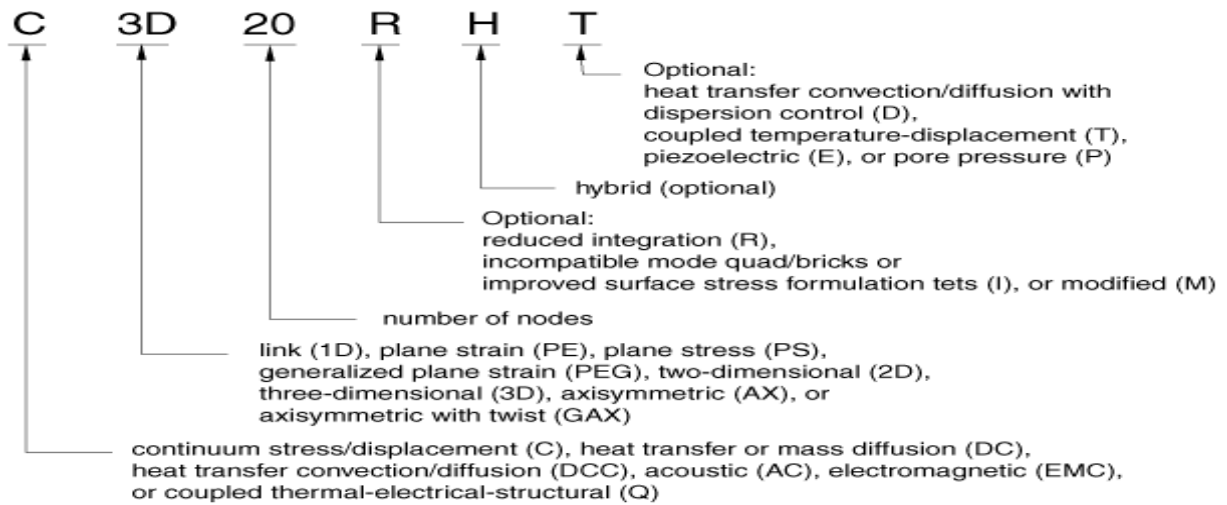
Figure 5.2.3 Name convention for solid elements in ABAQUS.

Mesh element shapes:

Most elements correspond to one of the shapes shown in Figure 5.2.4 (a), they are topologically equivalent to these shapes. For example, although the elements CPE4, CAX4R, and S4R are used for stress analysis, DC2D4 is used for heat transfer analysis, and AC2D4 is used for acoustic analysis, all five elements are topologically equivalent to a linear quadrilateral. As you can see in Figure 5.2.4 (b), a typically "Hex" (Hexahedra or brick) element shape is presented for the meshing of an element.

(a)   (b)
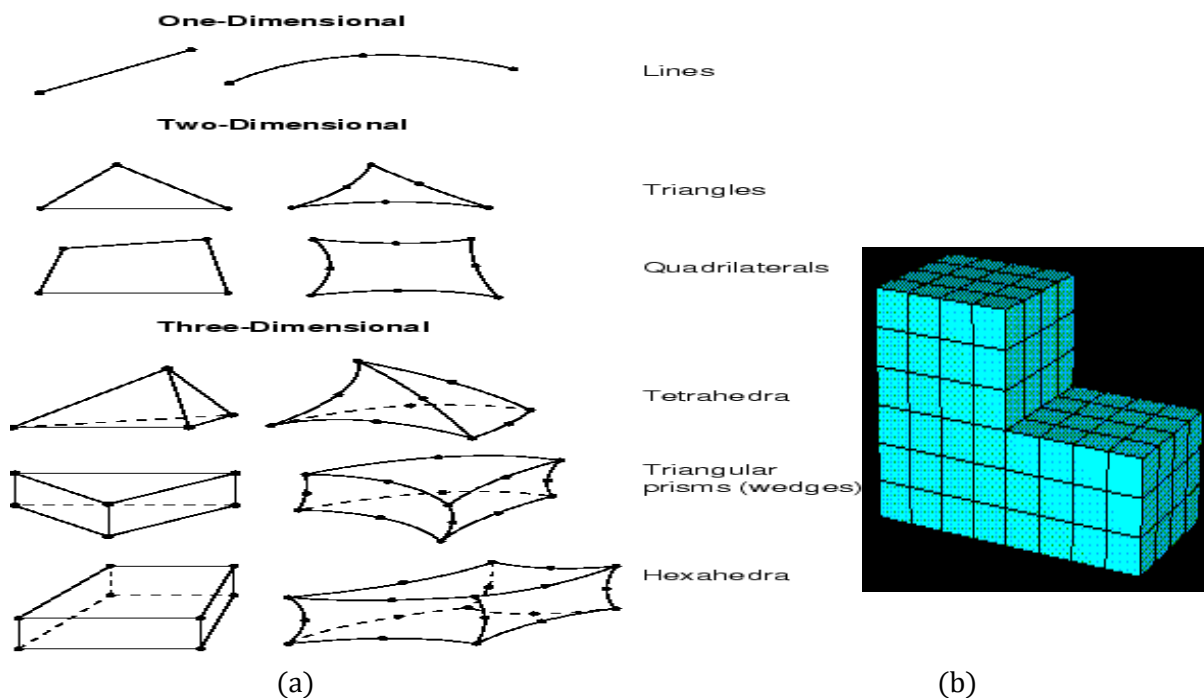
Figure 5.2.4. Hexahedra element shape (a) and Mesh element shapes (b) in ABAQUS.

Choosing between bricks/quadrilaterals and tetrahedra/triangles

Triangular and tetrahedral elements are geometrically versatile and are used in many automatic meshing algorithms. It is very convenient to mesh a complex shape with triangles or tetrahedra, and the second-order and modified triangular and tetrahedral elements (CPE6, CPE6M, C3D10, C3D10M, etc.) in Abaqus, thus they are suitable for general usage. However, a good mesh of hexahedral elements usually provides a solution of equivalent accuracy at less cost. Quadrilaterals and hexahedra have a better convergence rate than triangles and tetrahedra, and sensitivity to mesh orientation in regular meshes is not an issue. However, triangles and tetrahedra are less sensitive to initial element shape, whereas first-order quadrilaterals and hexahedra perform better if their shape is approximately rectangular.
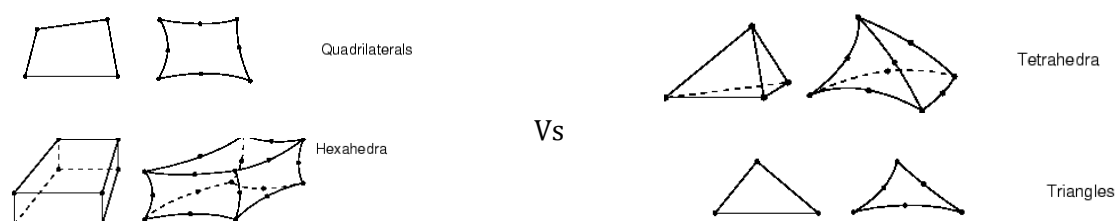
Figure 5.2.5. Comparison between bricks/quadrilaterals and tetrahedral/trinagles elements.

Mesh instability

Section control is used to choose a nondefault hourglass control approach for reduced-integration elements in Abaqus/Standard and Abaqus/Explicit and modified tetrahedral or triangular elements in Abaqus/Standard or to scale the default coefficients used in the hourglass control. In Abaqus/Explicit it is also used to select a nondefault kinematic formulation for 8-node brick elements (CPS4R, CAX4R, C3D8R, etc.), to choose the second-order accurate formulation for solids and shells, to activate distortion control for solid elements, to turn off the drill stiffness in small-strain shell elements S3RS and S4RS. Using values larger than the default values for hourglass control can produce excessively stiff response and sometimes can even lead to instability if the values are too large. Hourglassing that occurs with the default hourglass control parameters is usually an indication that the mesh is too coarse. Therefore, it is generally better to refine the mesh than to add stronger hourglass control.

According to the theory presented above, a 8-node linear brick, reduced integration, hourglass control (C3D8R) element type was selected for the member from standard element library. This type of element is a stress/displacement element. The family (the family has the meaning of the type of analysis that will be performed with the element) associated to the element was the 3D Stresses (i.e. 3D stress analysis). The column was meshed using structured mesh technique using hexahedral element shape (Figure 5.2.6).

Instead of global seeding of the elements, local seeding was chosen by number method, because this method is more accurate regarding the complex 3D models. The mesh sizes were defined along selected edges by prescribing the number of elements to create.
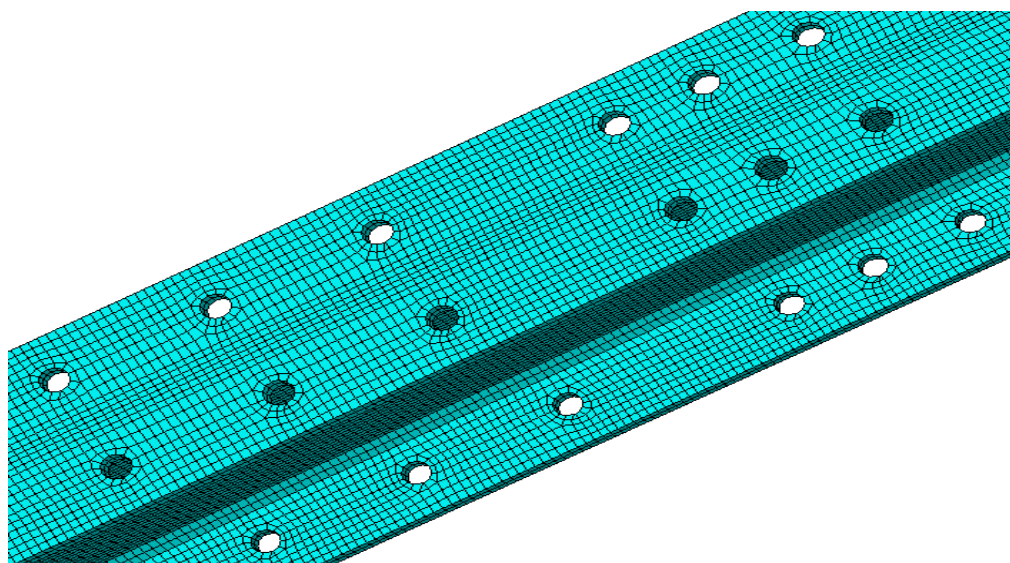
Figure 5.2.6.Interior column mesh at joint level.

5.3   Numerical model description

5.3.1   Steel S355 material model (Expected)

Structural steel is an isotropic material which has good strength and ductility. It undergoes large deformation prior to failure. Structural steel grade S355 (Expected,f_y= 1.25*355=443.75MPa) was used for most of the structural members (except bolts) during analysis. The elastic-plastic characteristics are presented in Figure 5.3.1.1. Firstly, the density of the material was defined, introducing 7.85E-009 (i.e. 7850 kg/m3) with uniform distribution. The isotropic elastic properties are completely defined by giving Young's modulus (E=210000 N/mm2) and Poisson's ratio (ν=0.3). The shear modulus (G) can be expressed by these two terms. For defining the classical metal plasticity property of the material, isotropic hardening model was used by defining yield stress and plastic strain data (Table 5.3.1.1).
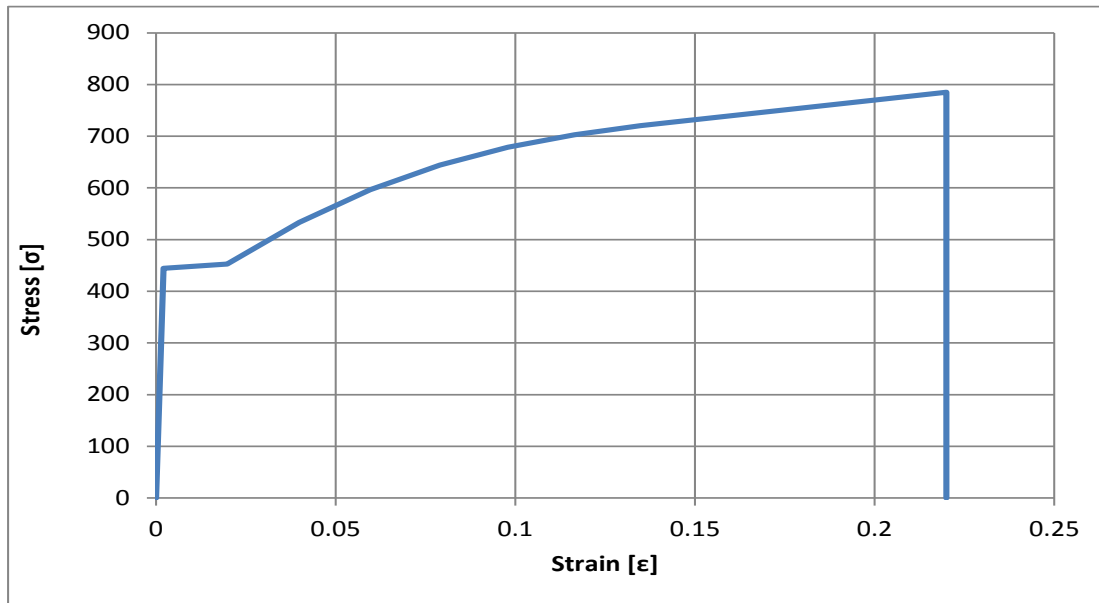
Figure 5.3.1.1.Stress-Strain relation of steel S355 (Expected).

Table 5.3.1.1.Steel material characteristics

Steel S355 (Expected)				
Density (ρ)	Young's modulus(E)	Poisson's ratio (μ)	Yield stress (f.y)	f.u/f.y
[kg/m^3]	[N/mm^2]		[N/mm^2]	
7850	210000	0.3	443.75	1.42
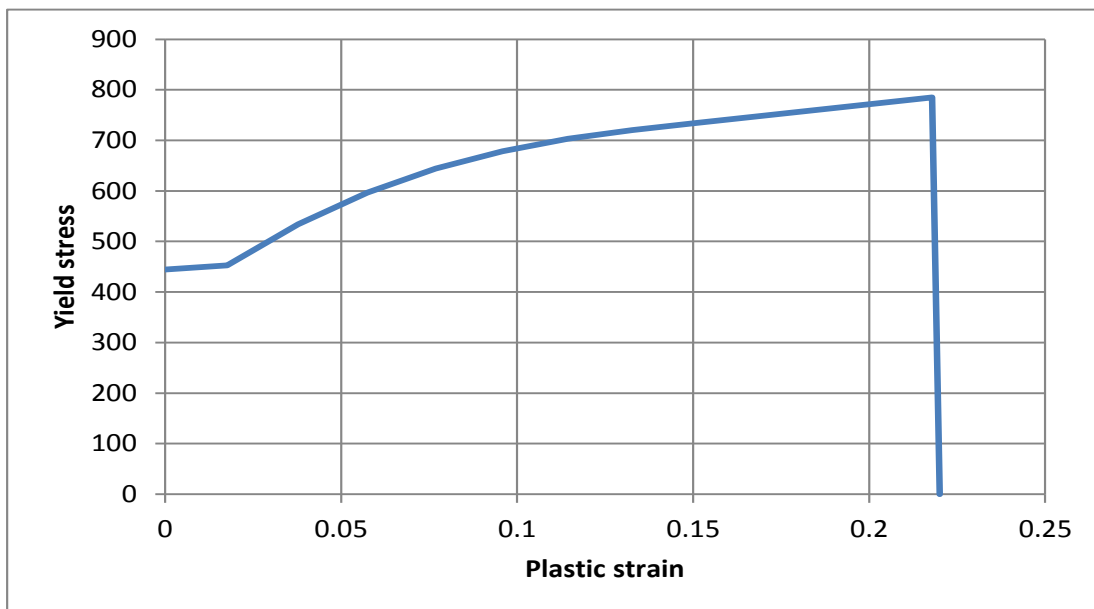
Figure 5.3.1.2.Isotropic hardening model data used for defining the nonlinear plastic behaviour of steel

5.3.2 Steel S355 material model (Nominal)

Structural steel is an isotropic material which has good strength and ductility. It undergoes large deformation prior to failure. Structural steel grade S355 (Nominal, f_y=355MPa) was used for most of the structural members (except bolts) during analysis. The elastic-plastic characteristics are presented in Figure 5.3.2.1. Firstly, the density of the material was defined, introducing 7.85E-009 (i.e. 7850 kg/m3) with uniform distribution. The isotropic elastic properties are completely defined by giving Young's modulus (E=210000 N/mm2) and Poisson's ratio (ν=0.3). The shear modulus (G) can be expressed by these two terms. For defining the classical metal plasticity property of the material, isotropic hardening model was used by defining yield stress and plastic strain data (Table 5.3.2.1).
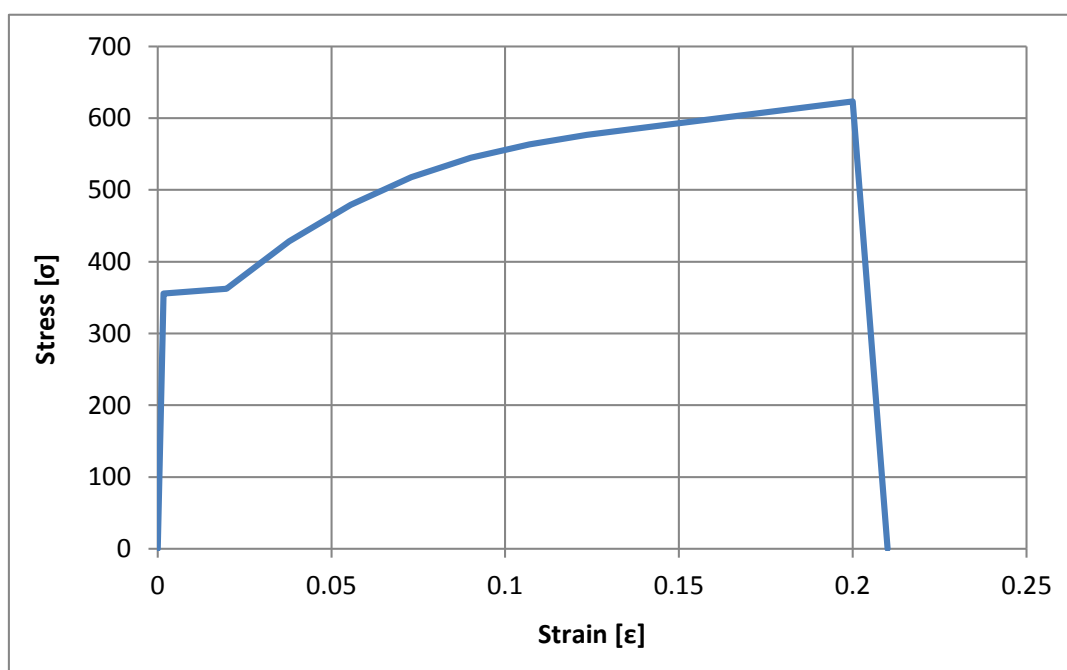
Figure 5.3.2.1. Stress-Strain relation of steel S355 (Nominal).

Table 5.3.2.1. Steel material characteristics

Steel S355 (Nominal)				
Density (ρ)	Young's modulus(E)	Poisson's ratio (μ)	Yield stress (f.y)	f.u/f.y
[kg/m^3]	[N/mm^2]		[N/mm^2]	
7850	210000	0.3	355	1.44
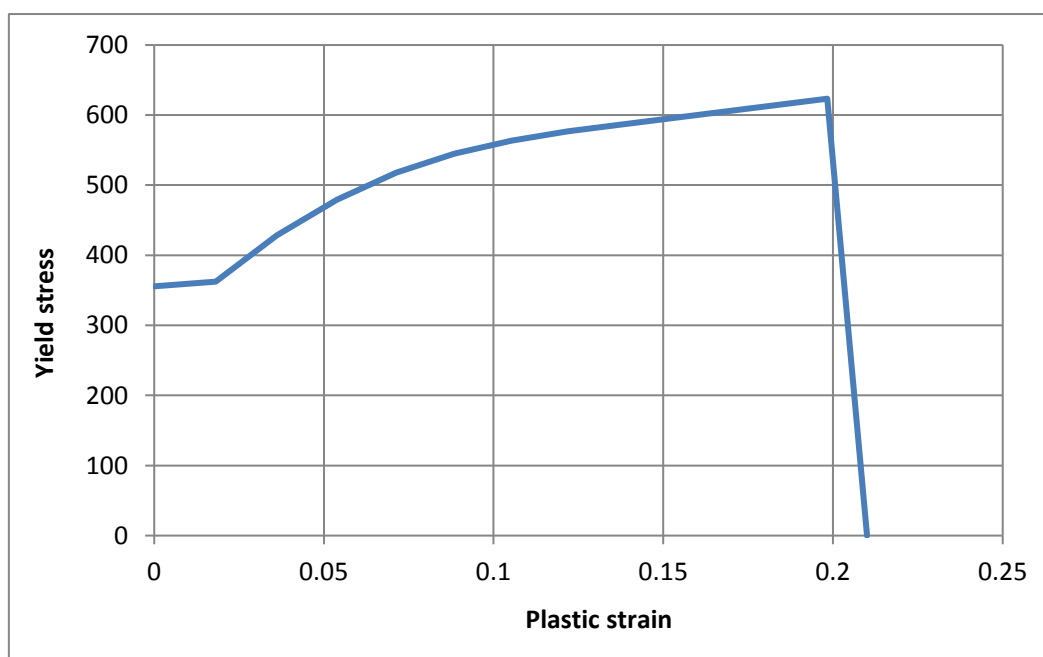
Figure 5.3.2.2. Isotropic hardening model data used for defining the nonlinear plastic behaviour of steel.

5.3.3   Bolt grade 10.9 material model (Expected)

Structural bolt grade 10.9 (Expected, f_y=940MPa) was used for all joints except in models for verification of design procedure. All bolts were modelled with solid type elements (C3D8R) with an equivalent diameter based on the effective cross-sectional area (threaded part) of the shank, with cylinders at the ends representing the head, nut and washer (Figure 5.3.3.1). Bolt thread was not modelled. The space between the head and nut was exactly the same as the thickness of the plates which it was supposed to holding. The diameters of the holes for the bolts were bigger than the shank as the code says for non-fitted bolts (typically 2 mm). The elastic-plastic characteristics are presented in Figure 5.3.3.2. Firstly, the density of the material was defined, introducing 7.85E-009 (i.e. 7850 kg/m3) with uniform distribution. The isotropic elastic properties are completely defined by giving Young's modulus (E=210000 N/mm2) and Poisson's ratio (ν=0.3). The shear modulus (G) can be expressed by these two terms. For defining the classical metal plasticity property of the material, isotropic hardening model was used by defining yield stress and plastic strain data (Figure 5.3.3.3).
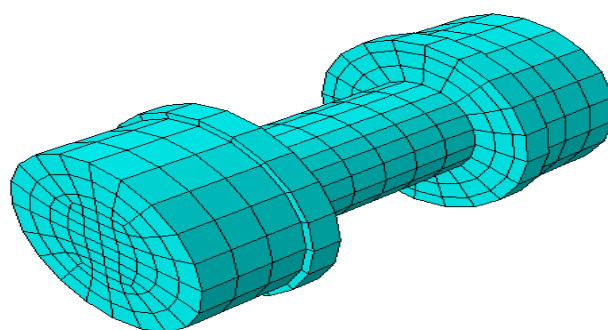
Figure 5.3.3.1.Numerical model of bolt.
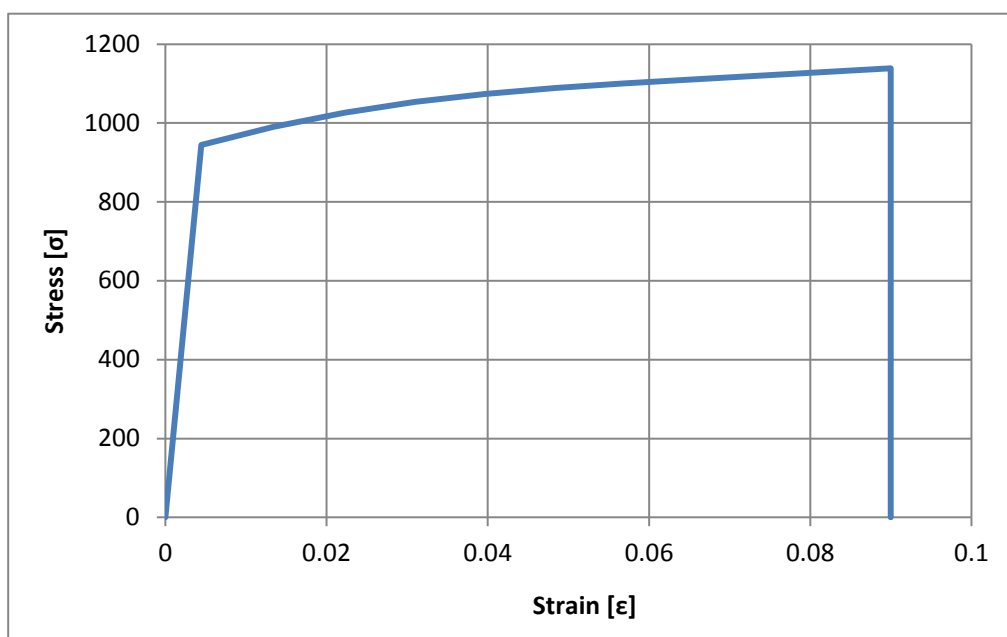
Figure 5.3.3.2.Stress-Strain relation of bolt grade 10.9 (Expected).

Table 5.3.3.1.Steel material characteristics

Bolt grade 10.9 (Expected)				
Density (ρ)	Young's modulus(E)	Poisson's ratio (μ)	Yield stress (f.y)	f.u/f.y
[kg/m^3]	[N/mm^2]		[N/mm^2]	
7850	210000	0.3	940	1.1
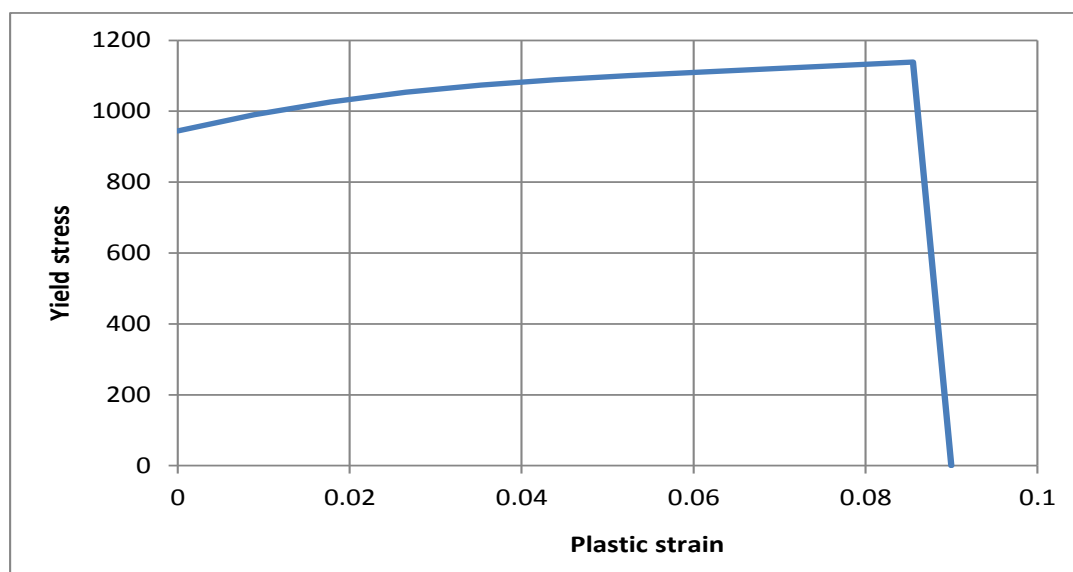
Figure 5.3.3.3. Isotropic hardening model data used for defining the nonlinear plastic behaviour of steel

5.3.4   Bolt grade 10.9 material model (Nominal)

Structural bolt grade 10.9 (Nominal, f_y=900MPa) was used for all joints in models for verification of design procedure. All bolts were modelled with solid type elements (C3D8R) with an equivalent diameter based on the effective cross-sectional area (threaded part) of the shank, with cylinders at the ends representing the head, nut and washer (Figure 5.3.4.1). Bolt thread was not modelled. The space between the head and nut was exactly the same as the thickness of the plates which it was supposed to holding. The diameters of the holes for the bolts were bigger than the shank as the code says for non-fitted bolts (typically 2 mm). The elastic-plastic characteristics are presented in Figure 5.3.4.2. Firstly, the density of the material was defined, introducing 7.85E-009 (i.e. 7850 kg/m3) with uniform distribution. The isotropic elastic properties are completely defined by giving Young's modulus (E=210000 N/mm2) and Poisson's ratio (ν=0.3). The shear modulus (G) can be expressed by these two terms. For defining the classical metal plasticity property of the material, isotropic hardening model was used by defining yield stress and plastic strain data (Figure 5.3.4.3).
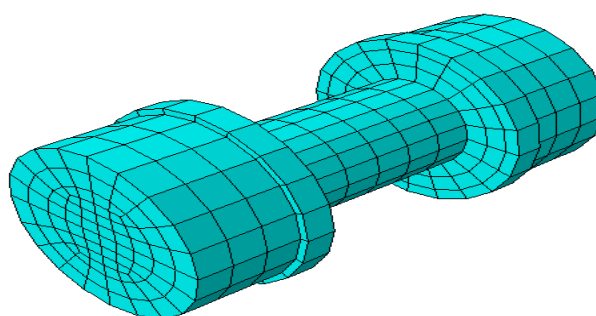
Figure 5.3.4.1. Numerical model of bolt.

European Erasmus Mundus Master
Sustainable Constructions under natural hazards and catastrophic events
520121-1-2011-1-CZ-ERA MUNDUS-EMMC

surcos
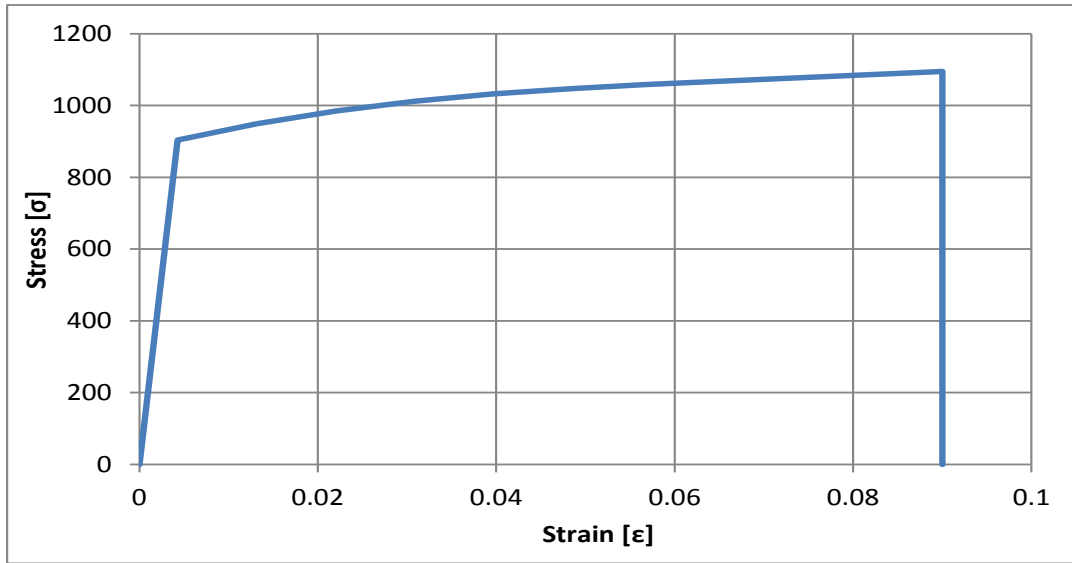
Figure 5.3.4.2. Stress-Strain relation of bolt grade 10.9 (Expected).

Table 5.3.4.1. Steel material characteristics

Bolt grade 10.9 (Nominal)				
Density (ρ)	Young's modulus(E)	Poisson's ratio (μ)	Yield stress (f.y)	f.u/f.y
[kg/m^3]	[N/mm^2]		[N/mm^2]	
7850	210000	0.3	900	1.11
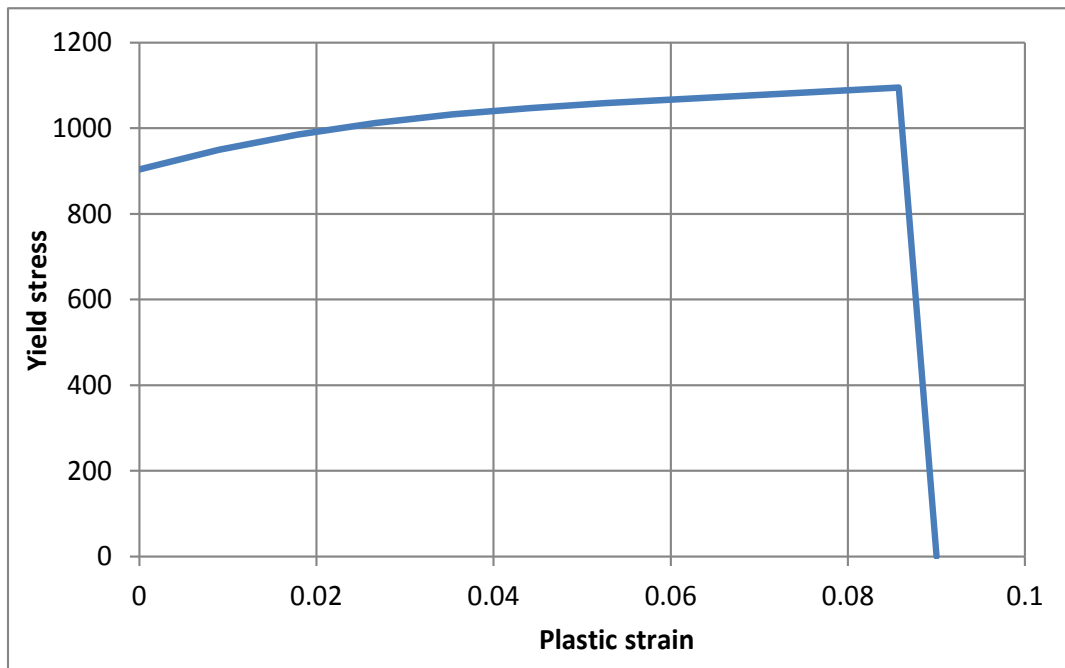
Figure 5.3.4.3. Isotropic hardening model data used for defining the nonlinear plastic behaviour of steel.

5.3.5   Cyclic loading protocol

The ECCS (1986) [93] procedure was considered for the cyclic loading. The yield displacement d_y can be obtained using the method recommended by the ECCS (1986) document, as the relative displacement corresponding to intersection of the initial stiffness (K_{ini}) line and a tangent to the moment-rotation curve with a stiffness equal to $K_{ini}/10$ (see Figure 5.3.5.1).

The cyclic loading procedure follows the steps below (ECCS), see Figure 5.3.5.1:

- one cycle at $0.25 \cdot d_y$
- one cycle at $0.5 \cdot d_y$
- one cycle at $0.75 \cdot d_y$
- one cycle at $d=1.0 \cdot d_y$
- three cycles at $m \cdot d_y$
- three cycles at $(m+m \cdot n) \cdot d_y$, with $n=1, 2, 3 \ldots$

The value of the m factor controls the magnitude of plastic excursions and the number of cycles performed in the plastic range. In the experimental tests a value of m=2 was considered.
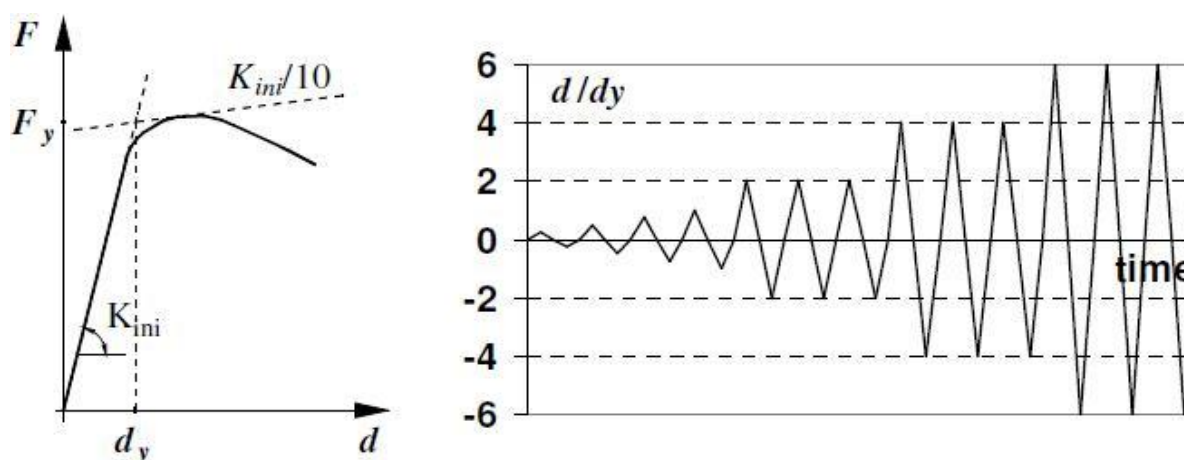
Figure 5.3.5.1.Determination of yield displacement, and ECCS loading procedure [93]

The ANSI/AISC 341-10 (2010) [94] loading procedure was also considered. The procedure is prescribed in absolute values of inter-storey drift θ (see Figure 5.3.5.2):

- 6 cycles at $\theta = 0.00375$ rad
- 6 cycles at $\theta = 0.005$ rad
- 6 cycles at $\theta = 0.0075$ rad
- 4 cycles at $\theta = 0.01$ rad
- 2 cycles at $\theta = 0.015$ rad
- 2 cycles at $\theta = 0.02$ rad

- 2 cycles at θ = 0.03 rad
- 2 cycles at θ = 0.04 rad

The loading is continued with increments of θ=0.01 rad, with 2 cycles/step.
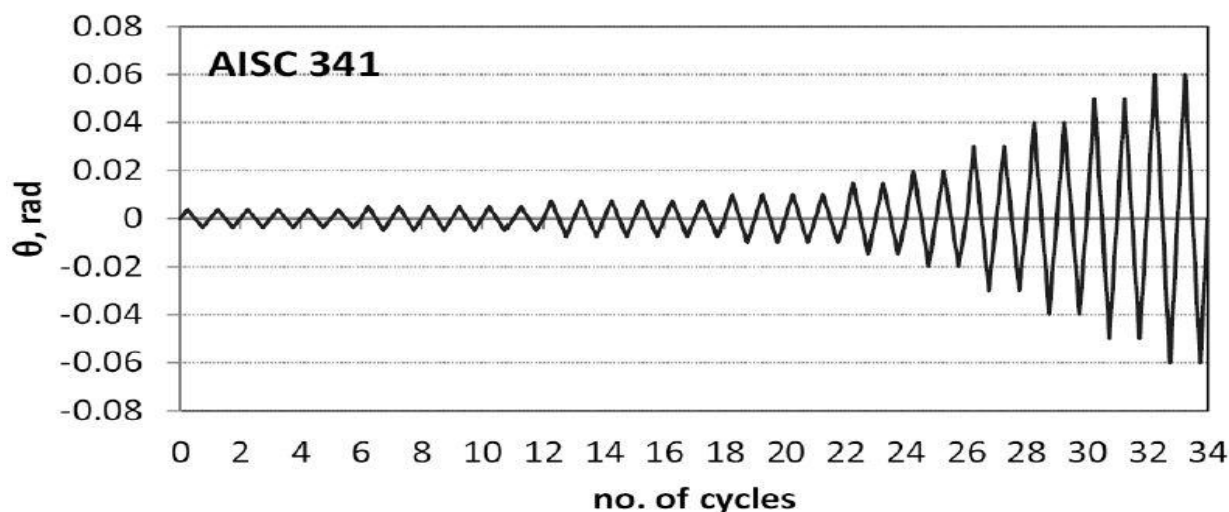
Figure 5.3.5.2.ANSI/AISC 341-10 (2010) cyclic loading procedure [94]

5.4   Results

5.4.1   Verification of design procedure

The objective of this section is to verify the design procedure and for this purpose two models EH3-TD-30-M(IPE600-HEB500) and EH3-TD-45-M(IPE600-HEB500) were chosen for numerical analysis. Both upward and downward displacement were applied corresponds to a magnitude of 0.1rad rotation on the tip of the beam in both models. Nominal material properties (f_y= 355MPa) were set for all the non-dissipative parts in the joints like haunch, endplate, column, stiffener etc. Only in the dissipative parts expected material properties (f_y= 1.25*355= 443.75MPa) were defined. For bolts (f_y=900MPa) was used. Figure 5.4.1.1 shows the moment-rotation capacity among those models. As we can see the difference is almost 4% between maximum and minimum moment capacity of the models EH3-TD-30-M-S and EH3-TD-45-M-H. In case of strength degradation in plastic yielding region, haunch position with 30 degree angle provides stiffer slope than 45 degree angle.
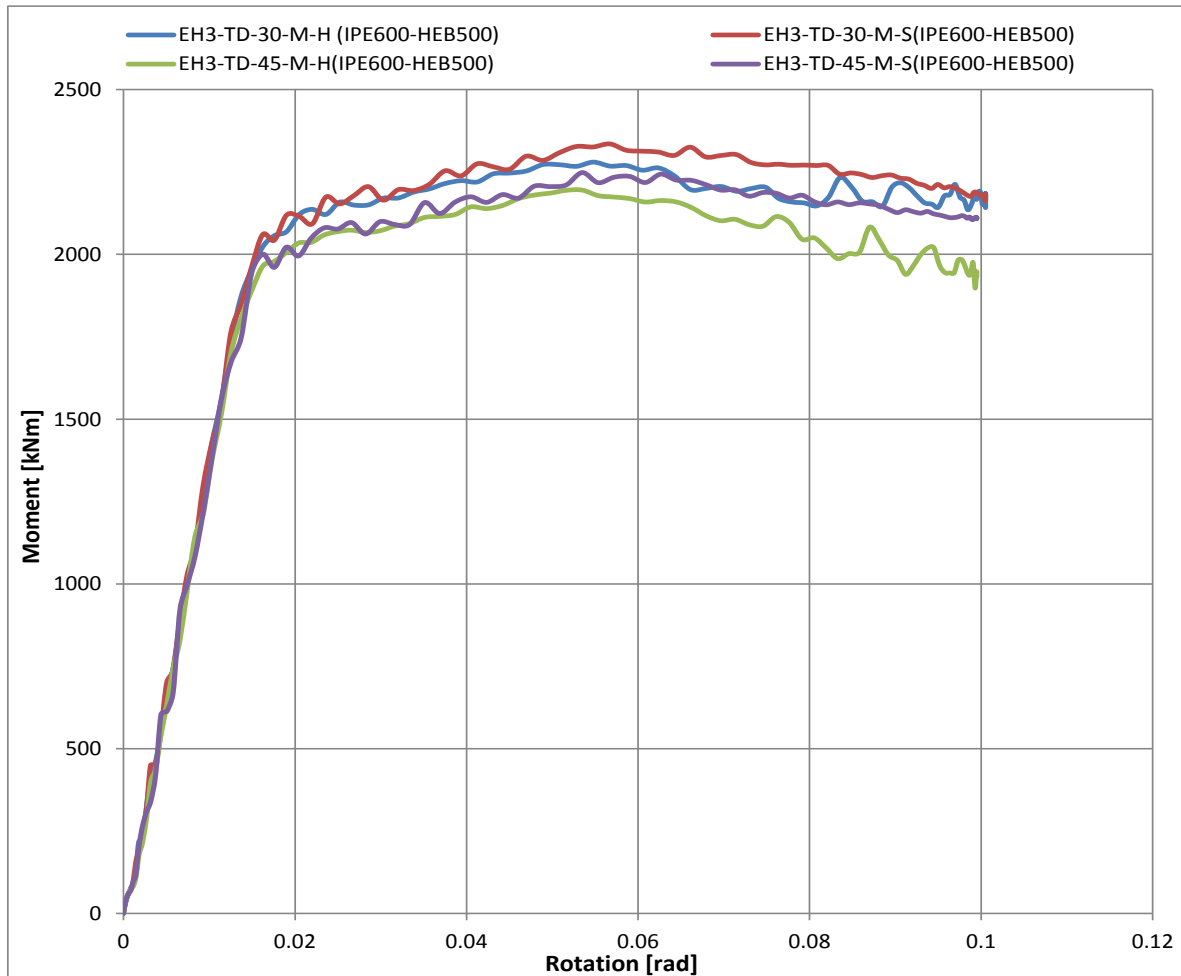
Figure 5.4.1.1.Comparision of moment–rotation among models EH3-TD-30-M-H, EH3-TD-30-M-S, EH3-TD-45-M-H, EH3-TD-45-M-S.

Figure 5.4.1.2 presents the von Mises stresses in models EH3-TD-30-M-S (a) and EH3-TD-30-M-H (b).It can be observed that beam flanges and web are exceeding the yield stress near the haunch end. Figure 5.4.1.3 represents the equivalent plastic strain in models EH3-TD-30-M-S (a) and EH3-TD-30-M-H (b). We can see plastic hinges are formed near to the haunch end. But in the design procedure it was assumed that plastic hinge forms at the end of the haunch. From the numerical analysis we have found that plastic hinges have occurred at a distance from the haunch end of 246mm $(0,41h_b)$ and 216mm$(0.36h_b)$ for models EH3-TD-30-M-S and EH3-TD-30-M-H. On the other hand, plastic hinges form at a distance from haunch end of 261mm $(0.43h_b)$ and 231mm $(0.38h_b)$ for models EH3-TD-45-M-S and EH3-TD-45-M-H. Figure 5.4.1.4 and Figure 5.4.1.5 depicts the von Mises stresses and equivalent plastic strain close up view in those two models. We can see that plastic strain in the top flange is close to column face and in bottom flange bit away from column face due to downward displacement and almost identical for upward displacement.

Due to safety reason, it is not desire to have plastic strain in the non-dissipative parts. Eventually from the analysis we have seen that some portion of the haunch, endplate,

column and bolts have plastic strain to the yield limit. Figure 5.4.1.6 and Figure 5.4.1.7 show the von Mises stresses & equivalent plastic strain for bolts. Upper and lower row of bolts are yielding under tension and bending. The yielding of bolts are taking place locally not along the full section. In overall we can say that joint performance is adequate.

Table 5.4.1.1 and

Table 5.4.1.2 present maximum von Mises stresses and equivalent plastic strain for all the parts in joint.

Models: EH3-TD-30-M-S(IPE600-HEB500)   EH3-TD-30-M-H(IPE600-HEB500)

(a)   (b)
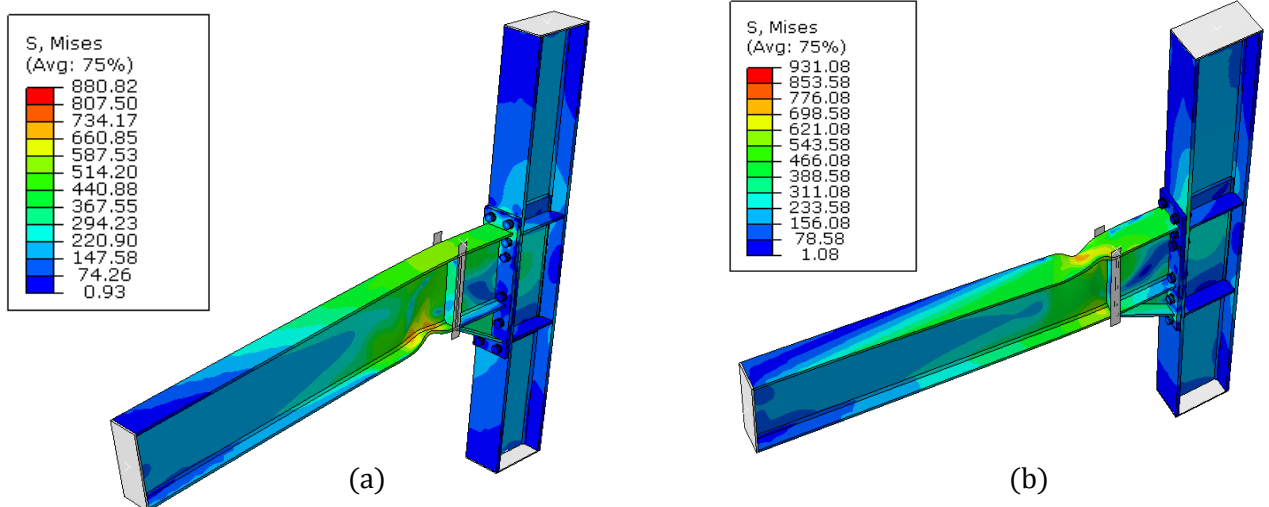
Figure 5.4.1.2.von Mises stresses in models EH3-TD-30-M-S (a) and EH3-TD-30-M-H (b)
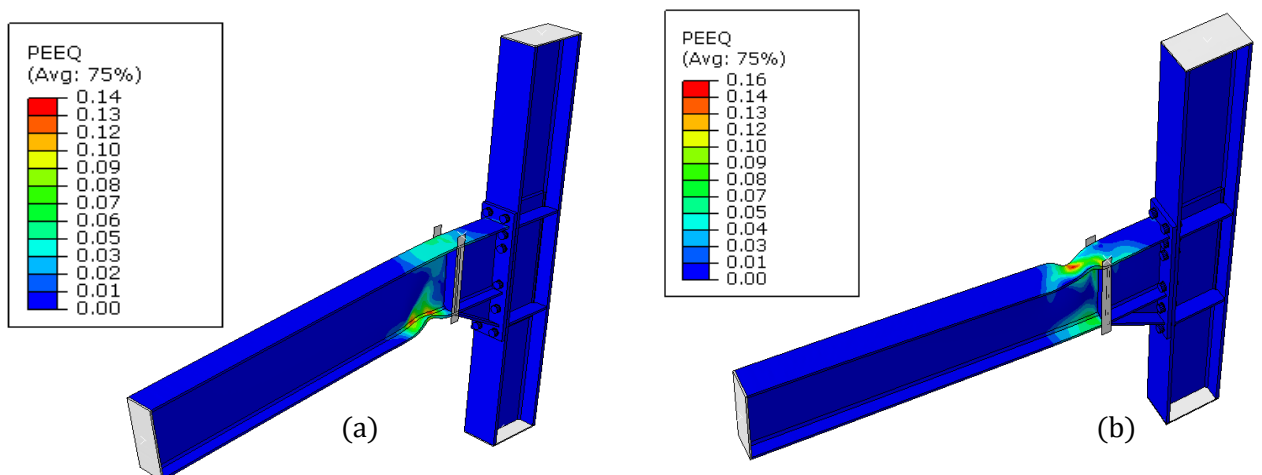
(a)   (b)

Figure 5.4.1.3.Equavalent plastic strain in models EH3-TD-30-M-S (a) and EH3-TD-30-M-H (b)
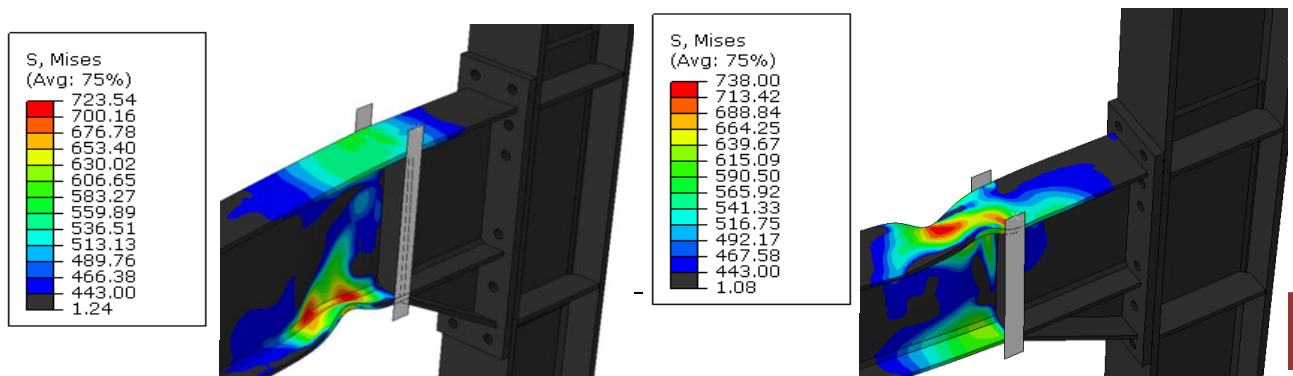
Figure 5.4.1.4. von Mises stresses close up view in models EH3-TD-30-M-S (a) and EH3-TD-30-M-H (b)

(a)   (b)
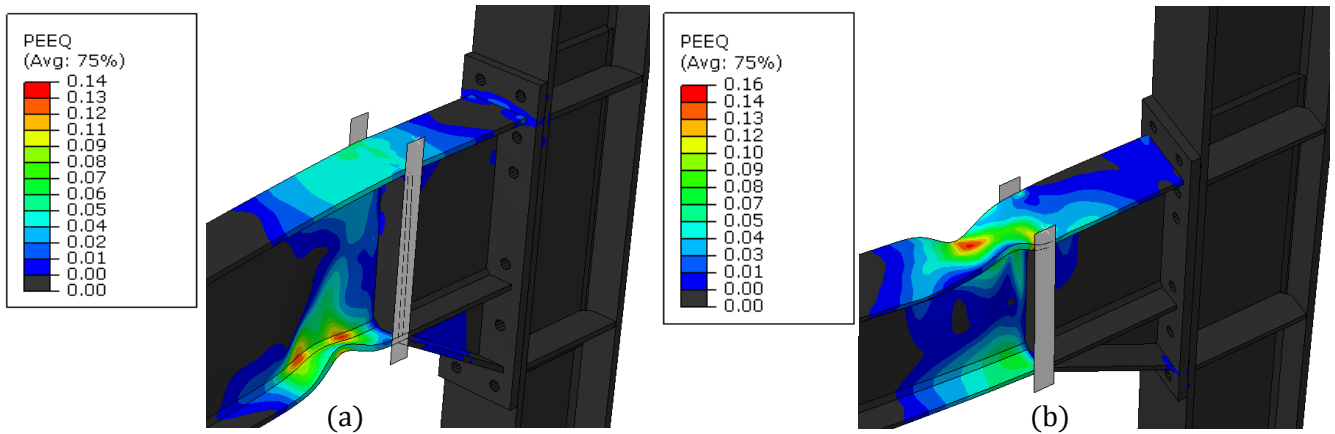
Figure 5.4.1.5. Equivalent plastic strain close up view in models EH3-TD-30-M-S (a) and EH3-TD-30-M-H (b)

(a)   (b)

Figure 5.4.1.6. von Mises stresses of bolts in models EH3-TD-30-M-S (a) and EH3-TD-30-M-H (b)

(a)   (b)

European Erasmus Mundus Master
Sustainable Constructions under natural hazards and catastrophic events
520121-1-2011-1-CZ-ERA MUNDUS-EMMC

surcos
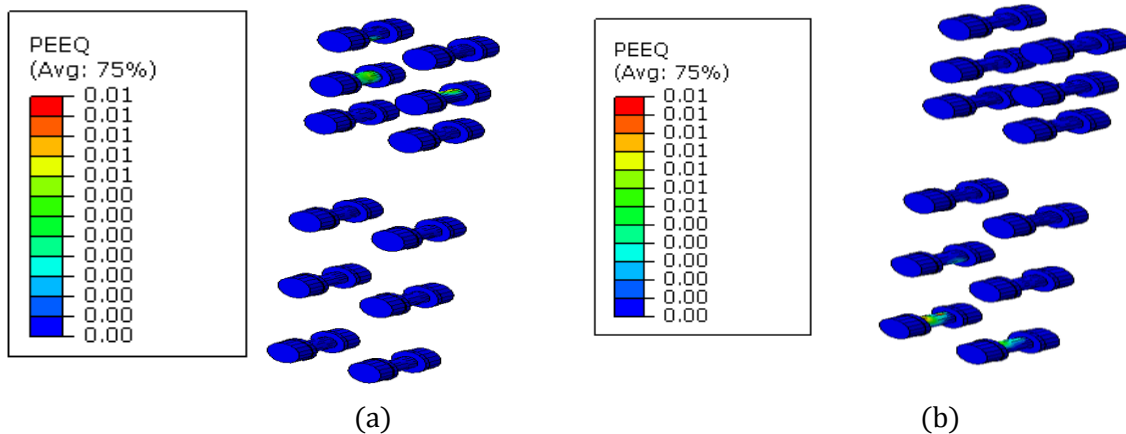
Figure 5.4.1.7. Equivalent plastic strain of bolts in models EH3-TD-30-M-S (a) and EH3-TD-30-M-H (b)

Models: EH3-TD-45-M-S (IPE600-HEB500)   EH3-TD-45-M-H (IPE600-HEB500)

(a)   (b)
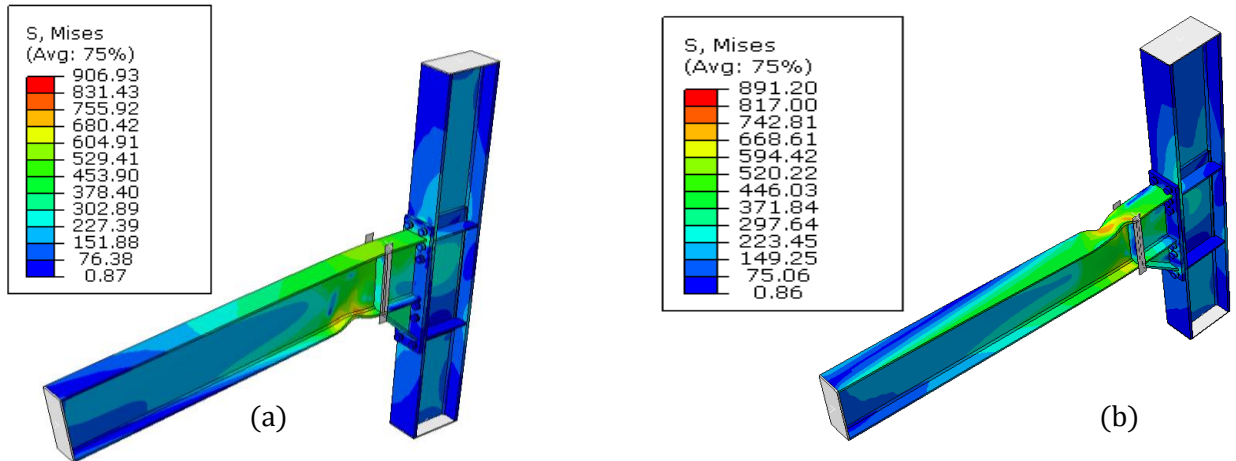
Figure 5.4.1.8. von Mises stresses in models EH3-TD-45-M-S(a) and EH3-TD-45-M-H(b)

(a)   (b)
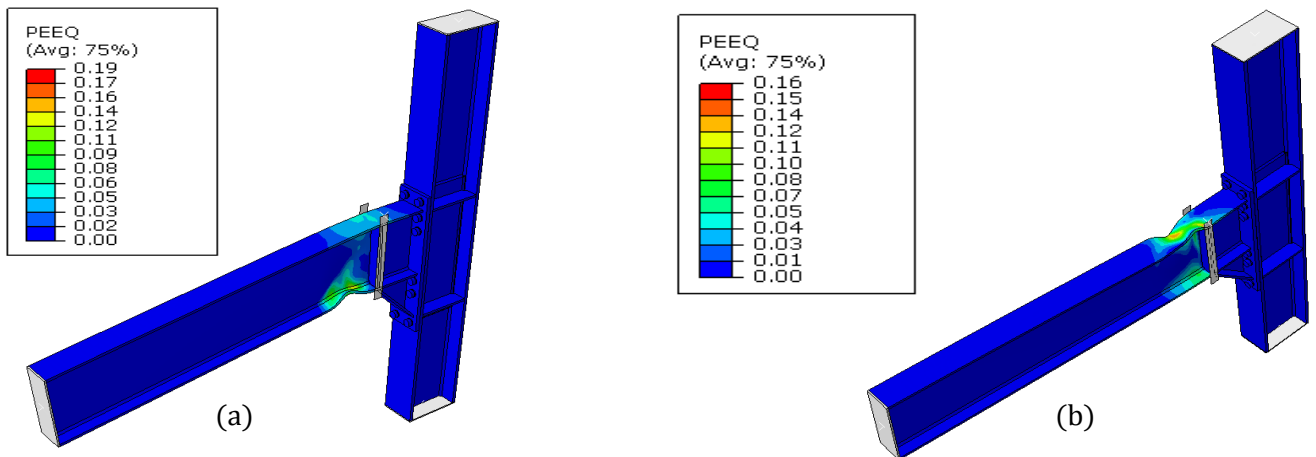
Figure 5.4.1.9. Equivalent plastic strain in mdoels EH3-TD-45-M-S(a) and EH3-TD-45-M-H(b)

(a)   (b)
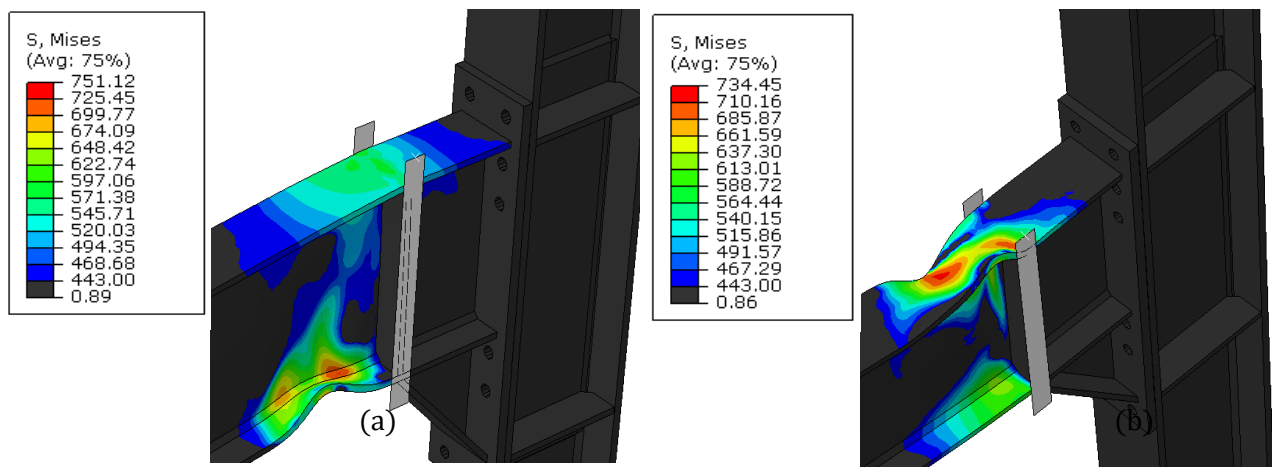
Figure 5.4.1.10. von Mises stresses close of view in models EH3-TD-45-M-S(a) and EH3-TD-45-M-H(b)

European Erasmus Mundus Master
Sustainable Constructions under natural hazards and catastrophic events
520121-1-2011-1-CZ-ERA MUNDUS-EMMC

ᒎᑌᒎᒐᓍᒎ
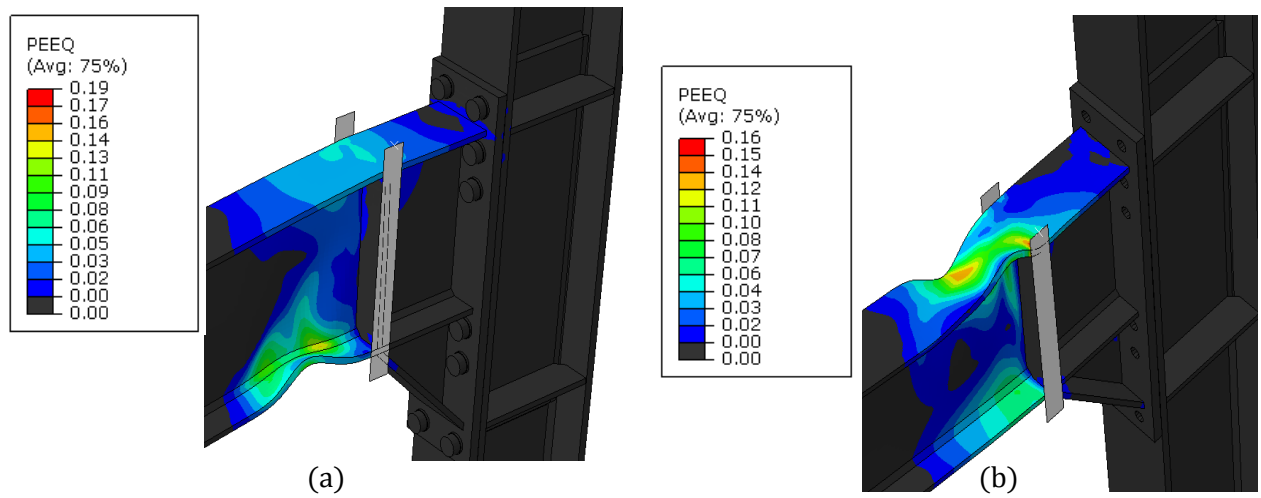
Figure 5.4.1.11.Equivalent plastic strain close up view in models EH3-TD-45-M-S(a) and EH3-TD-45-M-H(b)
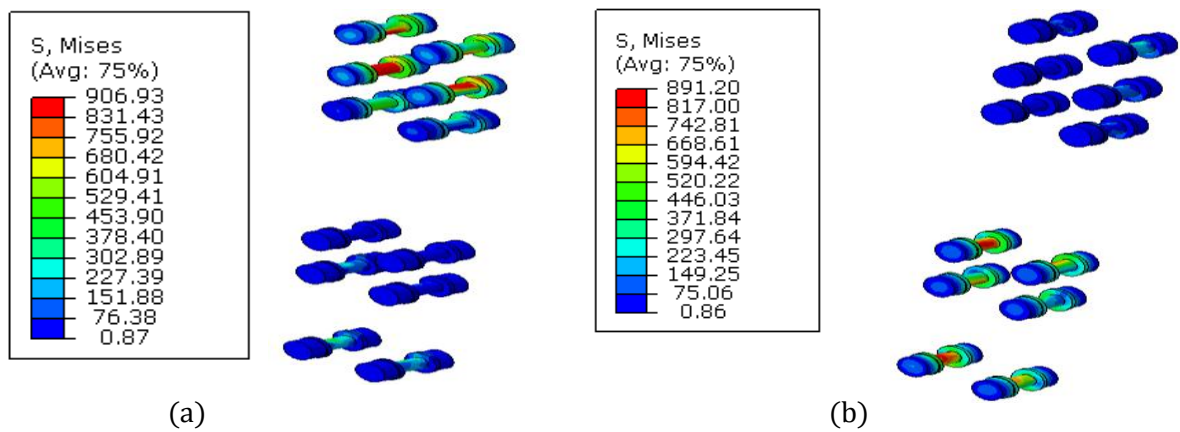
Figure 5.4.1.12.von Mises stresses of bolts in models EH3-TD-45-M-S(a) and EH3-TD-45-M-H(b)
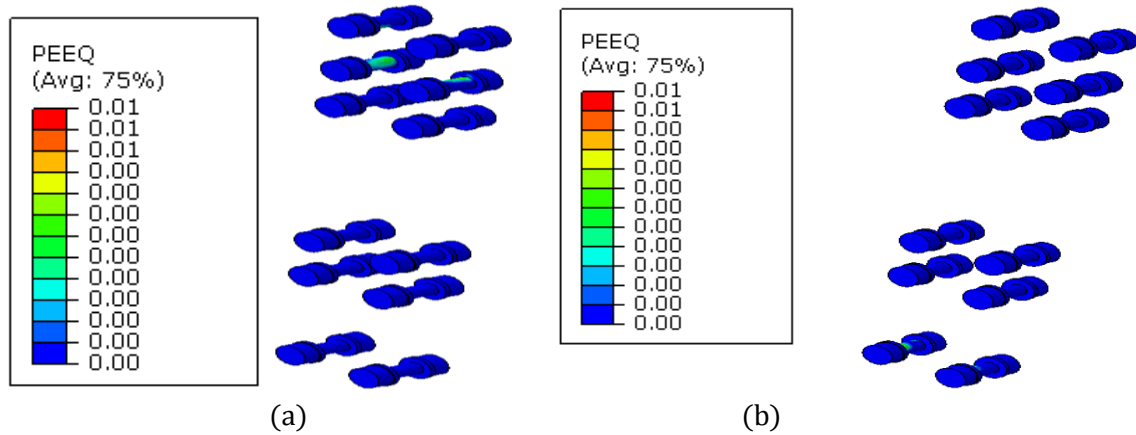
Figure 5.4.1.13. Equivalent plastic strain of bolts in models EH3-TD-45-M-S(a) and EH3-TD-45-M-H(b)

Table 5.4.1.1. von Mises stresses in models EH3-TD-30-M(IPE600-HEB500) and EH3-TD-45-M (IPE600-HEB500)

		von Mises stresses (N/mm²)	
		Group 1	Group 2
		EH3-TD-30-M(IPE600-HEB500)	EH3-TD-45-M(IPE600-HEB500)
Beam	S	723.5	751.1
	H	738.0	734.5
Haunch	S	501.1	453.2
	H	495.0	470.9
Endplate	S	350.0	354.5
	H	355.9	353.3
Bolt	S	880.8	906.9
	H	931.1	891.2
Column	S	343.9	354.5
	H	354.2	347.3

Table 5.4.1.2.Equivalent plastic strain in models EH3-TD-30-M(IPE600-HEB500) and EH3-TD-45-M (IPE600-HEB500)

		Equivalent plastic strain(PEEQ)	
		Group 1	Group 2
		EH3-TD-30-M(IPE600-HEB500)	EH3-TD-45-M(IPE600-HEB500)
Beam	S	0.140	0.187
	H	0.156	0.165
Haunch	S	0.064	0.047
	H	0.064	0.052
Endplate	S	0.020	0.012
	H	0.011	0.007
Bolt	S	0.008	0.006
	H	0.011	0.006
Column	S	0.013	0.011
	H	0.009	0.006

5.4.2   Influence of member size (group 1 and group 2)

The objective of this task is to assess the influence of member size in joints. For numerical analysis total 6 models were chosen from group1; EH1-TS-30-M(IPE360-HEB280),EH2-TS-30-M(IPE450-HEB340),EH3-TS-30-M(IPE600-HEB500)   and   from group 2;   EH1-TS-45-M(IPE360-HEB280),EH2-TS-45-M(IPE450-HEB340),EH3-TS-45-

M(IPE600-HEB500) Both upward and downward displacement were applied corresponds to a magnitude of 0.1rad rotation on the tip of the beam in all models. Expected material properties (f_y= 1.25*355= 443.75MPa) was defined for all parts in the joint except bolts. For bolts (f_y=940MPa) was used. Figure 5.4.2.1 and Figure 5.4.2.2 show the moment-rotation capacity among those models. From the curves we can see moment capacity of joint increases with large section which is quite obvious. During downward displacement moment capacity increases a bit than upward displacement. Strength degradation takes place for higher section of beam IPE600 in both situation of upward and downward displacement, while smaller section of beam IPE 360 does not show any strength degradation in any cases. From Figure 5.4.2.6 and Figure 5.4.2.10, we can see that in higher beam section local buckling takes place at flange. For beam IPE450, strength degradation occurs only in case of upward displacement both for 30 and 45 degree haunch angle.
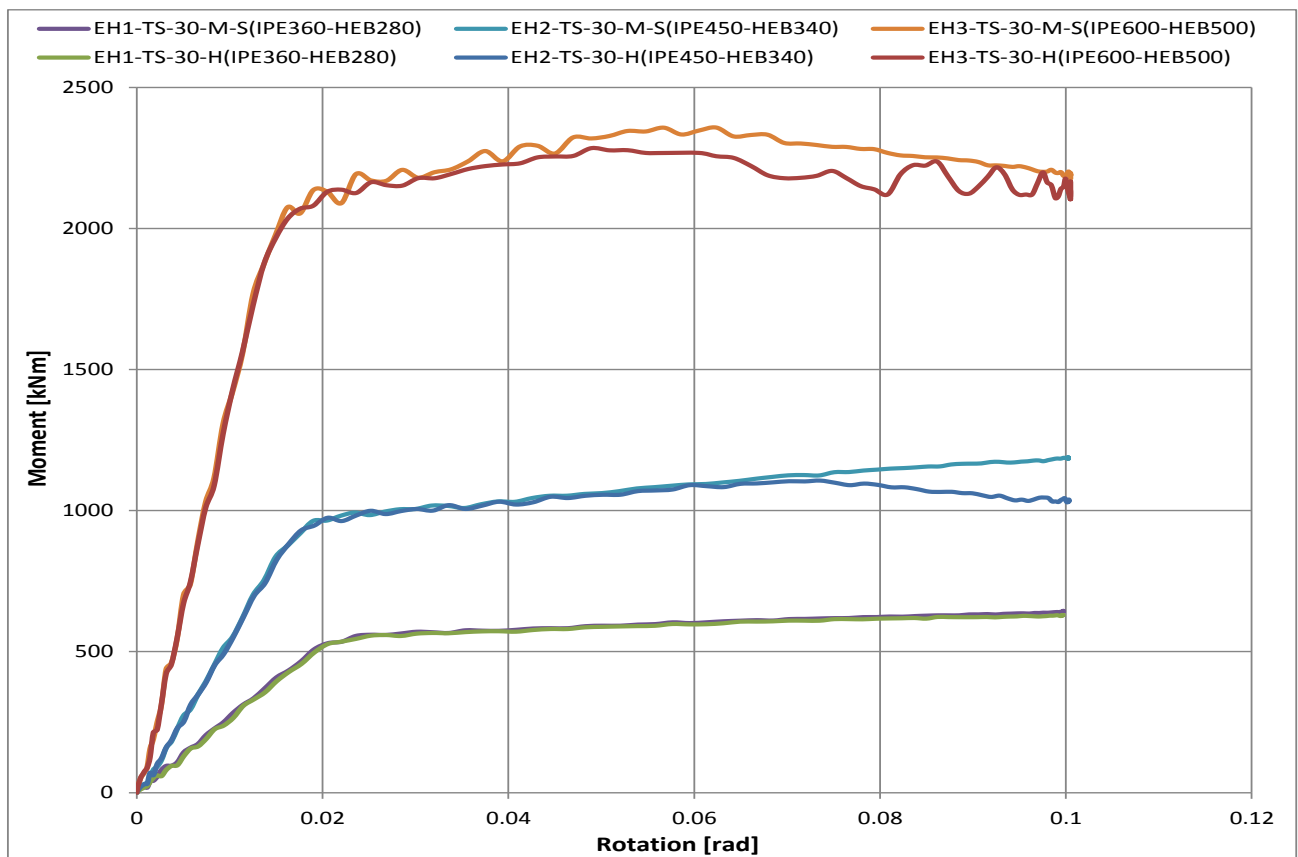
Figure 5.4.2.1.Comparision of moment–rotation among models EH1-TS-30-M-S, EH2-TS-30-M-S, EH3-TS-30-M-S, EH1-TS-30-H, EH2-TS-30-H, EH3-TS-30-H.
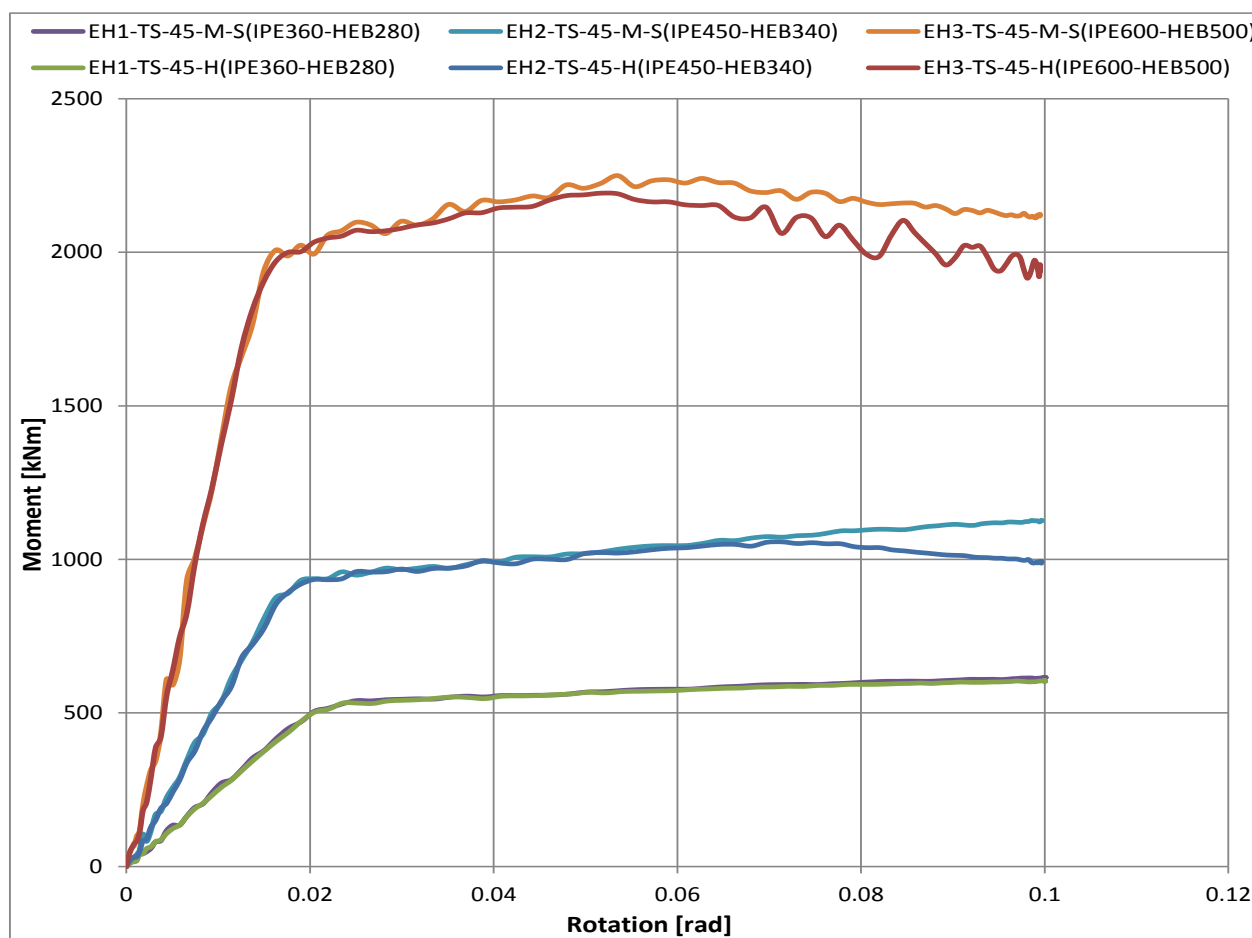
Figure 5.4.2.2. Comparision of moment–rotation among models EH1-TS-45-M-S, EH2-TS-45-M-S, EH3-TS-45-M-S, EH1-TS-45-H, EH2-TS-45-H, EH3-TS-45-H.

Figure 5.4.2.3 presents the von Mises stresses in models EH1-TS-30-M-S(a), EH2-TS-30-M-S(b) and EH3-TS-30-M-S(c).It can be observed that beam flanges and web are exceeding the yield stress near the haunch end. Figure 5.4.2.5 shows von Mises stresses close up view in models EH1-TS-30-M-S(a), EH2-TS-30-M-S(b) and EH3-TS-30-M-S(c). We can clearly see that local buckling takes place in bottom flange of beam IPE600 while other two beams do not show any local buckling. Inside the haunch, top flange of beam facing problem with stresses which are close to yield stress. Figure 5.4.2.4 represents the equivalent plastic strain in models EH1-TS-30-M-S(a), EH2-TS-30-M-S(b) and EH3-TS-30-M-S(c). We can see that plastic strain in the top flange is close to column face and in bottom flange bit away from column face due to downward displacement and almost identical for upward displacement. Figure 5.4.2.6 shows close view of equivalent plastic strain in models. We can see that plastic hinges are formed near to the haunch end. Although in the design procedure it was assumed that plastic hinge forms at the end of the haunch. From the numerical analysis we have found that plastic hinges have occurred at a distance from the end of haunch of 168mm $(0,47h_b)$, 179mm$(0.4h_b)$, 246mm$(0.41h_b)$ for models EH1-TS-30-M-S, EH2-TS-30-M-S, EH3-TS-30-M-S. On the

other hand, plastic hinges form at a distance from the end of haunch of 155mm (0,43h_b), 209mm(0.46h_b), 276mm(0.46h_b) for models EH1-TS-45-M-S, EH2-TS-45-M-S, EH3-TS-45-M-S. In case of upward displacement plastic hinges have occurred at a distance from the end of haunch of 93mm (0,26h_b), 134mm(0.3h_b), 231mm(0.38h_b) for models EH1-TS-30-M-H, EH2-TS-30-M-H, EH3-TS-30-M-H. On the other hand, plastic hinges form at a distance from the end of haunch of 155mm (0,43h_b), 209mm(0.46h_b), 231mm(0.39h_b) for models EH1-TS-45-M-H, EH2-TS-45-M-H, EH3-TS-45-M-H.

Figure 5.4.2.5, Figure 5.4.2.6, Figure 5.4.2.9 and Figure 5.4.2.10 depict the von Mises stresses and equivalent plastic strain close up view in those models.

Due to safety reason, it is not desire to have plastic strain in the non-dissipative parts. Eventually from the analysis we have seen that some portion of the haunch, endplate, column and bolts have plastic strain to the yield limit. So concerning member size, joint performance is adequate. Table 5.4.2.1, Table 5.4.2.2, Table 5.4.2.3 and Table 5.4.2.4 present maximum von Mises stresses and equivalent plastic strain for all the parts in joint.

Models:

EH1-TS-30-M-S(IPE360-HEB280)   EH2-TS-30-M-S(IPE450-HEB340)   EH3-TS-30-M-S(IPE600-HEB500)

(a)   (b)   (c)

Figure 5.4.2.3.von Mises stresses in models EH1-TS-30-M-S(a), EH2-TS-30-M-S(b) and EH3-TS-30-M-S(c)

(a)   (b)   (c)

Figure 5.4.2.4. Equivalent plastic strain in models EH1-TS-30-M-S(a), EH2-TS-30-M-S(b) and EH3-TS-30-M-S(c)

European Erasmus Mundus Master
Sustainable Constructions under natural hazards and catastrophic events
520121-1-2011-1-CZ-ERA MUNDUS-EMMC

ᓚᑌᖇᑕᓍᔕ
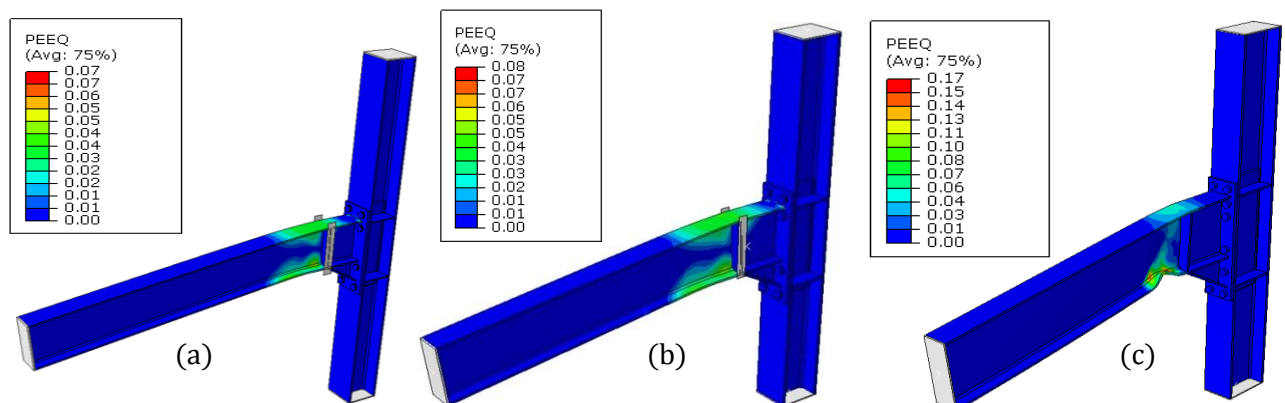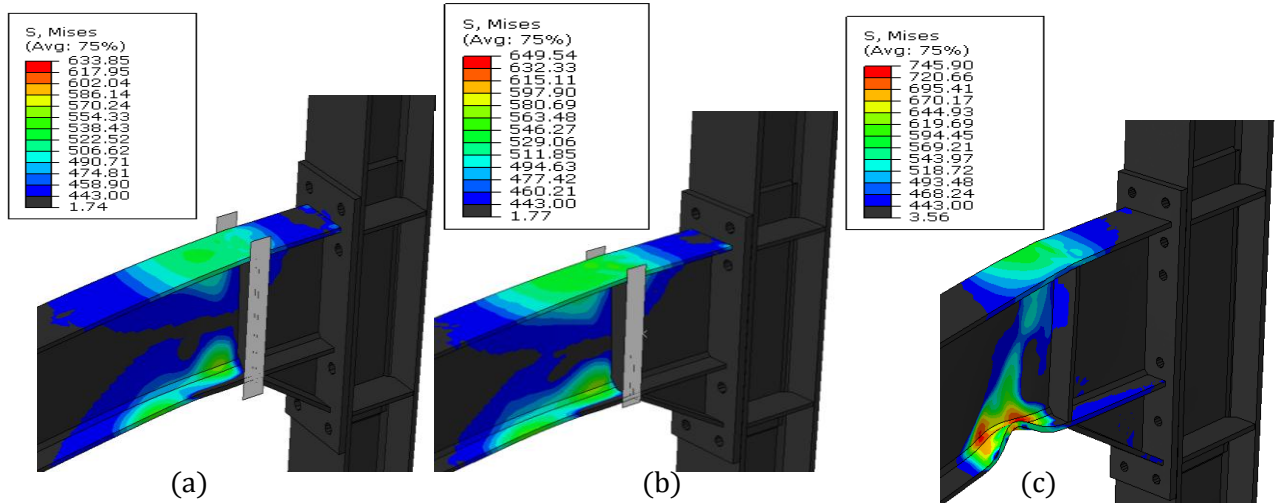
Figure 5.4.2.5. von Mises stresses close of view in models EH1-TS-30-M-S(a), EH2-TS-30-M-S(b) and EH3-TS-30-M-S(c)
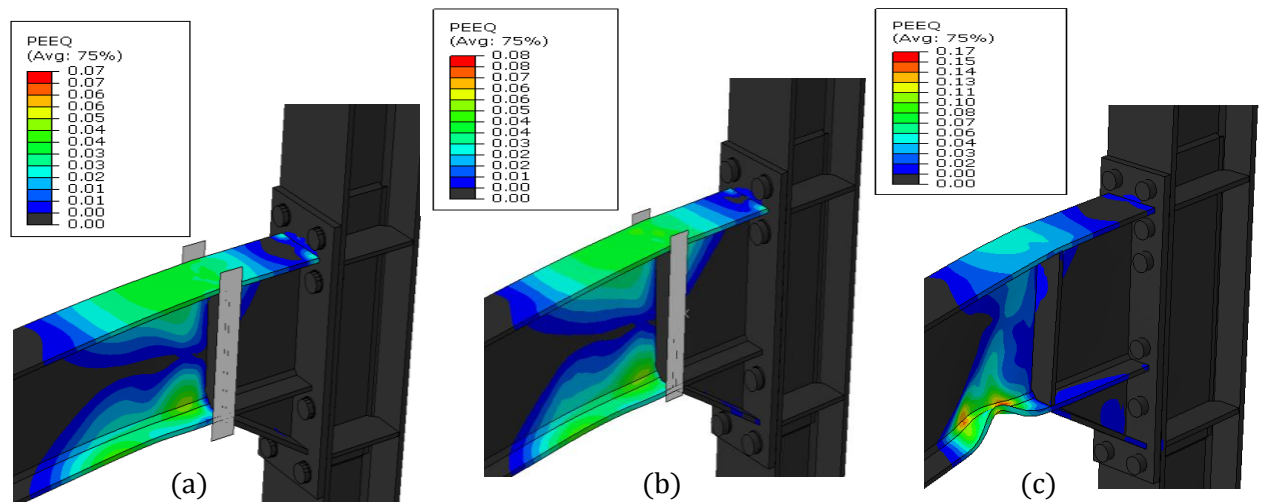
Figure 5.4.2.6. Equivalent plastic strain close up view in models EH1-TS-30-M-S(a), EH2-TS-30-M-S(b) and EH3-TS-30-M-S(c)
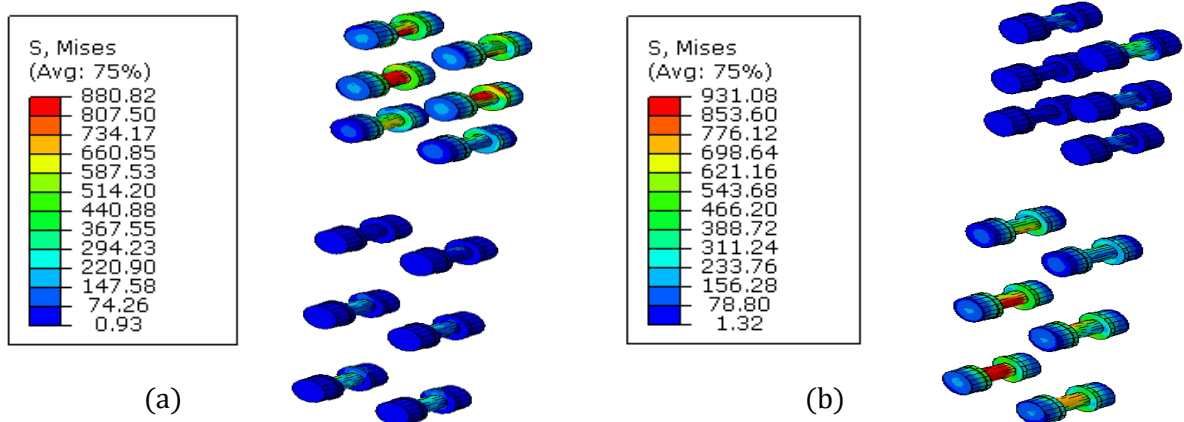
Models:

EH1-TS-30-M-H(IPE360-HEB280)   EH2-TS-30-M-H(IPE450-HEB340)   EH3-TS-30-M-H(IPE600-HEB500)
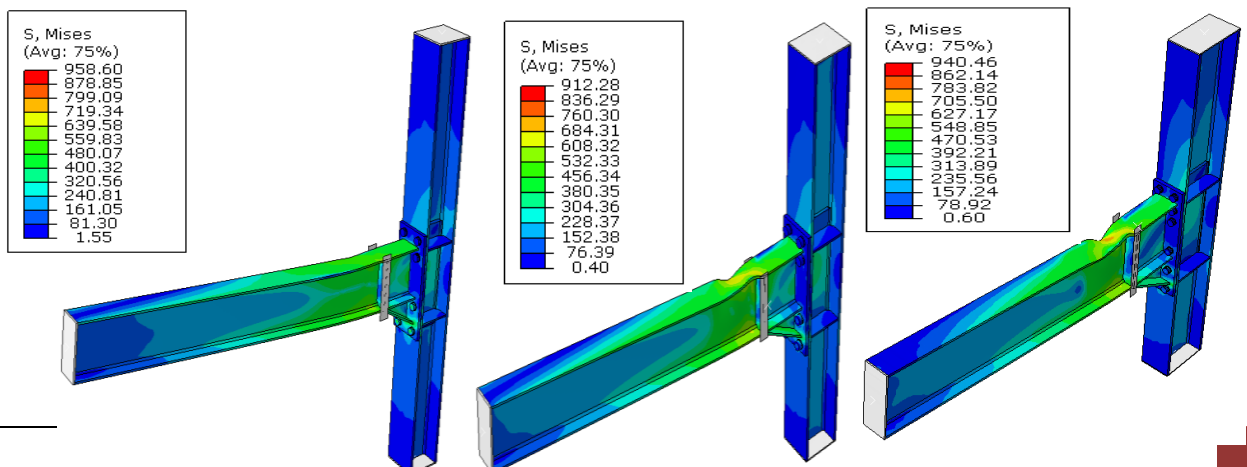
(a)   (b)   (c)

Figure 5.4.2.7.von Mises stresses in models EH1-TS-30-M-H(a), EH2-TS-30-M-H(b) and EH3-TS-30-M-H(c)

(a)   (b)   (c)
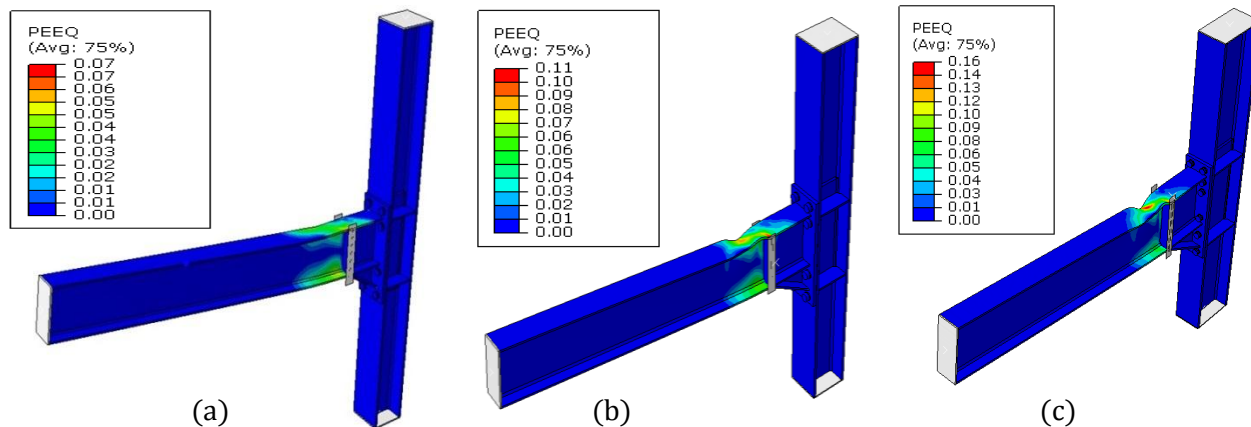
Figure 5.4.2.8 Equivalent plastic strain in models EH1-TS-30-M-H(a), EH2-TS-30-M-H(b) and EH3-TS-30-M-H(c)

(a)   (b)   (c)
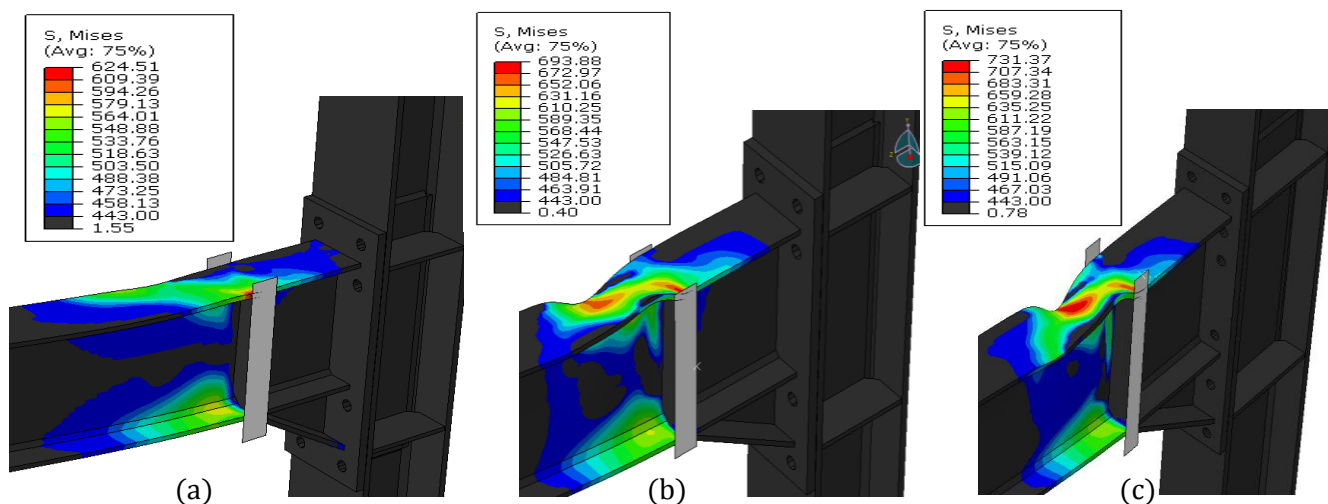
Figure 5.4.2.9.von Mises stresses close up view in models EH1-TS-30-M-H(a), EH2-TS-30-M-H(b) and EH3-TS-30-M-H(c)
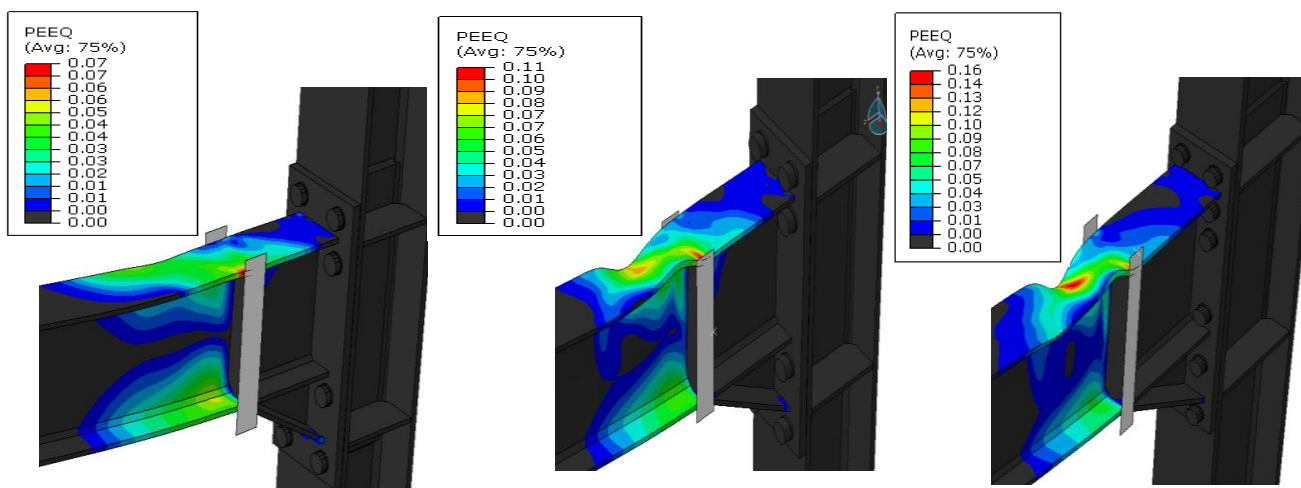
(a)   (b)   (c)

Figure 5.4.2.10. Equivalent plastic strain close up view in models EH1-TS-30-M-H(a), EH2-TS-30-M-H(b) and EH3-TS-30-M-H(c)

Models:

EH1-TS-45-M-S(IPE360-HEB280)   EH2-TS-45-M-S(IPE450-HEB340)   EH3-TS-45-M-S(IPE600-HEB500)
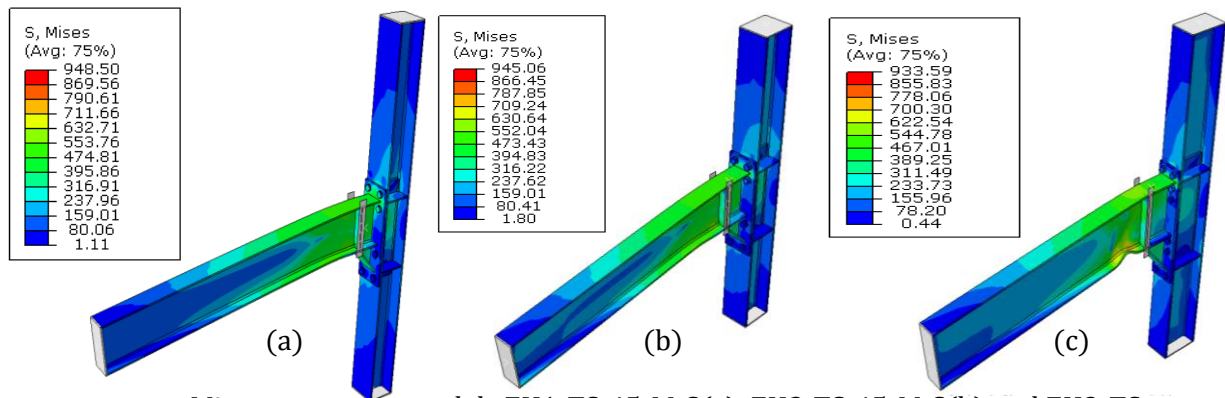
Figure 5.4.2.11. von Mises stresses in models EH1-TS-45-M-S(a), EH2-TS-45-M-S(b) and EH3-TS-45-M-S(c)
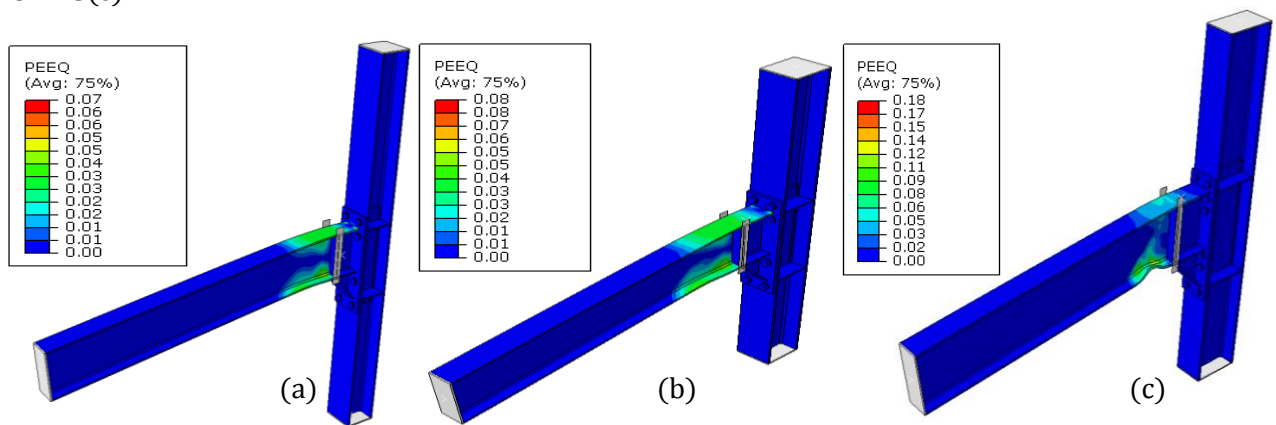
Figure 5.4.2.12. Equivalent plastic strain in models EH1-TS-45-M-S(a), EH2-TS-45-M-S(b) and EH3-TS-45-M-S(c)

European Erasmus Mundus Master
Sustainable Constructions under natural hazards and catastrophic events
520121-1-2011-1-CZ-ERA MUNDUS-EMMC

 รบโตอร
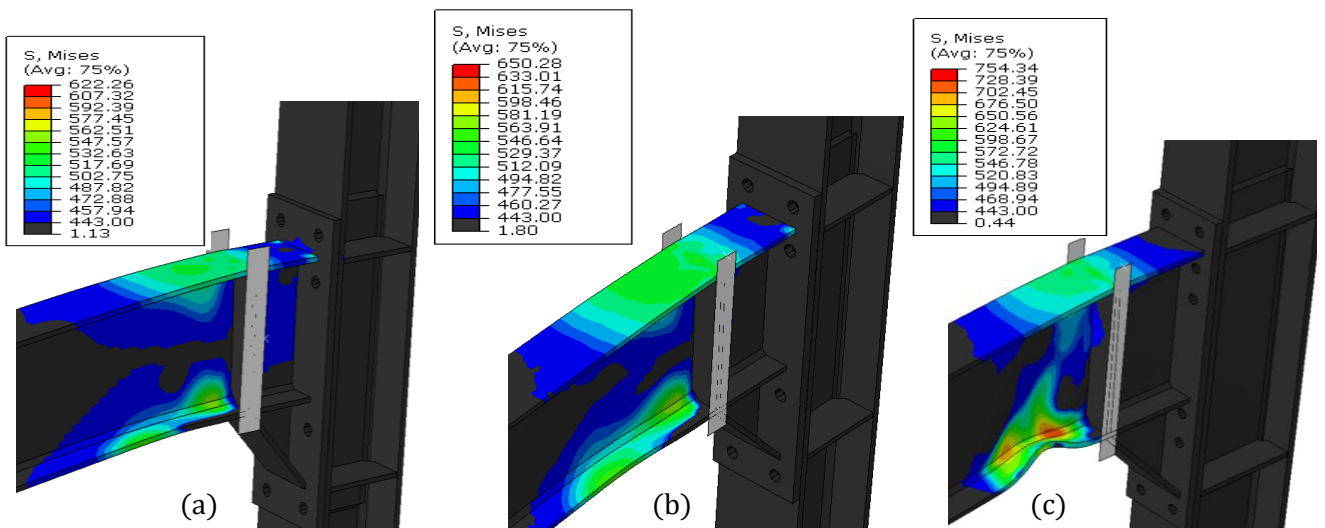
Figure 5.4.2.13.von Mises stresses close up view in models EH1-TS-45-M-S(a), EH2-TS-45-M-S(b) and EH3-TS-45-M-S(c)

(a)　　　　　　　　(b)　　　　　　　　(c)
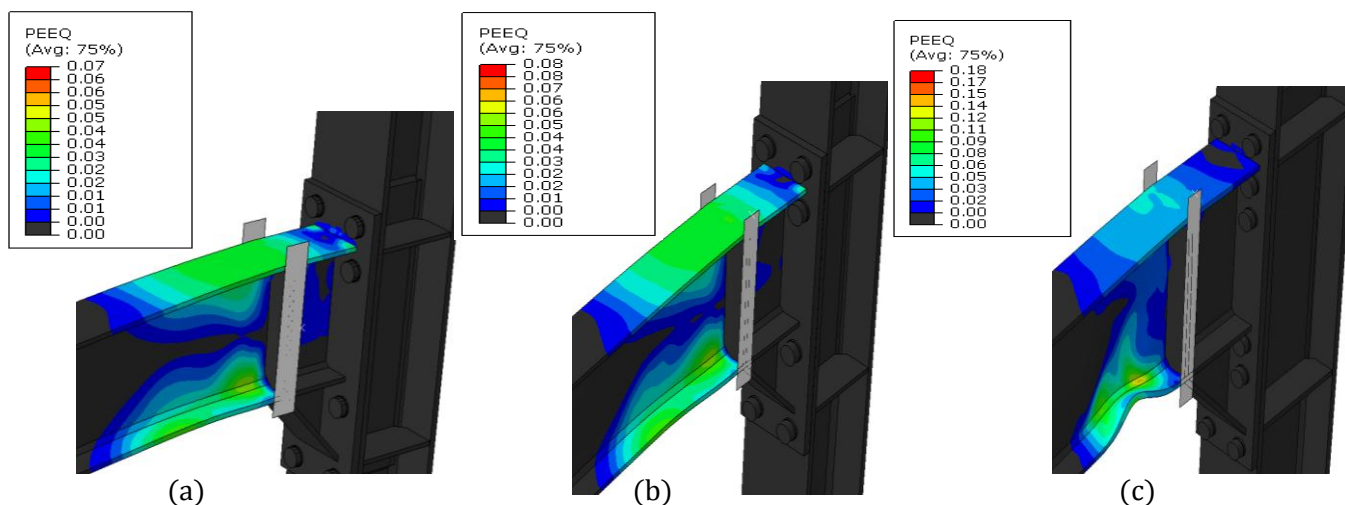
Figure 5.4.2.14.Equivalent plastic strain close up view in models EH1-TS-45-M-S(a), EH2-TS-45-M-S(b) and EH3-TS-45-M-S(c)

Models:

EH1-TS-45-M-H(IPE360-HEB280)　　EH2-TS-45-M-H(IPE450-HEB340)　　EH3-TS-45-M-H(IPE600-HEB500)

(a)　　　　　　　　(b)　　　　　　　　(c)
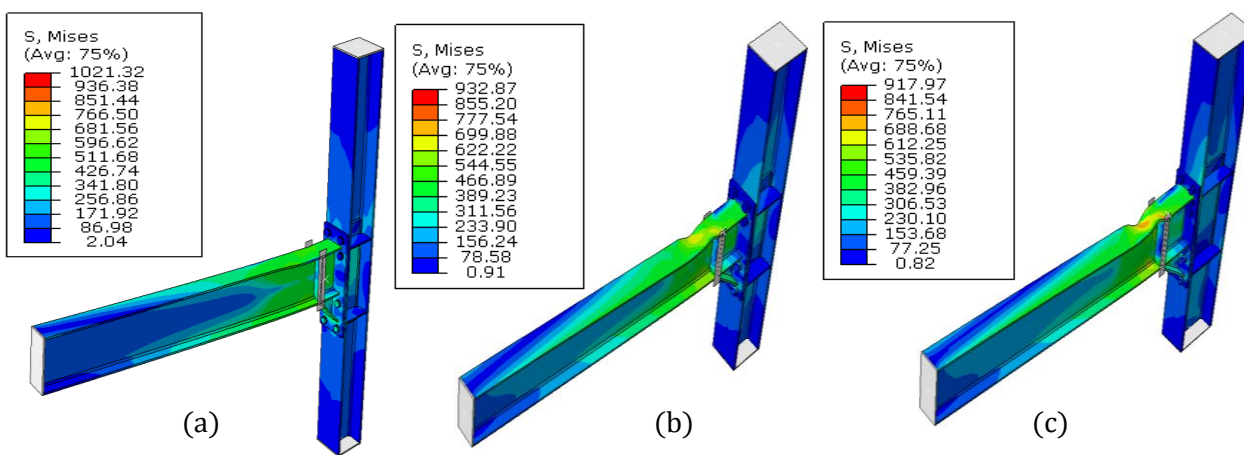
Figure 5.4.2.15.von Mises stresses in models EH1-TS-45-M-H(a), EH2-TS-45-M-H(b) and EH3-TS-45-M-H(c)

(a)　　　　　　　　(b)　　　　　　　　(c)
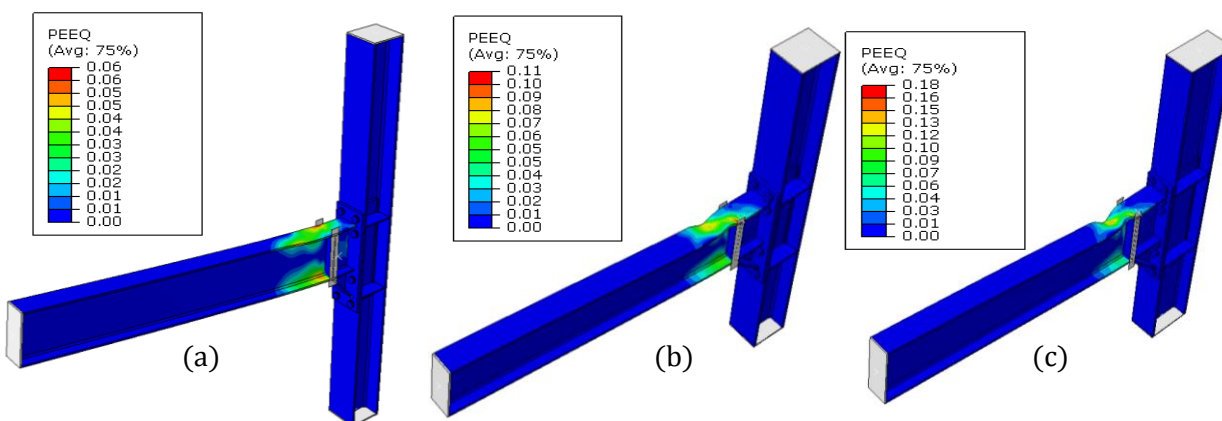
Figure 5.4.2.16. Equivalent plastic strain in models EH1-TS-45-M-H(a), EH2-TS-45-M-H(b) and EH3-TS-45-M-H(c)

(a) (b) (c)
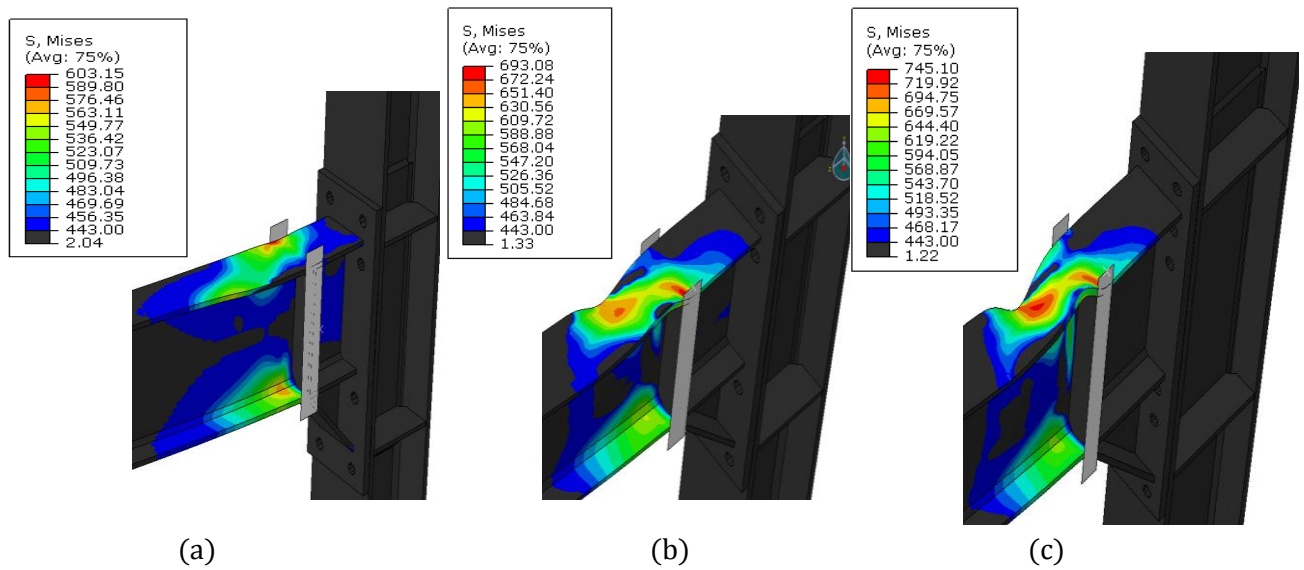
Figure 5.4.2.17. von Mises stresses close up view in models EH1-TS-45-M-H(a), EH2-TS-45-M-H(b) and EH3-TS-45-M-H(c)

(a) (b) (c)
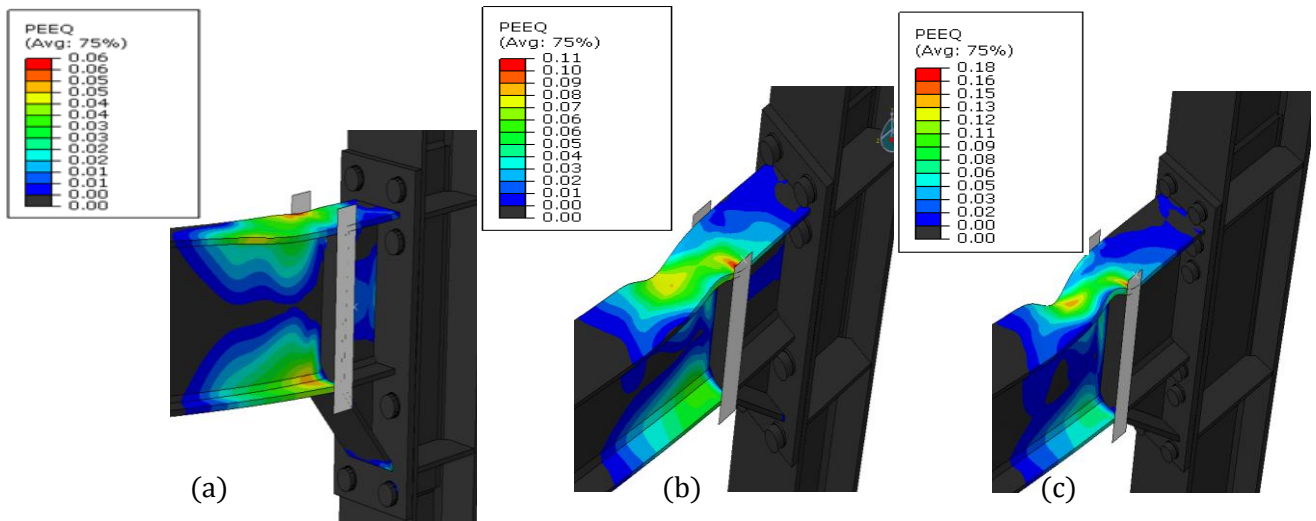
Figure 5.4.2.18. Equivalent plastic strain close up view in models EH1-TS-45-M-H(a), EH2-TS-45-M-H(b) and EH3-TS-45-M-H(c)

Table 5.4.2.1. von Mises stresses in models EH1-TS-30-M(IPE360-HEB280), EH2-TS-30-M(IPE450-HEB340) and EH3-TS-30-M(IPE600-HEB500)

	Von Mises stresses (N/mm²)		
	Group 1		
	EH1-TS-30-M(IPE360-HEB280)	EH2-TS-30-M(IPE450-HEB340)	EH3-TS-30-M(IPE600-HEB500)
S	633.9	649.5	765.1
H	624.5	693.9	731.4
S	527.3	518.5	611.8
H	487.1	506.3	598.1
S	444.6	444.5	428.9
H	444.9	429.7	433.9
S	947.6	952.3	919.3
H	958.6	912.3	940.5
S	443.9	442.9	441.5
H	443.4	438.9	436.1

Table 5.4.2.2. von Mises stresses in models EH1-TS-45-M(IPE360-HEB280), EH2-TS-45-M(IPE450-HEB340) and EH3-TS-45-M(IPE600-HEB500)

		von Mises stresses (N/mm²)		
		Group 2		
		EH1-TS-45-M(IPE360-HEB280)	EH2-TS-45-M(IPE450-HEB340)	EH3-TS-45-M(IPE600-HEB500)
Beam	S	622.3	650.3	754.3
	H	603.2	693.1	745.1
Haunch	S	598.3	476.1	545.5
	H	585.0	461.8	559.5
Endplate	S	447.1	441.0	439.3
	H	442.8	427.5	434.1
Bolt	S	948.5	945.1	933.6
	H	1021.3	932.9	918.0
Column	S	445.4	441.2	442.5
	H	445.0	441.4	431.2

Table 5.4.2.3. Equivalent plastic strain in models EH1-TS-30-M(IPE360-HEB280), EH2-TS-30-M(IPE450-HEB340) and EH3-TS-30-M(IPE600-HEB500)
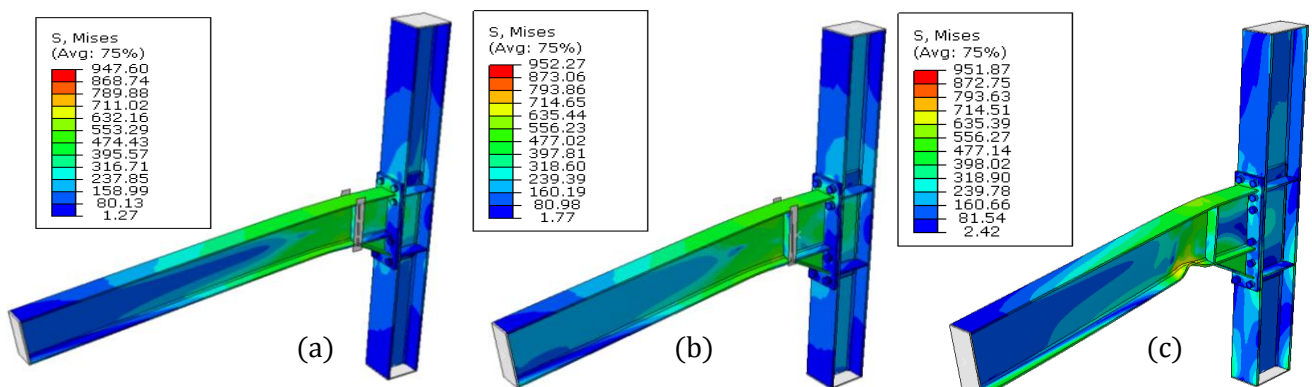
		Equivalent plastic strain (PEEQ)		
		Group 1		
		EH1-TS-30-M(IPE360-HEB280)	EH2-TS-30-M(IPE450-HEB340)	EH3-TS-30-M(IPE600-HEB500)
Beam	S	0.073	0.082	0.202
	H	0.073	0.110	0.155
Haunch	S	0.037	0.034	0.064
	H	0.027	0.031	0.058
Endplate	S	0.009	0.011	0.004
	H	0.008	0.007	0.006
Bolt	S	0.006	0.004	0.004
	H	0.009	0.008	0.010
Column	S	0.009	0.008	0.005
	H	0.010	0.006	0.006

Table 5.4.2.4. Equivalent plastic strain in models EH1-TS-45-M(IPE360-HEB280), EH2-TS-45-M(IPE450-HEB340) and EH3-TS-45-M(IPE600-HEB500)

		Equivalent plastic strain (PEEQ)		
		Group 2		
		EH1-TS-45-M(IPE360-HEB280)	EH2-TS-45-M(IPE450-HEB340)	EH3-TS-45-M(IPE600-HEB500)
Beam	S	0.069	0.082	0.185
	H	0.060	0.110	0.179
Haunch	S	0.060	0.024	0.043
	H	0.054	0.020	0.046
Endplate	S	0.011	0.008	0.005
	H	0.004	0.001	0.005
Bolt	S	0.003	0.004	0.003
	H	0.034	0.006	0.005
Column	S	0.008	0.006	0.005
	H	0.009	0.004	0.003

5.4.3 Influence of haunch geometry (group 1 vs group 2)

The objective of this study is to assess the influence of haunch geometry in joints. For numerical analysis total 6 models were chosen from group1; EH1-TS-30-M(IPE360-HEB280),EH2-TS-30-M(IPE450-HEB340),EH3-TS-30-M(IPE600-HEB500)   and   from

group 2; EH1-TS-45-M(IPE360-HEB280),EH2-TS-45-M(IPE450-HEB340),EH3-TS-45-M(IPE600-HEB500) Both upward and downward displacement were applied corresponds to a magnitude of 0.1rad rotation on the tip of the beam in all models. Expected material properties (f_y= 1.25*355= 443.75MPa) was defined for all parts in the joint except bolts. For bolts (f_y=940MPa) was used. Figure 5.4.3.1, Figure 5.4.3.2 and Figure 5.4.3.3 show the moment-rotation capacity among those models. From the curves we can see that moment capacity of joint increases with 30 degree haunch than 45 degree angle of haunch. In fact 30 degree angle provides larger haunch length. Strength degradation takes place for higher section of beam IPE600 in both situation of 30 & 45 degree angle haunch, while smaller section of beam IPE 360 does not show any strength degradation in any cases. From Figure 5.4.3.14 and Figure 5.4.3.26, we can see that in higher beam section IPE600 local buckling takes place at flange. For beam IPE450, Figure 5.4.3.22 shows strength degradation only in case of upward displacement both for 30 and 45 degree haunch angle. The elastic yield moment capacity is very close to each other for every model.
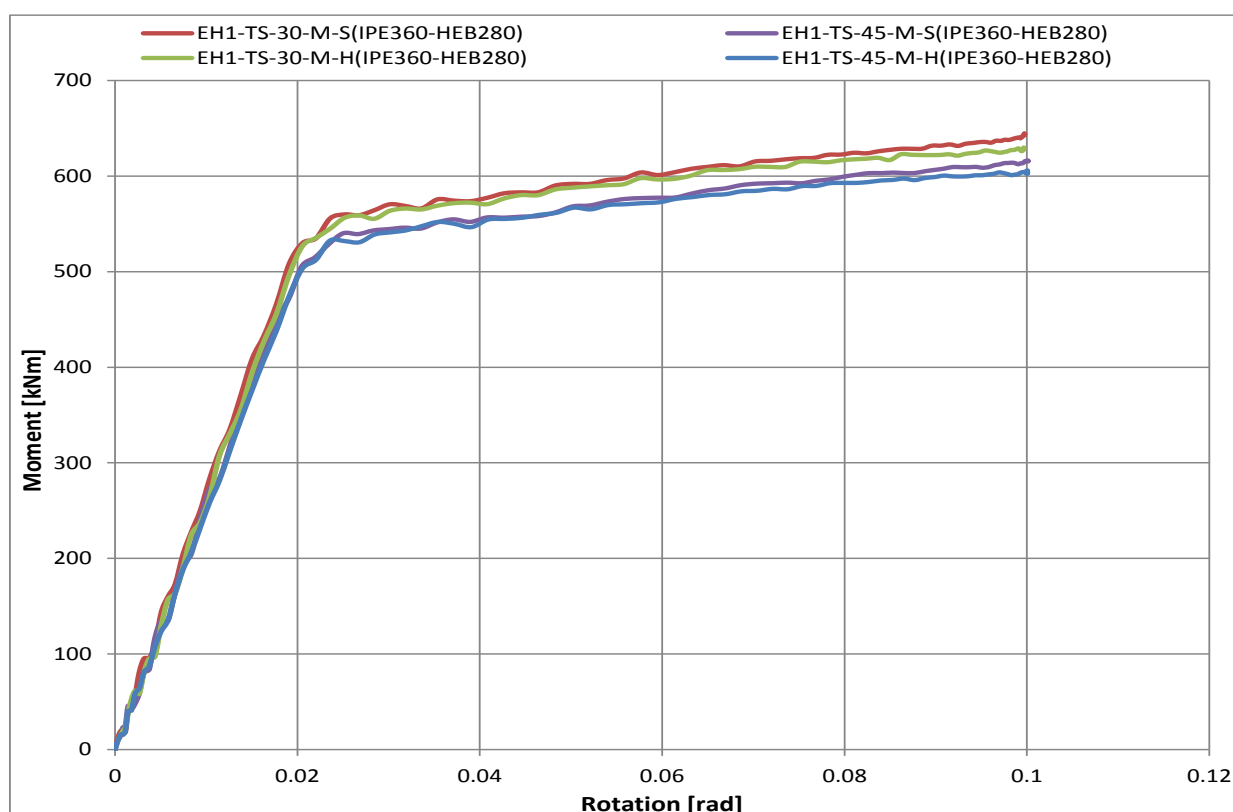
Figure 5.4.3.1.Comparision of moment-rotation among models EH1-TS-30-M-S, EH1-TS-30-M-H, EH1-TS-45-M-S, and EH1-TS-45-M-H.
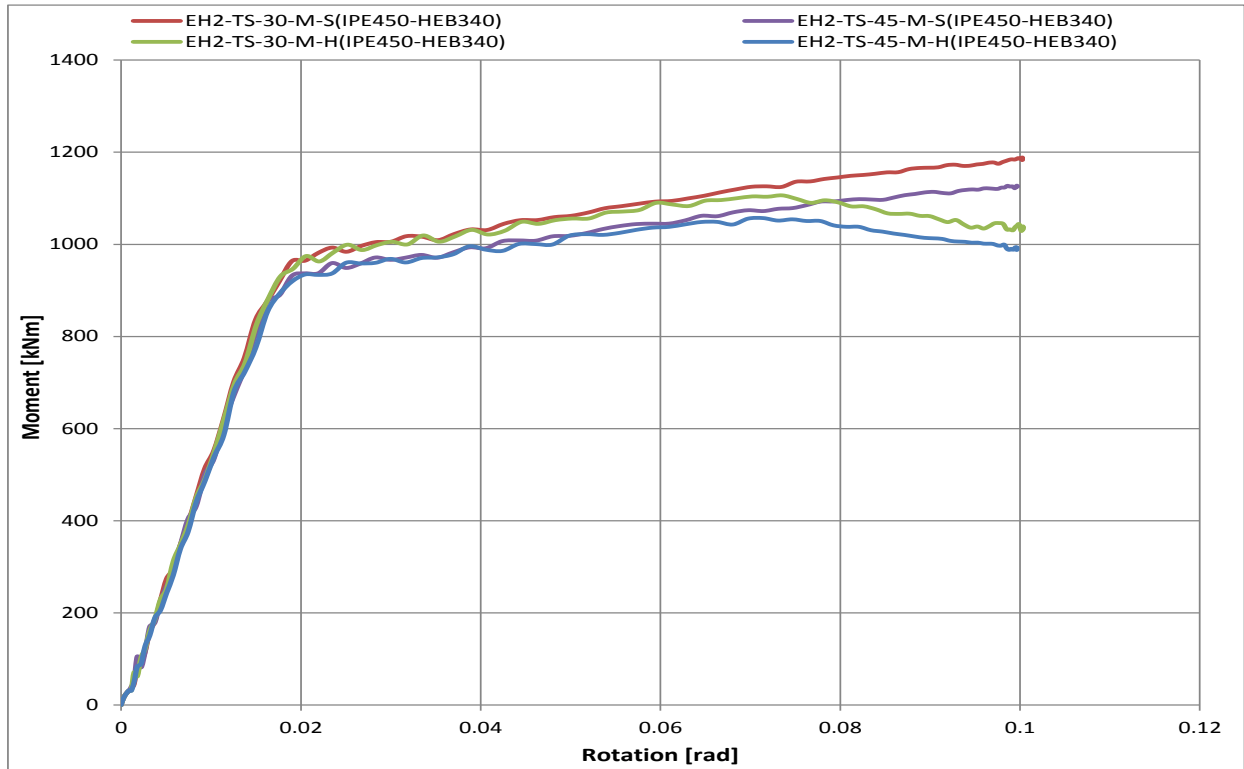
Figure 5.4.3.2. Comparision of moment-rotation among models EH2-TS-30-M-S, EH2-TS-30-M-H, EH2-TS-45-M-S, and EH2-TS-45-M-H.
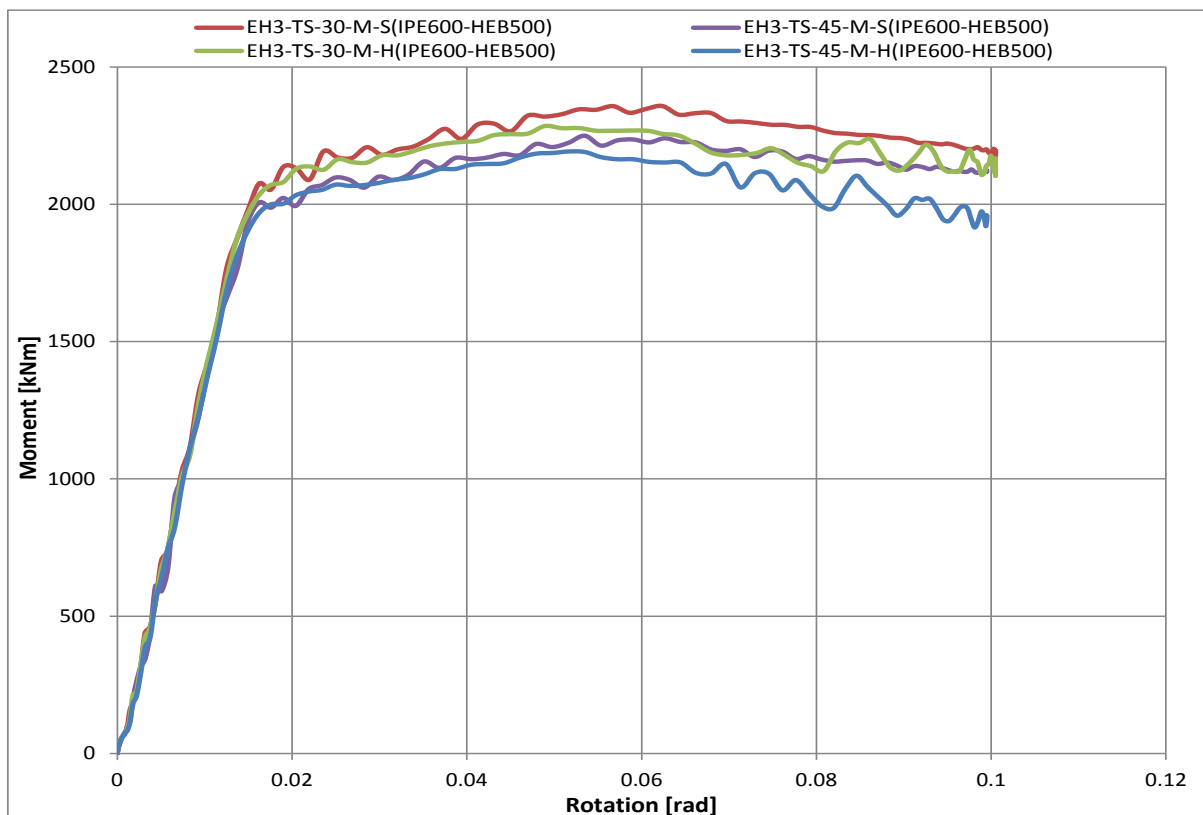
Figure 5.4.3.3. Comparision of moment-rotation among models EH3-TS-30-M-S, EH3-TS-30-M-H, EH3-TS-45-M-S, and EH3-TS-45-M-H.

Figure 5.4.3.4 presents the von Mises stresses in models EH1-TS-30-M-S(a) and EH1-TS-45-M-S(b).It can be observed that beam flanges and web are exceeding the yield stress near the haunch end. Figure 5.4.3.6 shows von Mises stresses close up view in models EH1-TS-30-M-S(a) and EH1-TS-45-M-S(b). Figure 5.4.3.11 shows equivalent plastic strain in models EH2-TS-30-S(a) and EH2-TS-45-S(b) where we can't see any local buckling in beam flange. From Figure 5.4.3.22, We can clearly see that local buckling takes place in upper flange of beam IPE450. Inside the haunch, top flange of beam facing problem with stresses which are close to yield stress. Figure 5.4.3.23 represents the equivalent plastic strain in models EH2-TS-30-M-H(a) and EH2-TS-30-M-S(b). Figure 5.4.3.15 shows close view of equivalent plastic strain in models EH3-TS-30-M-S(a) and EH3-TS-45-M-S(b). From Figure 5.4.3.15 and Figure 5.4.3.27, we can see that plastic strain in the top flange is close to column face and in bottom flange bit away from column face due to downward displacement and almost identical for upward displacement. As we know that assumption for design procedure was to consider plastic hinge formation at the end of the haunch but we have found from the analysis that plastic hinges have occurred at a distance from the end of haunch of 168mm (0,47h_b) and 155mm(0.43h_b) for models EH1-TS-30-M-S, EH1-TS-45-M-S; 179mm (0,4h_b) and 209mm(0.46h_b) for models EH2-TS-30-M-S and EH2-TS-45-M-S; 246mm(0.41h_b) and 276mm(0.46h_b) for models EH3-TS-30-M-S and EH3-TS-45-M-S; 93mm(0.26h_b) and 155mm(0.43h_b) for models EH1-TS-30-M-H, EH1-TS-45-M-H; 134mm(0.3h_b) and 209mm(0.46h_b) for models EH2-TS-30-M-H, EH2-TS-45-M-H; 231mm(0.38h_b) and 230mm(0.38h_b) for models EH3-TS-30-M-H, EH3-TS-45-M-H

Figure 5.4.3.14, Figure 5.4.3.15, Figure 5.4.3.26 and Figure 5.4.3.27 depict the von Mises stresses and equivalent plastic strain close up view in those models.

Due to safety reason, it is not desire to have plastic strain in the non-dissipative parts. Eventually from the analysis we have seen that some portion of the haunch, endplate, column and bolts have plastic strain to the yield limit. So concerning haunch angle, joint performance is adequate. Table 5.4.3.1 and Table 5.4.3.2 present maximum von Mises stresses and equivalent plastic strain for all the parts in joint.

Models:

EH1-TS-30-M-S(IPE360-HEB280)   EH1-TS-45-M-S(IPE360-HEB280)

European Erasmus Mundus Master
Sustainable Constructions under natural hazards and catastrophic events
520121-1-2011-1-CZ-ERA MUNDUS-EMMC

ᓱᓯᒧᓯ
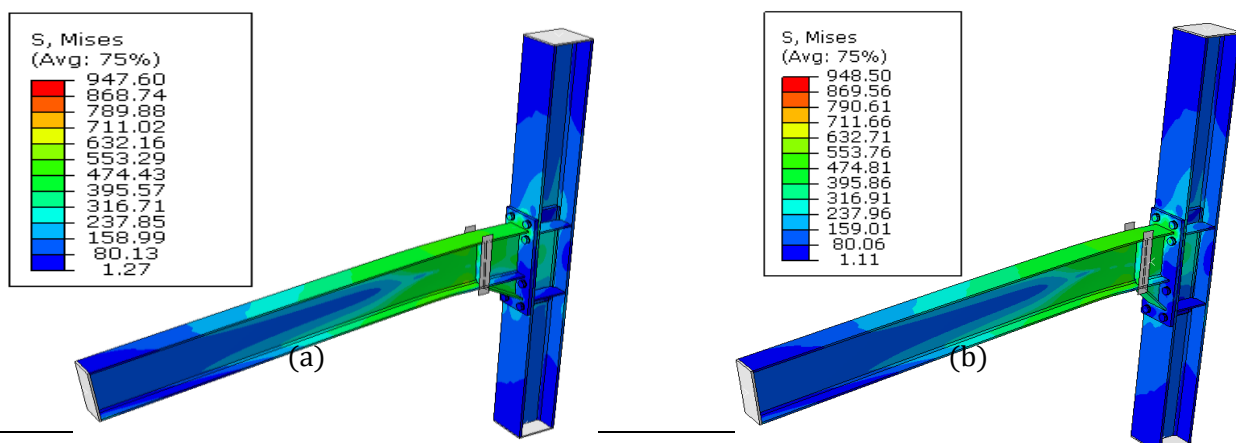
Figure 5.4.3.4.von Mises stresses in models EH1-TS-30-M-S(a) and EH1-TS-45-M-S(b)

(a)   (b)
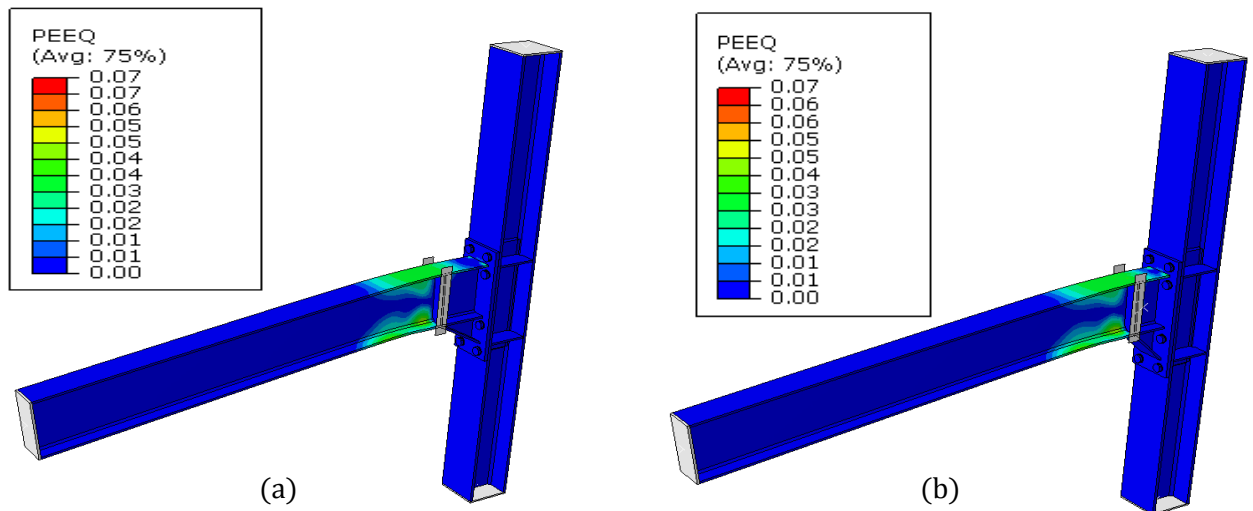
Figure 5.4.3.5.Equivalent plastic strain in models EH1-TS-30-M-S(a) and EH1-TS-45-M-S(b)

(a)   (b)

Figure 5.4.3.6.von Mises stresses close up view in models EH1-TS-30-M-S(a) and EH1-TS-45-M-S(b)

(a)   (b)

Figure 5.4.3.7.Equivalent plastic strain close up view in models EH1-TS-30-M-S(a) and EH1-TS-45-M-S(b)

Models:

EH2-TS-30-M-S(IPE450-HEB340)   EH2-TS-45-M-S(IPE450-HEB340)

(a)   (b)
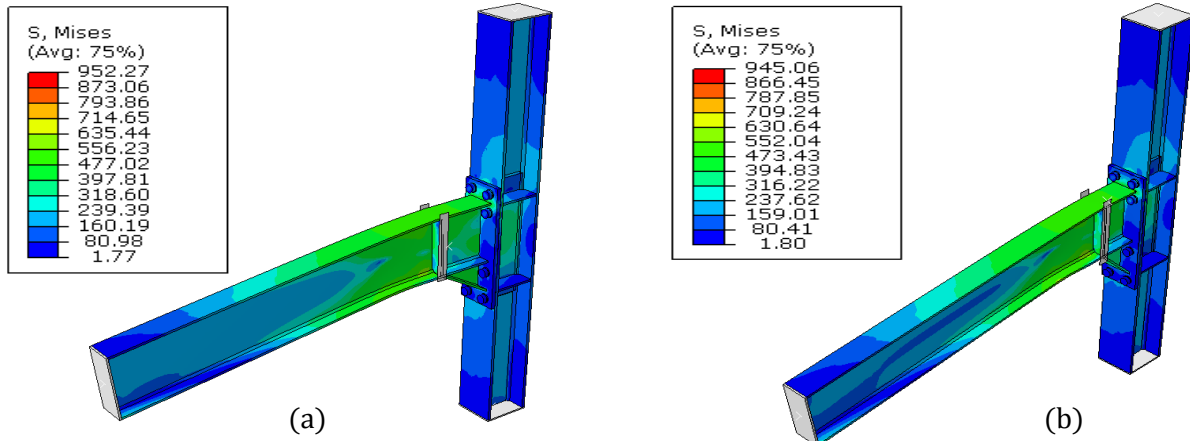
Figure 5.4.3.8.von Mises stresses in models EH2-TS-30-M-S(a) and EH2-TS-45-M-S(b)

(a)   (b)
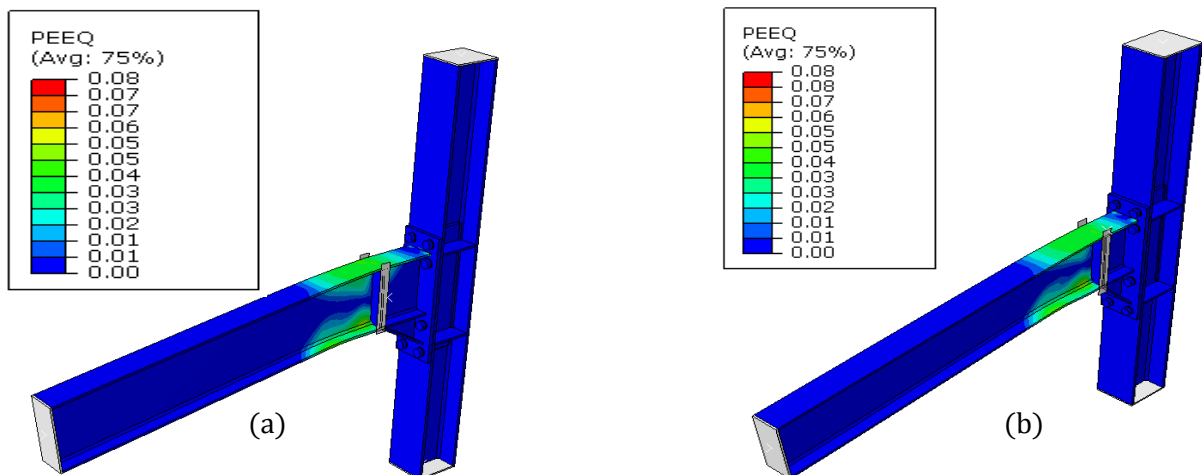
Figure 5.4.3.9.Equivalent plastic strain in models EH2-TS-30-M-S(a) and EH2-TS-45-M-S(b)

(a)   (b)

European Erasmus Mundus Master
Sustainable Constructions under natural hazards and catastrophic events
520121-1-2011-1-CZ-ERA MUNDUS-EMMC

รนรcอร

Figure 5.4.3.10.von Mises stresses close up view in models EH2-TS-30-M-S(a) and EH2-TS-45-M-S(b)

(a)   (b)

Figure 5.4.3.11.Equivalent plastic strain close up view in models EH2-TS-30-M-S(a) and EH2-TS-45-M-S(b)

Models:

EH3-TS-30-M-S(IPE600-HEB500)   EH3-TS-45-M-S(IPE600-HEB500)

(a)   (b)

Figure 5.4.3.12.von Mises stresses in models EH3-TS-30-M-S(a) and EH3-TS-45-M-S(b)

Figure 5.4.3.13. Equivalent plastic strain in models EH3-TS-30-M-S(a) and EH3-TS-45-M-S(b)

Figure 5.4.3.14. von Mises stresses close up view in models EH3-TS-30-M-S(a) and EH3-TS-45-M-S(b)
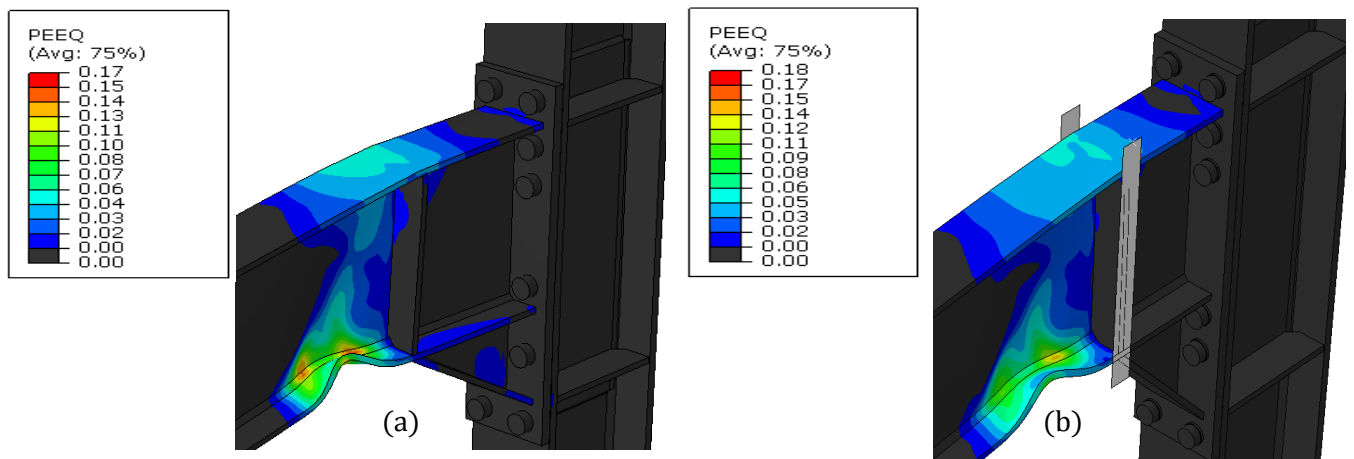
Figure 5.4.3.15.Equivalent plastic strain close up view in models EH3-TS-30-M-S(a) and EH3-TS-45-M-S(b)

Models:

EH1-TS-30-M-H(IPE360-HEB280)   EH1-TS-45-M-H(IPE360-HEB280)

(a)   (b)
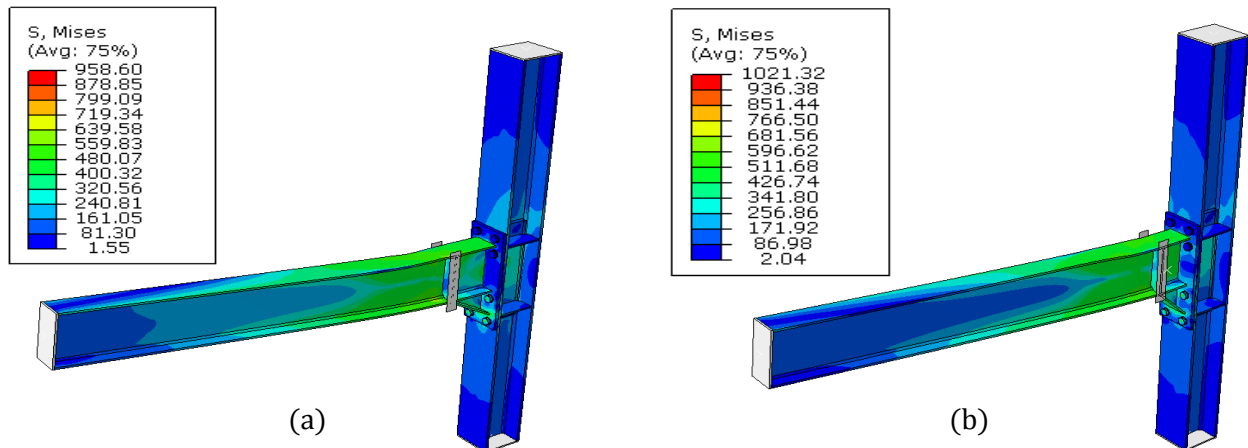
Figure 5.4.3.16.von Mises stresses in models EH1-TS-30-M-H(a) and EH1-TS-45-M-H(b)

(a)   (b)
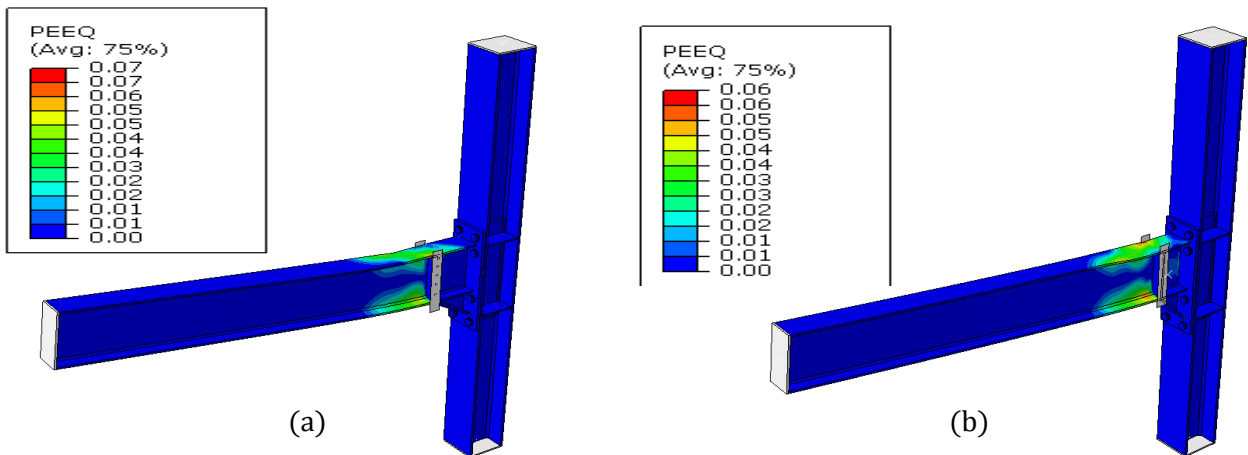
Figure 5.4.3.17.Equivalent plastic strain in models EH1-TS-30-M-H(a) and EH1-TS-45-M-H(b)

European Erasmus Mundus Master
Sustainable Constructions under natural hazards and catastrophic events
520121-1-2011-1-CZ-ERA MUNDUS-EMMC

ᒋᘮᒋᒋᐤᒋ
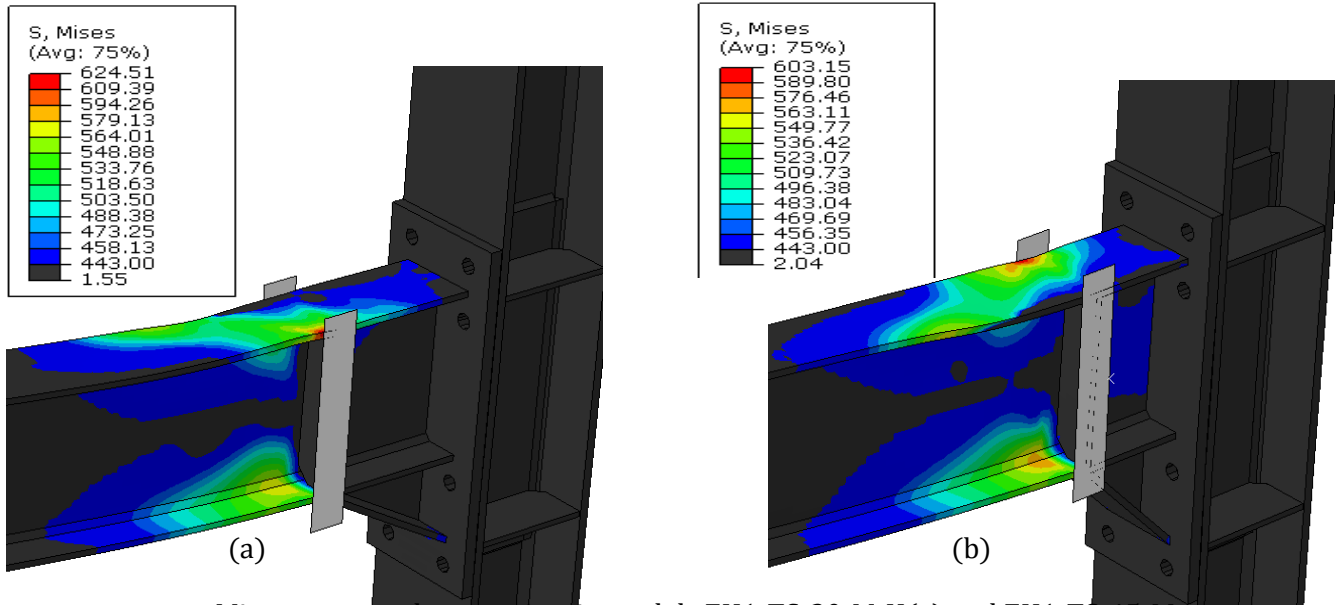
Figure 5.4.3.18. von Mises stresses close up view in models EH1-TS-30-M-H(a) and EH1-TS-45-M-H(b)
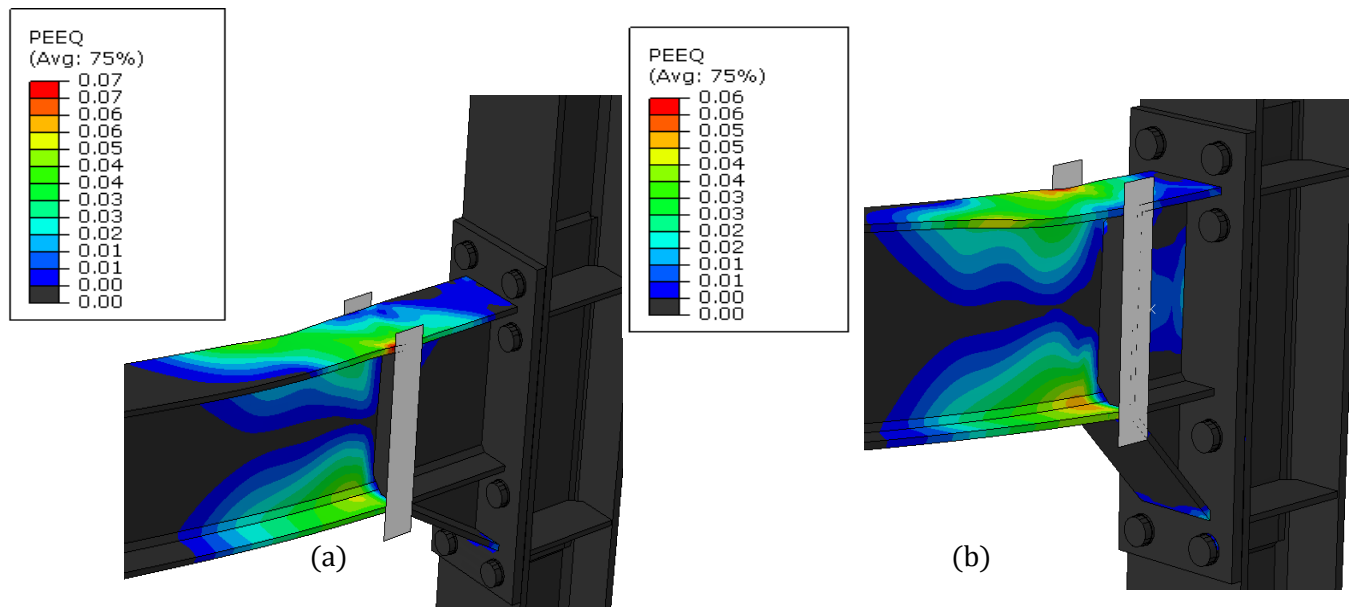
Figure 5.4.3.19. Equivalent plastic strain close up view in models EH1-TS-30-M-H(a) and EH1-TS-45-M-H(b)

European Erasmus Mundus Master
Sustainable Constructions under natural hazards and catastrophic events
520121-1-2011-1-CZ-ERA MUNDUS-EMMC

surcos

Models:

EH2-TS-30-M-H(IPE450-HEB340)   EH2-TS-45-M-H(IPE450-HEB340)
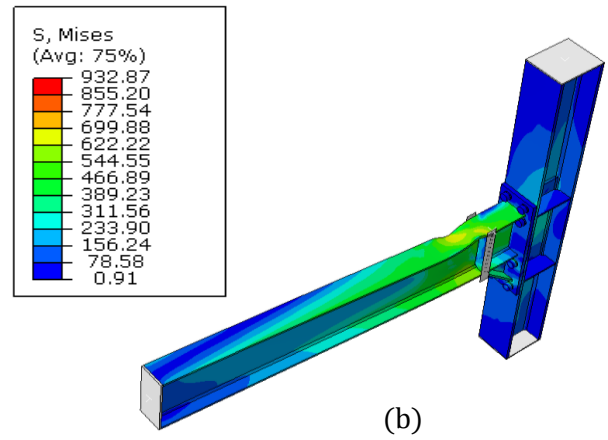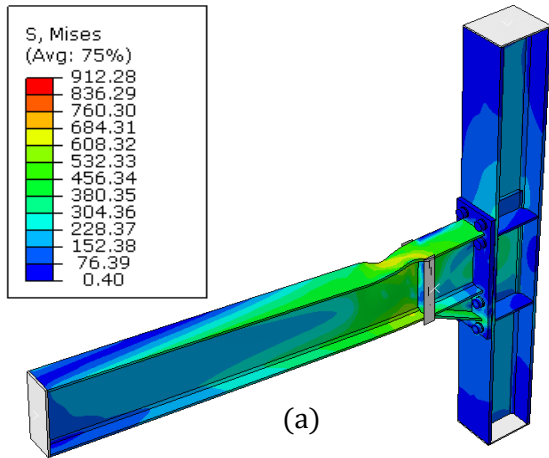
Figure 5.4.3.20.von Mises stresses in models EH2-TS-30-M-H(a) and EH2-TS-45-M-H(b)
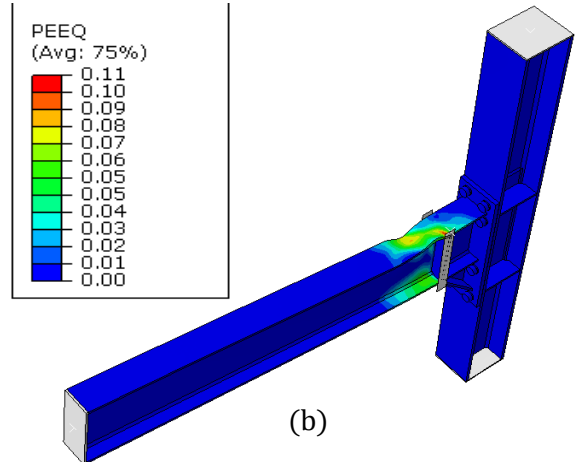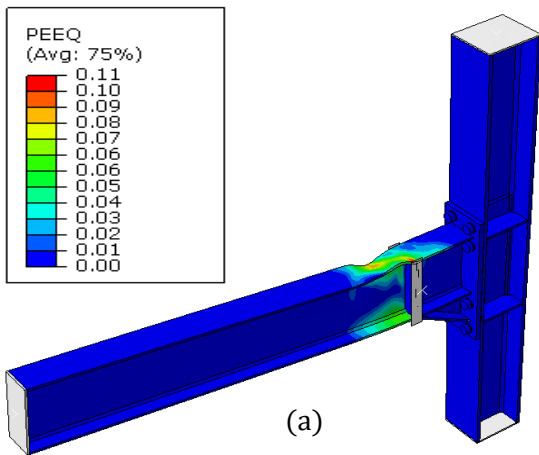
Figure 5.4.3.21.Equivalent plastic strain in models EH2-TS-30-M-H(a) and EH2-TS-45-M-H(b)

European Erasmus Mundus Master
Sustainable Constructions under natural hazards and catastrophic events
520121-1-2011-1-CZ-ERA MUNDUS-EMMC

ſuℛcoſ
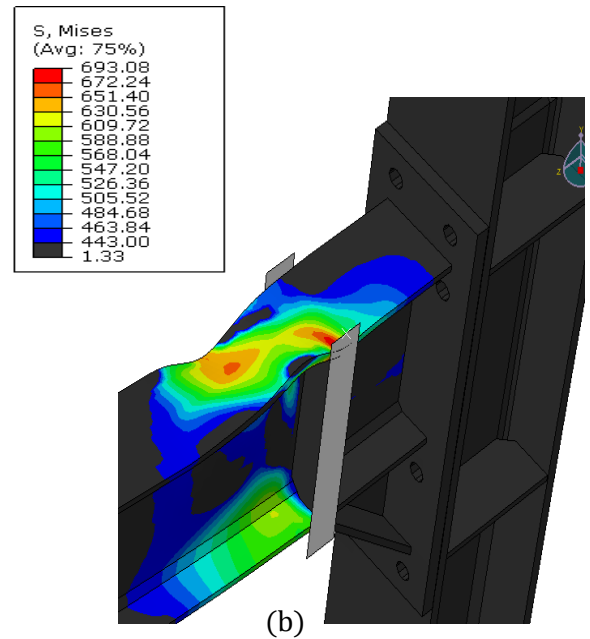
Figure 5.4.3.22. von Mises stresses close up view in models EH2-TS-30-M-H(a) and EH2-TS-45-M-H(b)

(a)   (b)
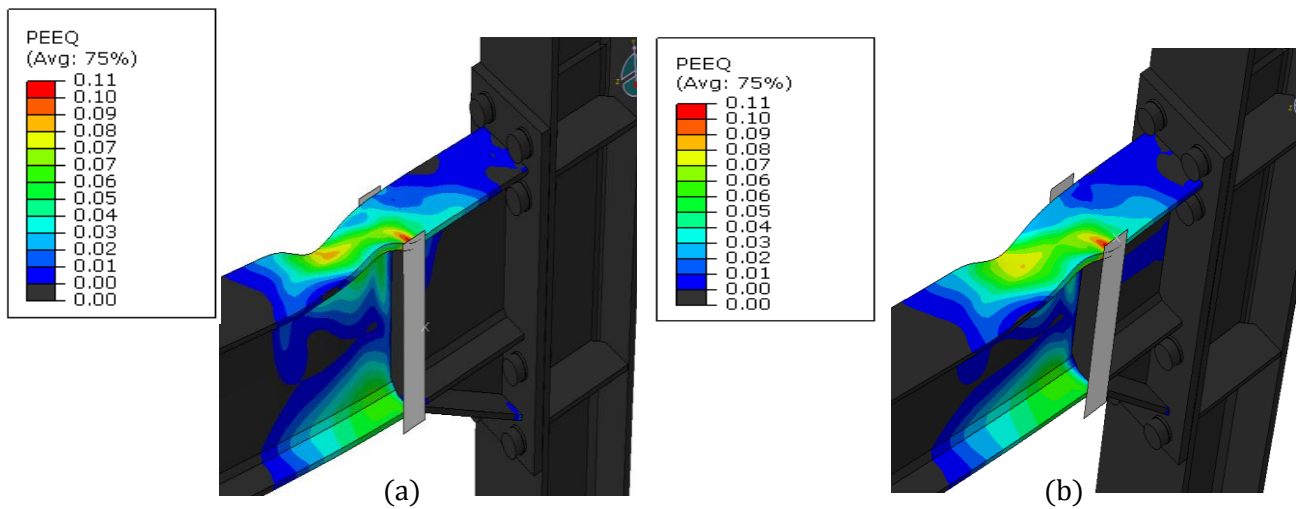
Figure 5.4.3.23. Equivalent plastic strain close up view in models EH2-TS-30-M-H(a) and EH2-TS-45-M-H(b)

Models:

EH3-TS-30-M-H(IPE600-HEB500)   EH3-TS-45-M-H(IPE600-HEB500)

(a)   (b)

Figure 5.4.3.24. von Mises stresses in models EH3-TS-30-M-H(a) and EH3-TS-45-M-H(b)

European Erasmus Mundus Master
Sustainable Constructions under natural hazards and catastrophic events
520121-1-2011-1-CZ-ERA MUNDUS-EMMC

rusros

(a)   (b)

Figure 5.4.3.25.Equivalent plastic strain in models EH3-TS-30-M-H(a) and EH3-TS-45-M-H(b)

(a)   (b)
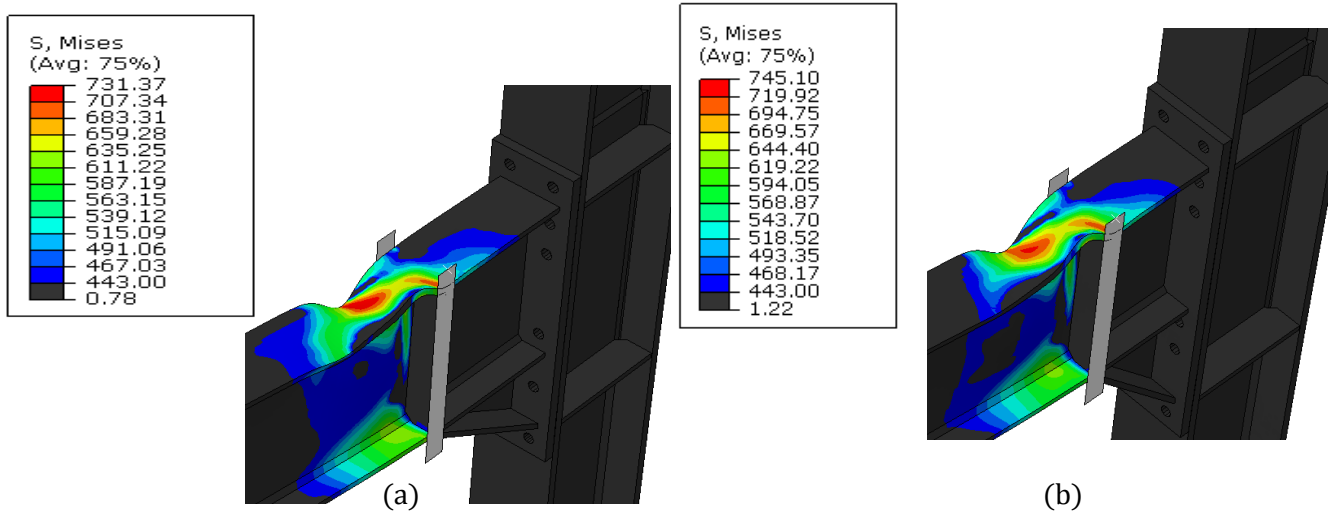
Figure 5.4.3.26.von Mises stresses close up view in models EH3-TS-30-M-H(a) and EH3-TS-45-M-H(b)

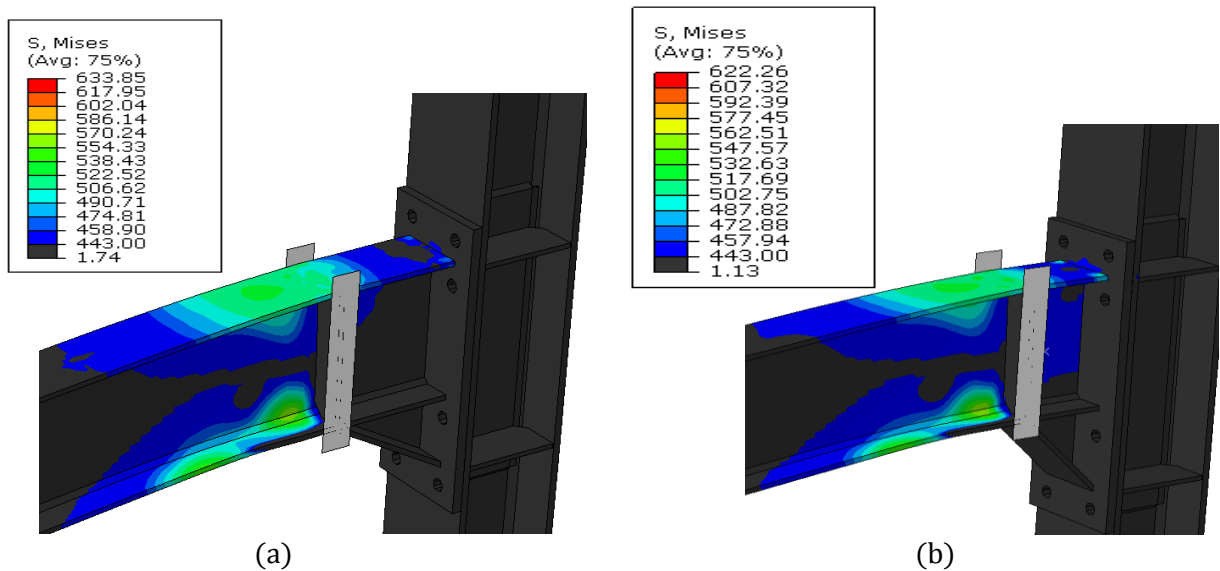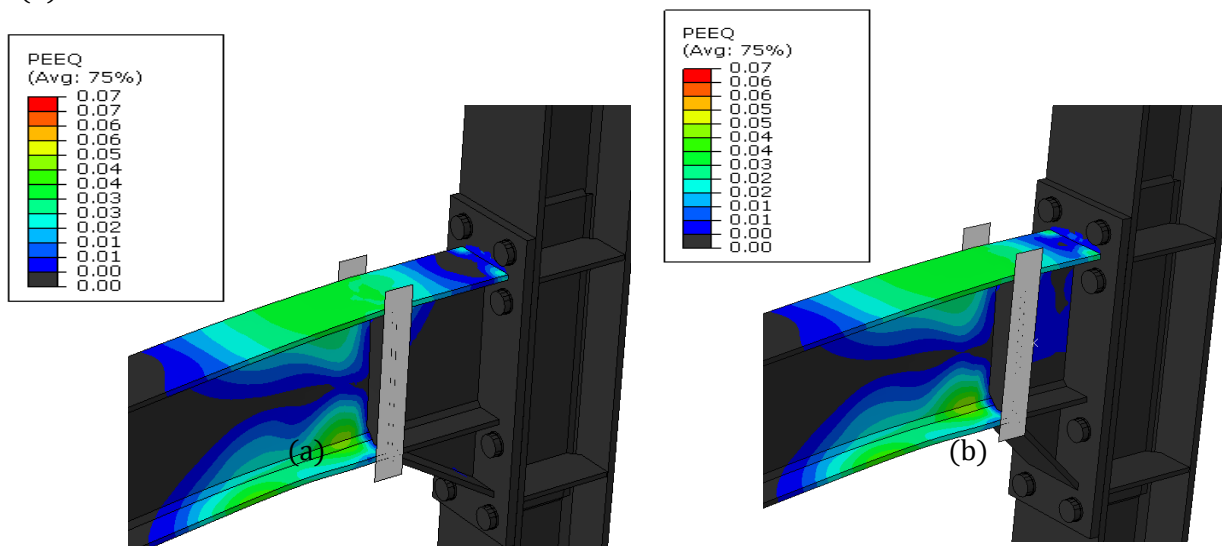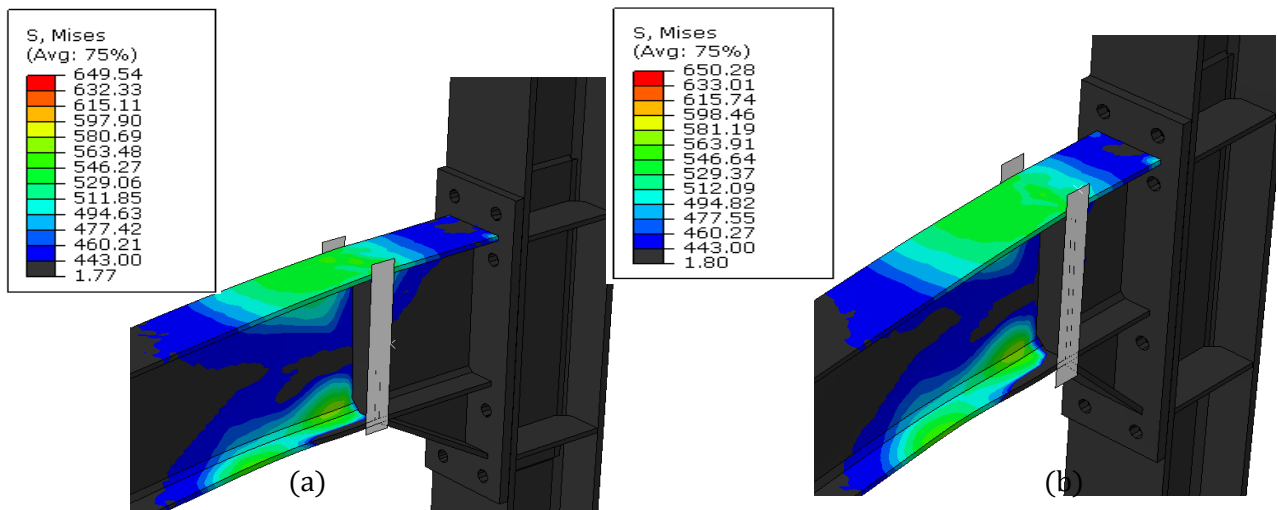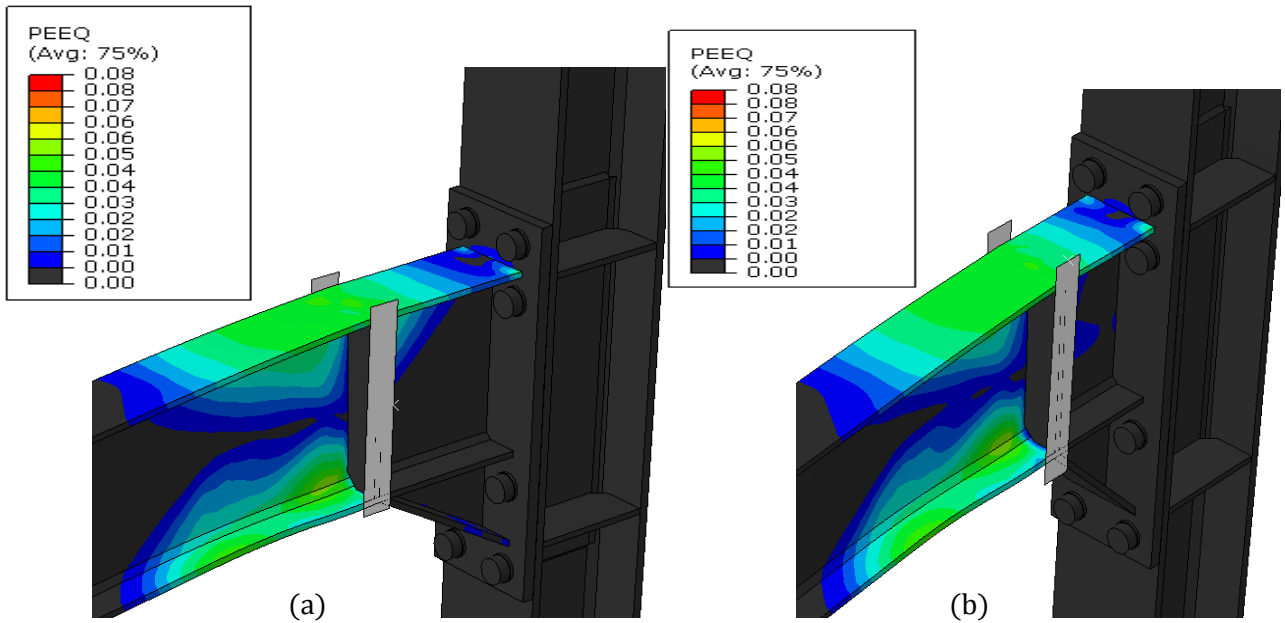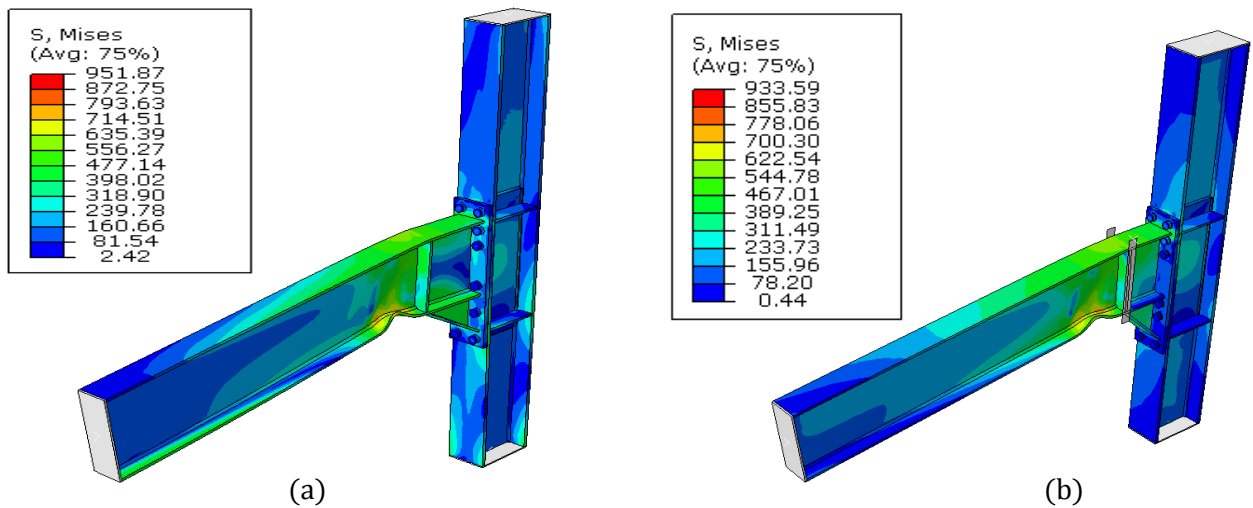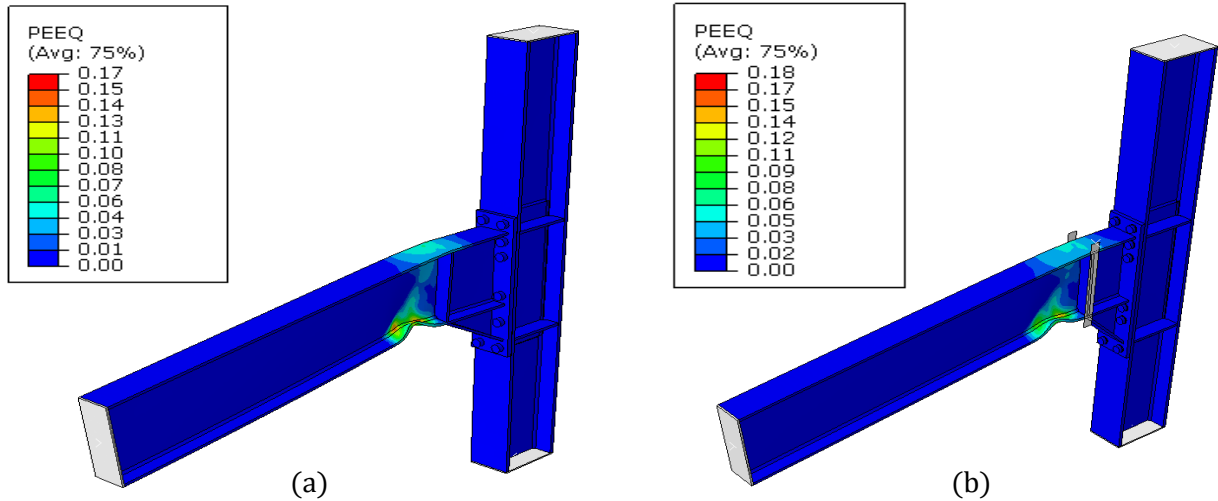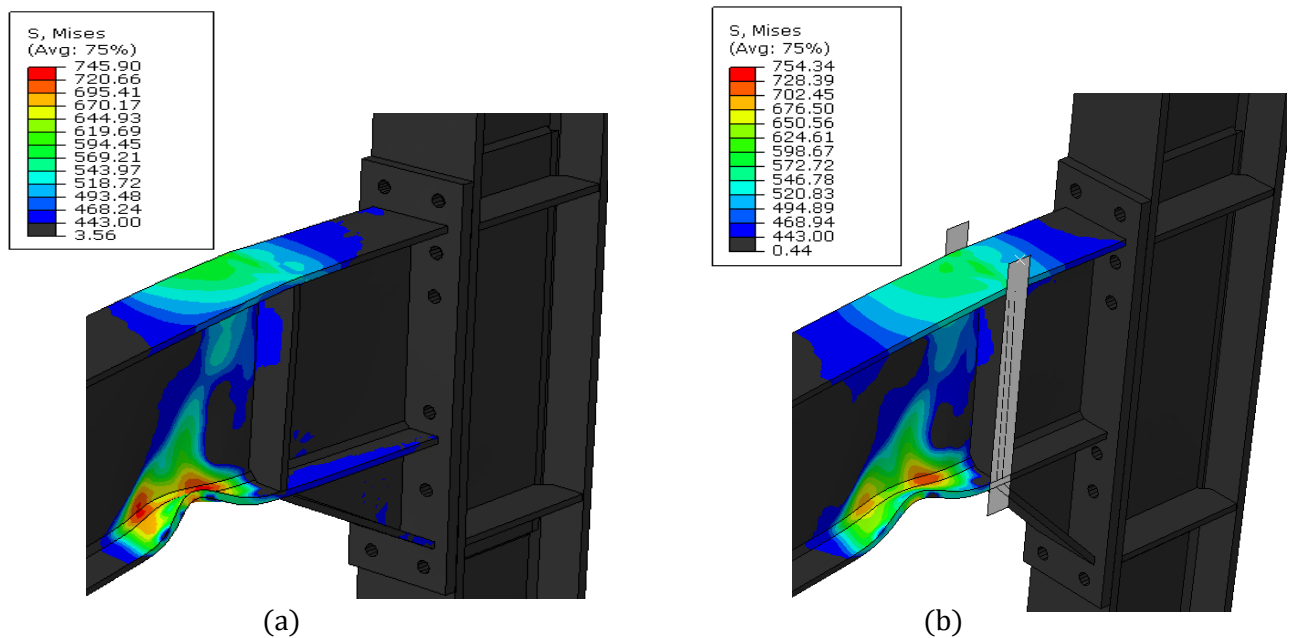(a)   (b)
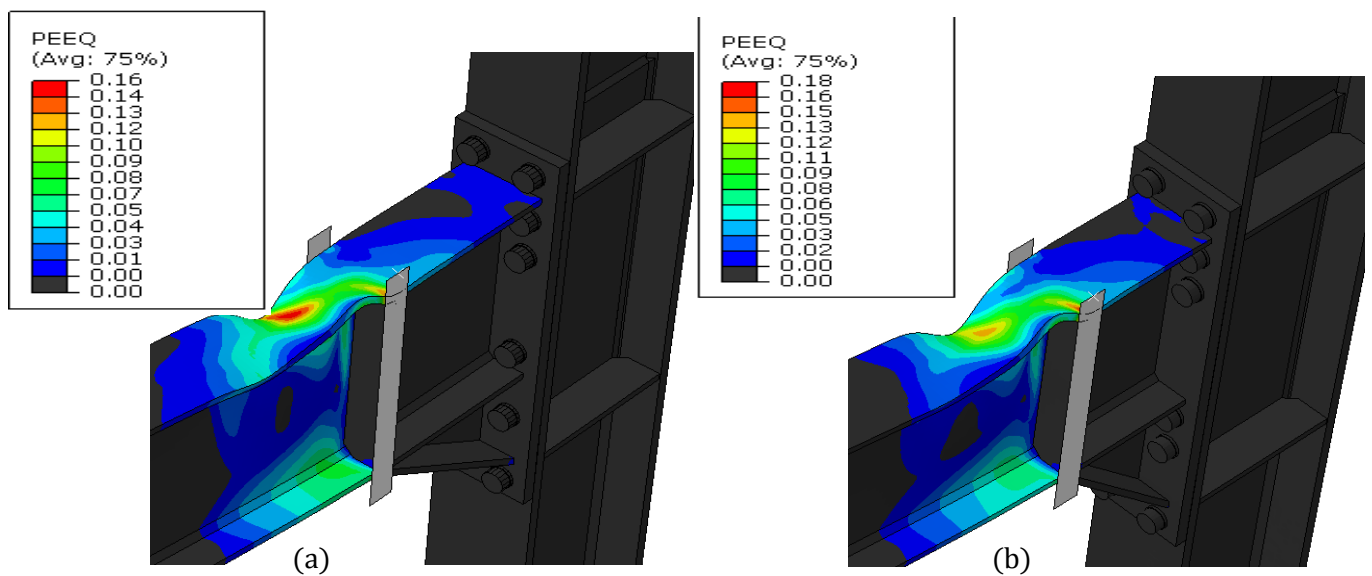
Figure 5.4.3.27.Equivalent plastic strain close up view in models EH3-TS-30-M-H(a) and EH3-TS-45-M-H(b)

Table 5.4.3.1. von Mises stresses in models EH1-TS-30-M(IPE360-HEB280), EH1-TS-45-M(IPE360-HEB280), EH2-TS-30-M(IPE450-HEB340), EH2-TS-45-M(IPE450-HEB340), EH3-TS-30-M(IPE600-HEB500) and EH3-TS-45-M(IPE600-HEB500)

		Von Mises stresses (N/mm²)					
		Group 1	Group 2	Group 1	Group 2	Group 1	Group 2
		EH1-TS-30-M	EH1-TS-45-M	EH2-TS-30-M	EH2-TS-45-M	EH3-TS-30-M	EH3-TS-45-M
Beam	S	633.9	622.3	649.5	650.3	765.1	754.3
	H	624.5	603.2	693.9	693.1	731.4	745.1
Haunch	S	527.3	598.3	518.5	476.1	611.8	545.5
	H	487.1	585.0	506.3	461.8	598.1	559.5
Endplate	S	444.6	447.1	444.5	441.0	428.9	439.3
	H	444.9	442.8	429.7	427.5	433.9	434.1
Bolt	S	947.6	948.5	952.3	945.1	919.3	933.6
	H	958.6	1021.3	912.3	932.9	940.5	918.0
Column	S	443.9	445.4	442.9	441.2	441.5	442.5
	H	443.4	445.0	438.9	441.4	436.1	431.2

Table 5.4.3.2. Equivalent plastic strain in models EH1-TS-30-M(IPE360-HEB280), EH1-TS-45-M(IPE360-HEB280), EH2-TS-30-M(IPE450-HEB340), EH2-TS-45-M(IPE450-HEB340), EH3-TS-30-M(IPE600-HEB500) and EH3-TS-45-M(IPE600-HEB500)

		Equivalent plastic strain (PEEQ)					
		Group 1	Group 2	Group 1	Group 2	Group 1	Group 2
		EH1-TS-30-M	EH1-TS-45-M	EH2-TS-30-M	EH2-TS-45-M	EH3-TS-30-M	EH3-TS-45-M
Beam	S	0.073	0.069	0.082	0.082	0.202	0.185
	H	0.073	0.060	0.110	0.110	0.155	0.179
Haunch	S	0.037	0.060	0.034	0.024	0.064	0.043
	H	0.027	0.054	0.031	0.020	0.058	0.046
Endplate	S	0.009	0.011	0.011	0.008	0.004	0.005
	H	0.008	0.004	0.007	0.001	0.006	0.005
Bolt	S	0.006	0.003	0.004	0.004	0.004	0.003
	H	0.009	0.034	0.008	0.006	0.010	0.005
Column	S	0.009	0.008	0.008	0.006	0.005	0.005
	H	0.010	0.009	0.006	0.004	0.006	0.003

5.4.4   Influence of panel zone strength (group 1 vs group 3)

The objective of this study is to assess the contribution of panel zone strength in joints. For numerical analysis total 6 models were chosen from group1; EH1-TS-30-M(IPE360-HEB280),EH2-TS-30-M(IPE450-HEB340),EH3-TS-30-M(IPE600-HEB500)   and   from group 3; EH1-XB-30-M(IPE360-HEB340),EH2-XB-30-M(IPE450-HEB500),EH3-XB-30-M(IPE600-HEB650) Both upward and downward displacement were applied corresponds to a magnitude of 0.1rad rotation on the tip of the beam in all models. Expected material properties (f_y= 1.25*355= 443.75MPa) was defined for all parts in the joint except bolts. For bolts (f_y=940MPa) was used. Figure 5.4.4.1, Figure 5.4.4.2 and Figure 5.4.4.3 show the moment-rotation capacity among those models. From the curves we can see that moment capacity of joint is identical for beam IPE360. Strength degradation takes place for beam IPE450 in correspond to upward displacement. For beam IPE600 strength degradation occurs in downward and upward displacement. From Figure 5.4.4.14 and Figure 5.4.4.15, we can see that in higher beam section IPE600 local buckling takes place at beam flange. The elastic yield moment capacity is very close to each other for every model.
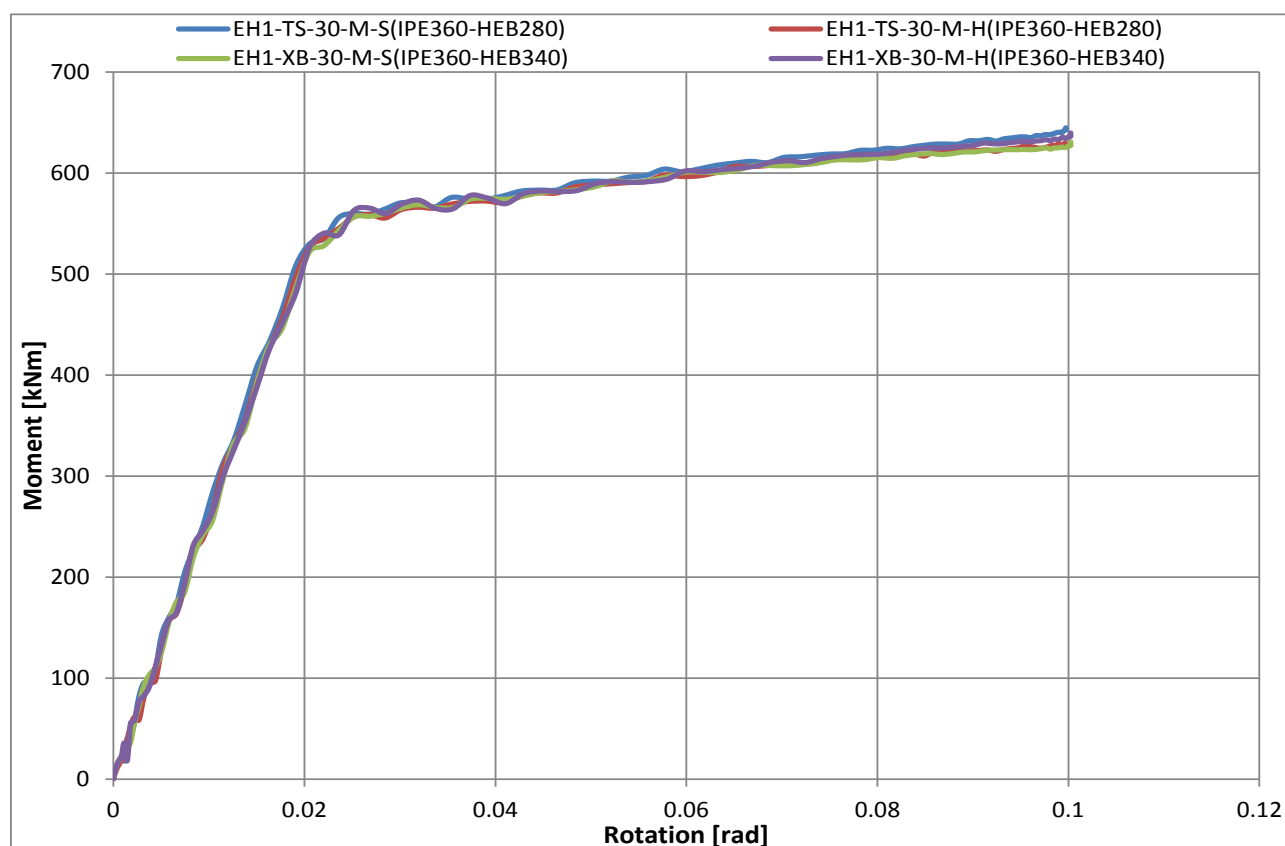
Figure 5.4.4.1.Comparision of moment–rotation among models EH1-TS-30-M-S(IPE360-HEB280), EH1-TS-30-M-H(IPE360-HEB280) and EH1-XB-30-M(IPE360-HEB340).
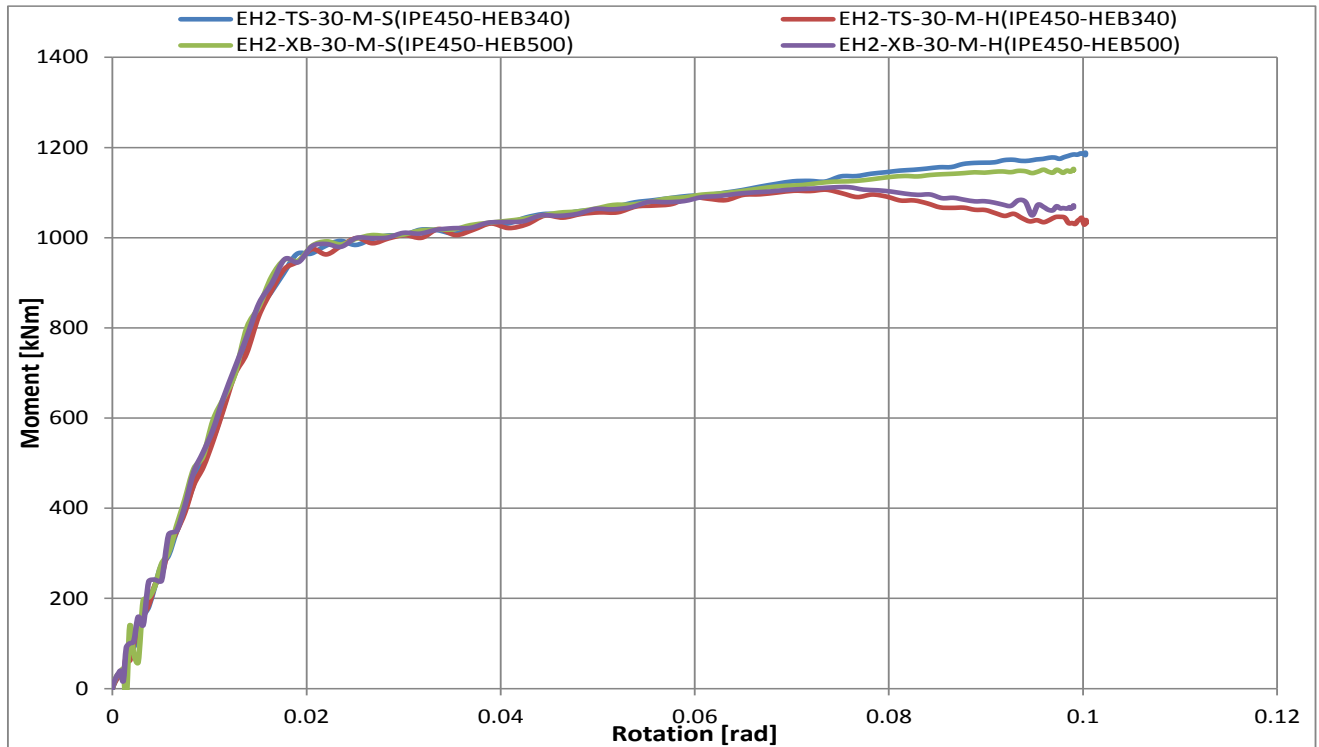
Figure 5.4.4.2.Comparision of moment–rotation among models EH2-TS-30-M-S(IPE450-HEB340), EH2-TS-30-M-H(IPE450-HEB340) and EH2-XB-30-M(IPE450-HEB500).
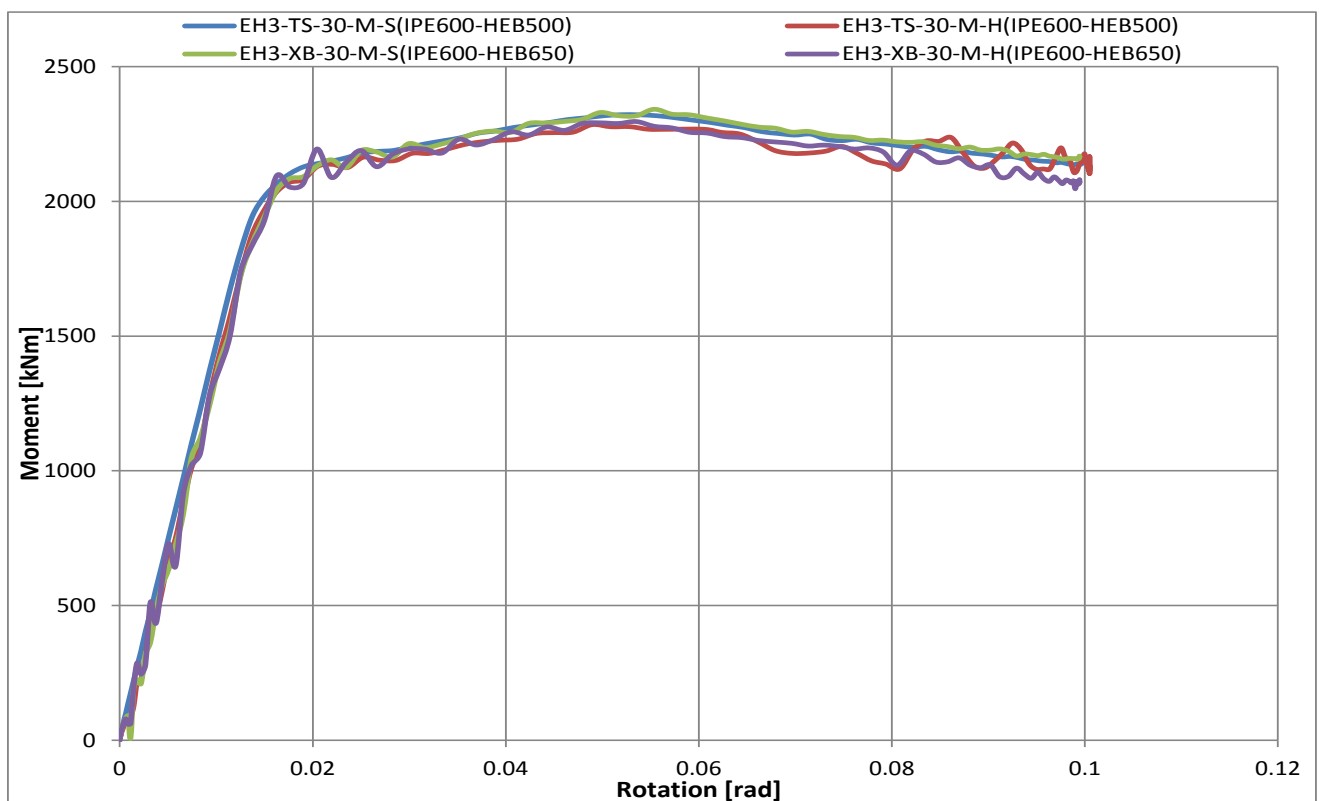
Figure 5.4.4.3.Comparision of moment–rotation among models EH3-TS-30-M-S(IPE600-HEB500), EH2-TS-30-M-H(IPE600-HEB500) and EH2-XB-30-M(IPE600-HEB650).

Figure 5.4.4.4 presents the von Mises stresses in models EH1-TS-30-M-S(a), EH1-TS-30-M-H(b).and EH1-XB-30-M(c). It can be observed that beam flanges and web are exceeding the yield stress near the haunch end. Figure 5.4.4.6 shows von Mises stresses close up view in models. EH1-TS-30-M-S(a), EH1-TS-30-M-H(b).and EH1-XB-30-M(c). Figure 5.4.4.5 shows equivalent plastic strain in models, where we can't see any local buckling in beam flange. From Figure 5.4.4.8, we can clearly see that local buckling takes place in upper flange of beam IPE450. Inside the haunch, top flange of beam facing problem with stresses which are close to yield stress. Figure 5.4.4.9 represents the equivalent plastic strain in models EH2-TS-30-M-S(a), EH2-TS-30-M-H(b).and EH2-XB-30-M(c). Figure 5.4.4.15 shows close view of equivalent plastic strain in models EH3-TS-30-M-S(a), EH3-TS-30-M-H(b).and EH3-XB-30-M(c). We can see that plastic strain in the top flange is close to column face and in bottom flange bit away from column face due to downward displacement and almost identical for upward displacement. We have found from the analysis that plastic hinges have occurred at a distance from the end of haunch of 168mm (0,47h_b), 93mm(0.26h_b), 108mm (0.3h_b) for models EH1-TS-30-M-S, EH1-TS-30-M-H, EH1-XB-30-M-S, EH1-XB-30-M-H; 179mm(0.4h_b), 134mm(0.3h_b), 179mm(0.4h_b), 164mm(0.36h_b) for models EH2-TS-30-M-S, EH2-TS-30-M-H, EH2-XB-30-M-S, EH2-XB-30-M-H; 246mm(0.41h_b), 231mm(0.39h_b), 261mm(0.43h_b), 171mm(0.29h_b) for models EH3-TS-30-M-S, EH3-TS-30-M-H, EH3-XB-30-M-S, EH3-XB-30-M-H.

Figure 5.4.4.14 and Figure 5.4.4.15 depict the von Mises stresses and equivalent plastic strain close up view in models.

Due to safety reason, it is not desire to have plastic strain in the non-dissipative parts. Eventually from the analysis we have seen that some portion of the haunch, endplate, column and bolts have plastic strain to the yield limit. In overall, joint performance is adequate. Table 5.4.4.1 and Table 5.4.4.2 present maximum von Mises stresses and equivalent plastic strain for all the parts in joint.

Models:

EH1-TS-30-M-S   EH1-TS-30-M-H   EH1-XB-30-M.

(a)   (b)   (c)
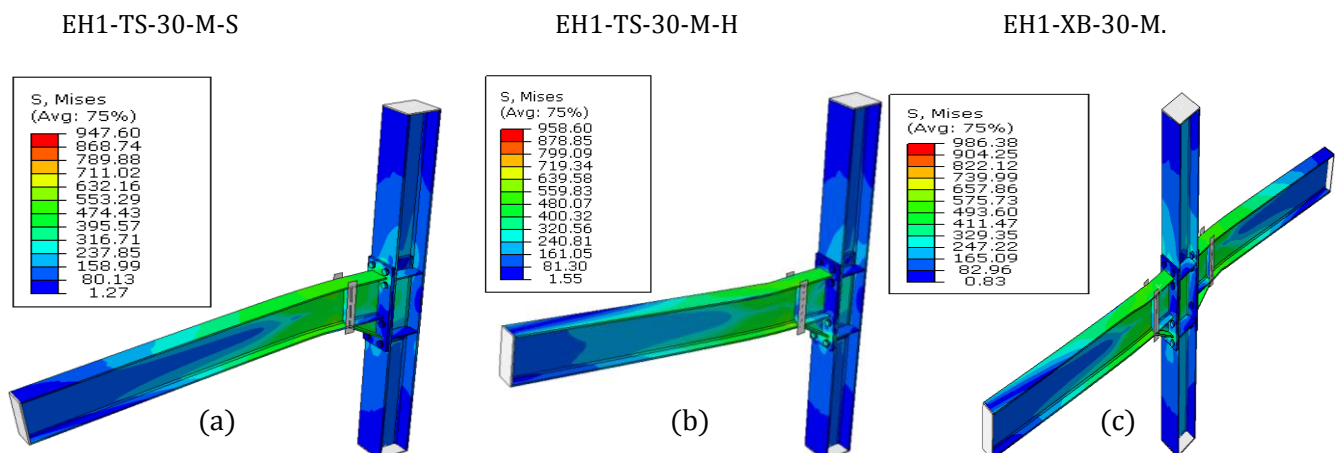
Figure 5.4.4.4.von Mises stresses in models EH1-TS-30-M-S(a), EH1-TS-30-M-H(b) and EH1-XB-30-M(c)
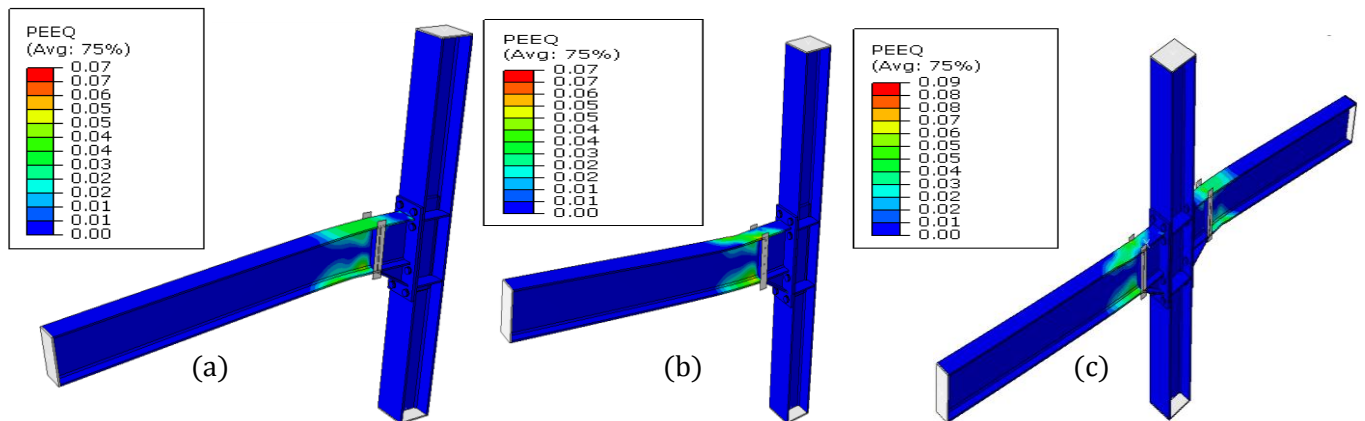
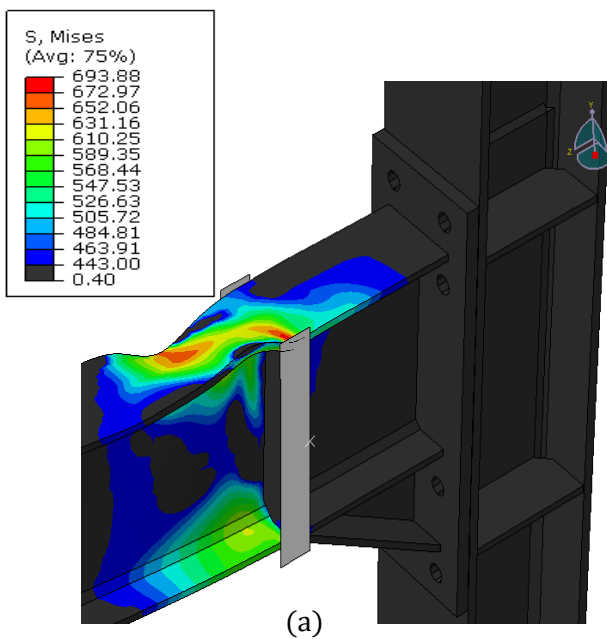Figure 5.4.4.5.Equivalent plastic strain in models EH1-TS-30-M-S(a), EH1-TS-30-M-H(b) and EH1-XB-30-M(c)

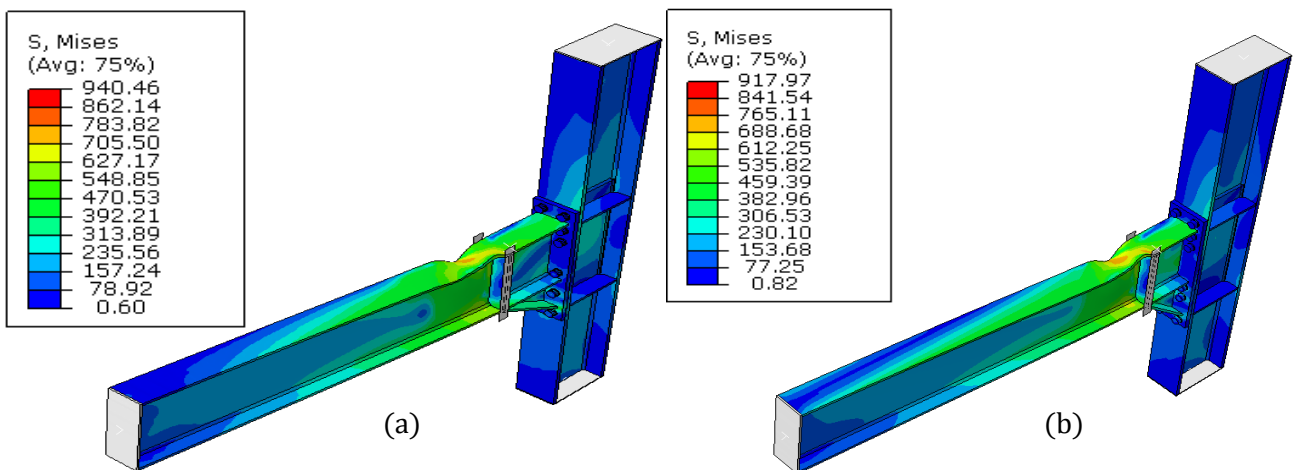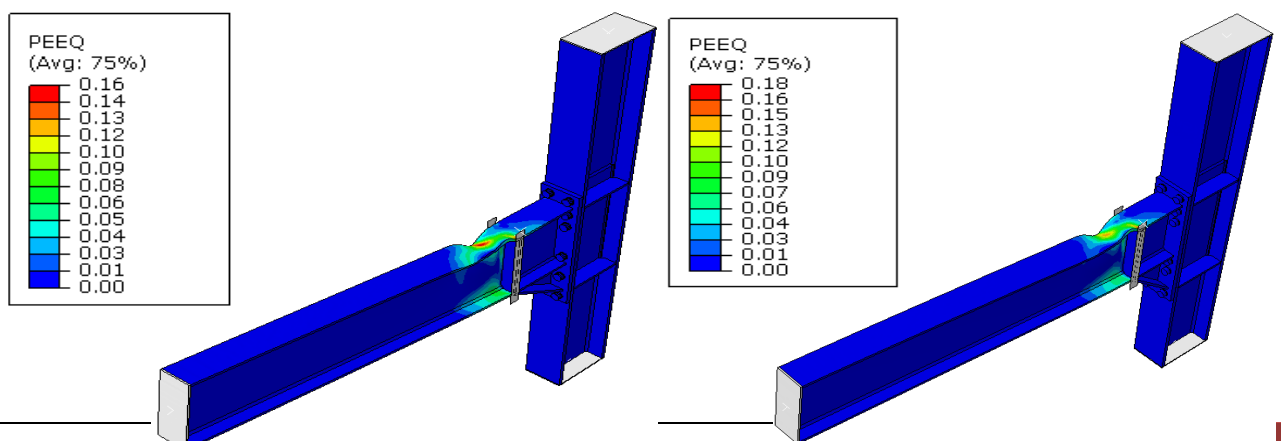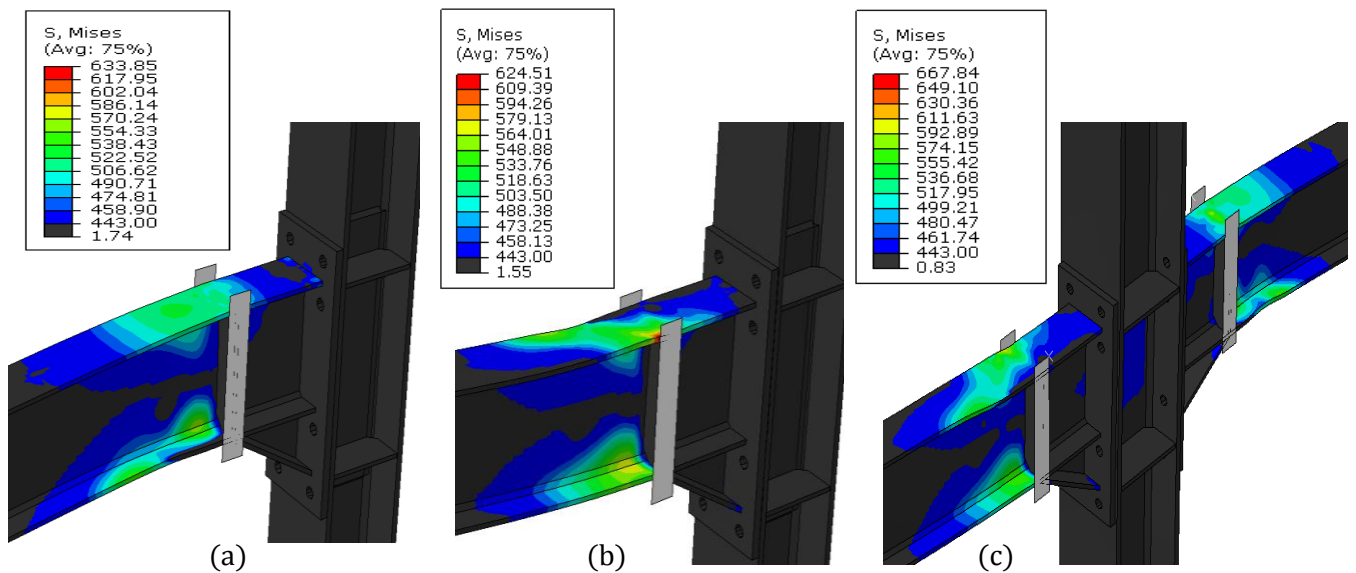Figure 5.4.4.6.von Mises stresses close up view in models EH1-TS-30-M-S(a), EH1-TS-30-M-H(b) and EH1-XB-30-M(c)
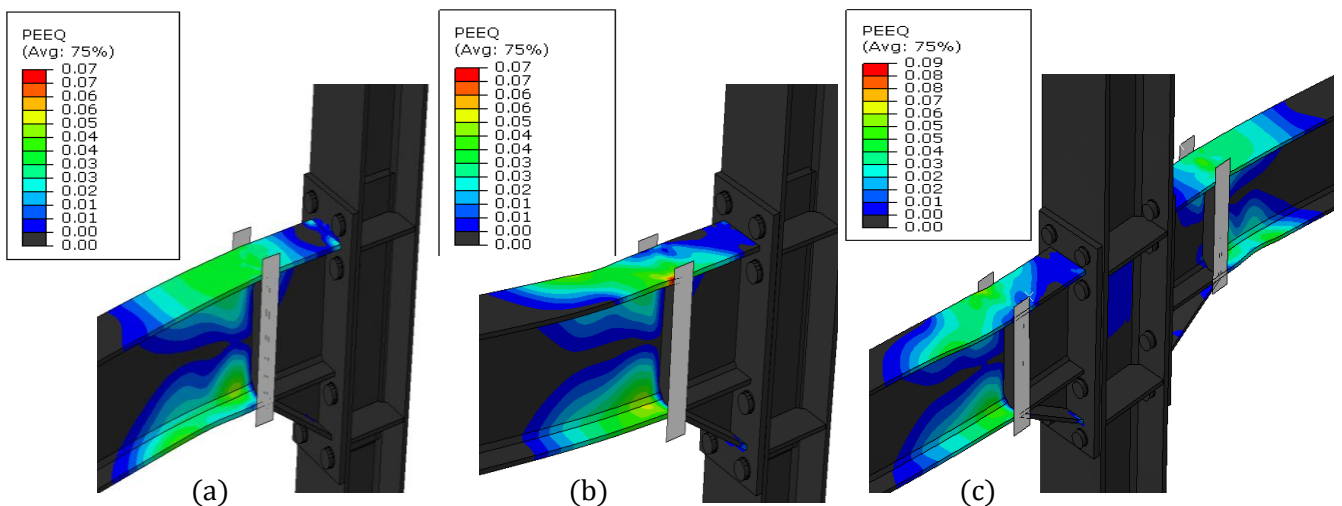
Figure 5.4.4.7. Equivalent plastic strain close up view in models EH1-TS-30-M-S(a), EH1-TS-30-M-H(b) and EH1-XB-30-M(c)

Models:

EH2-TS-30-M-S   EH2-TS-30-M-H   EH2-XB-30-M
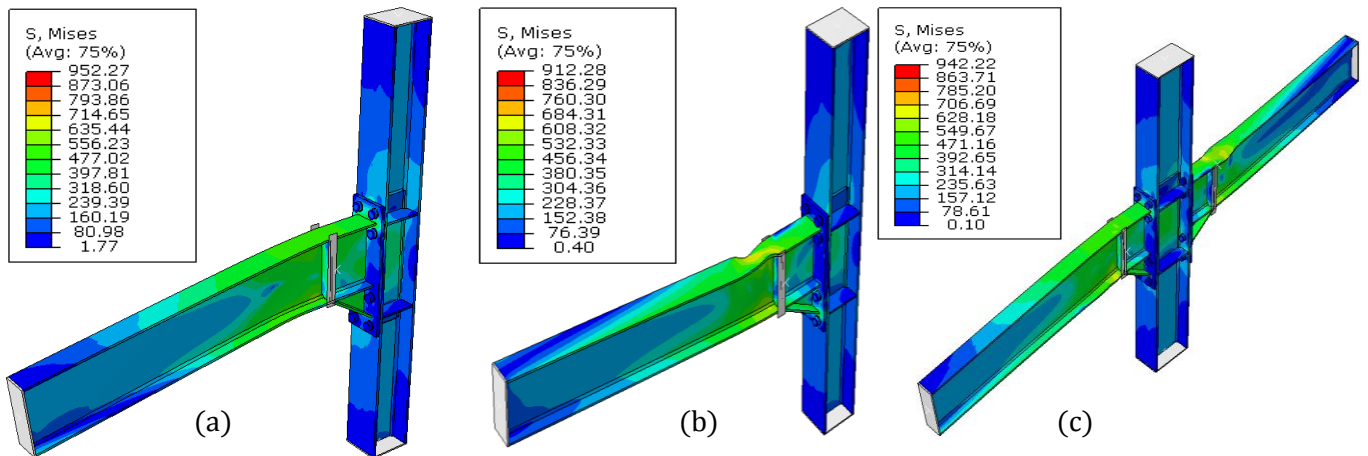
Figure 5.4.4.8. von Mises stresses in models EH2-TS-30-M-S(a), EH2-TS-30-M-H(b) and EH2-XB-30-M(c)
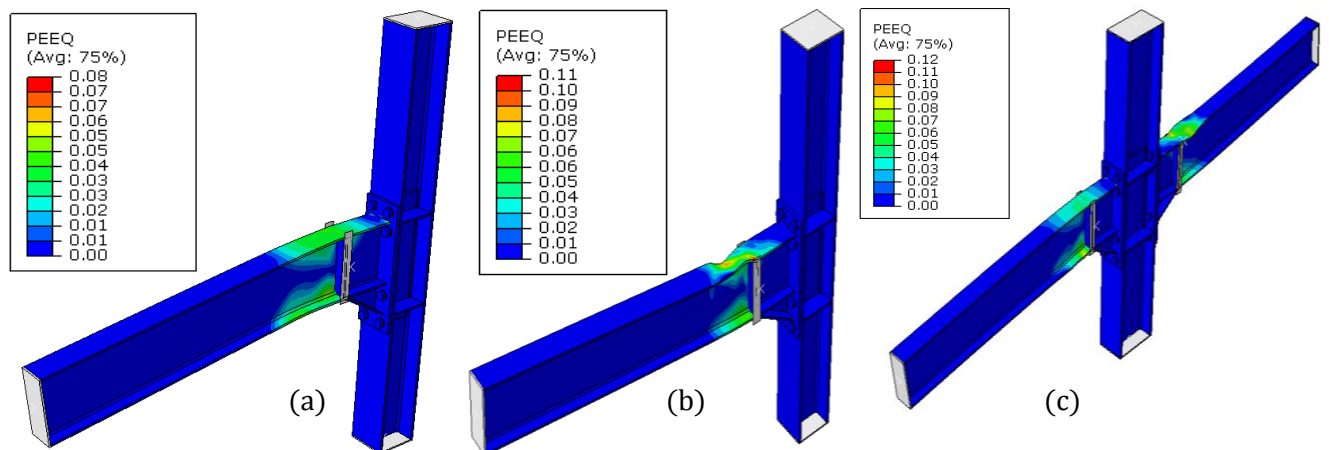
Figure 5.4.4.9. Equivalent plastic strain in models EH2-TS-30-M-S(a), EH2-TS-30-M-H(b) and EH2-XB-30-M(c)

European Erasmus Mundus Master
Sustainable Constructions under natural hazards and catastrophic events
520121-1-2011-1-CZ-ERA MUNDUS-EMMC

SUSCOS
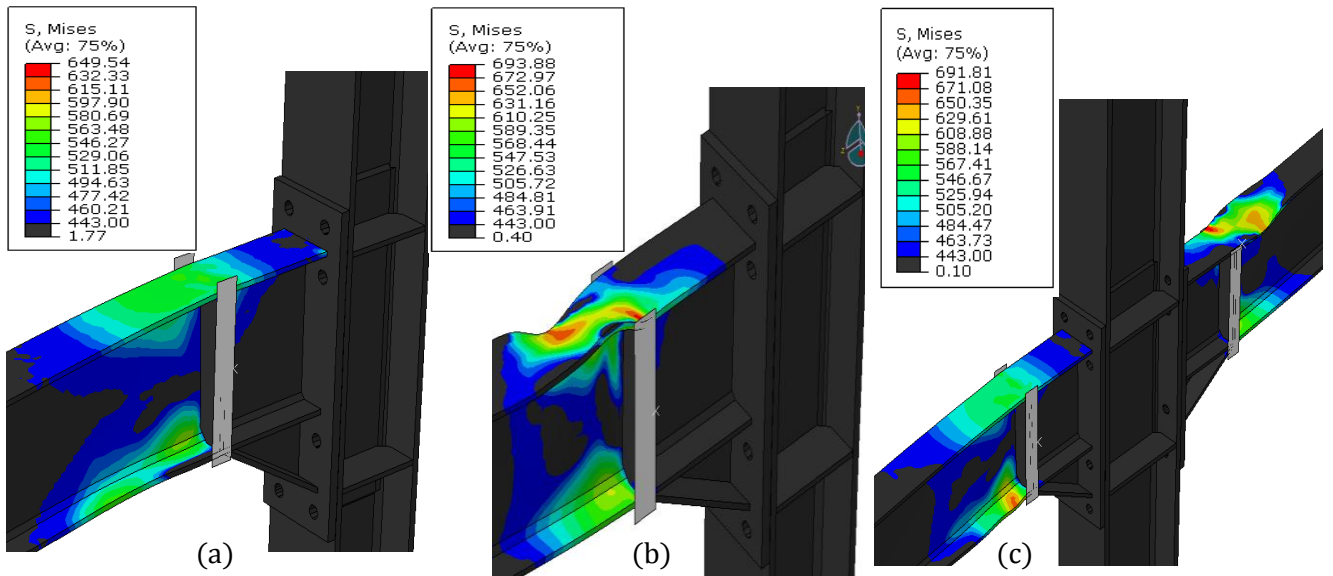
Figure 5.4.4.10. von Mises stresses close up view in models EH2-TS-30-M-S(a), EH2-TS-30-M-H(b) and EH2-XB-30-M(c)
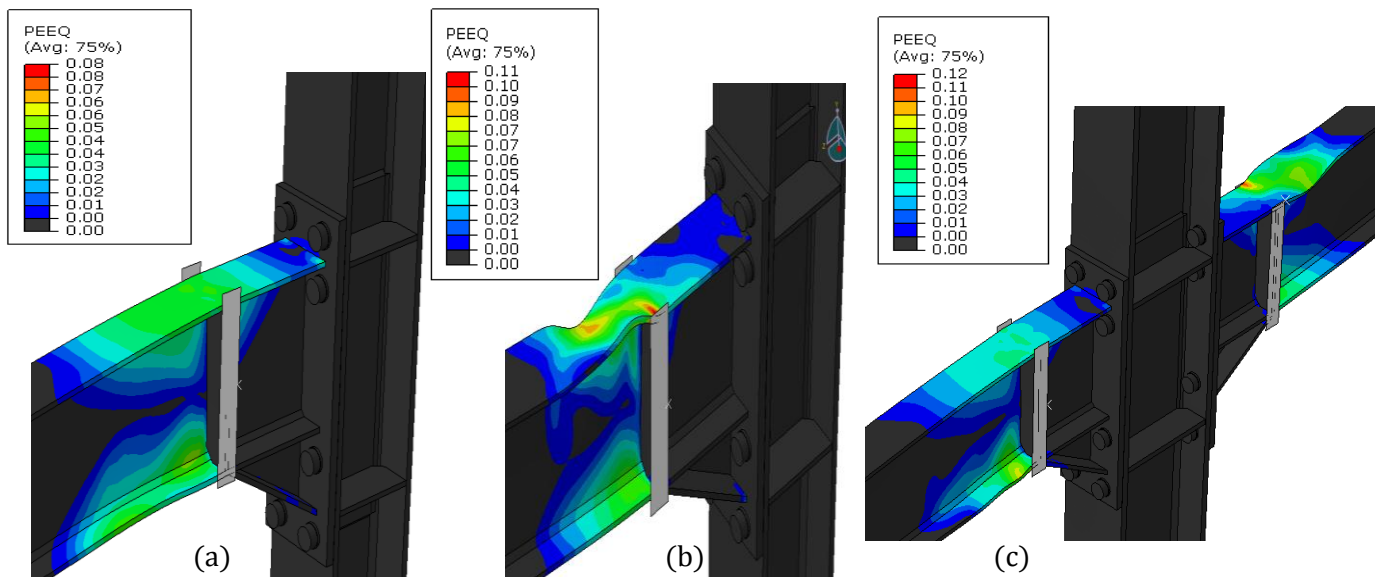
Figure 5.4.4.11. Equivalent plastic strain close up view in models EH2-TS-30-M-S(a), EH2-TS-30-M-H(b) and EH2-XB-30-M(c)

Models:

EH3-TS-30-M-S   EH3-TS-30-M-H   EH3-XB-30-M

European Erasmus Mundus Master
Sustainable Constructions under natural hazards and catastrophic events
520121-1-2011-1-CZ-ERA MUNDUS-EMMC

ЛЛГСОЛ
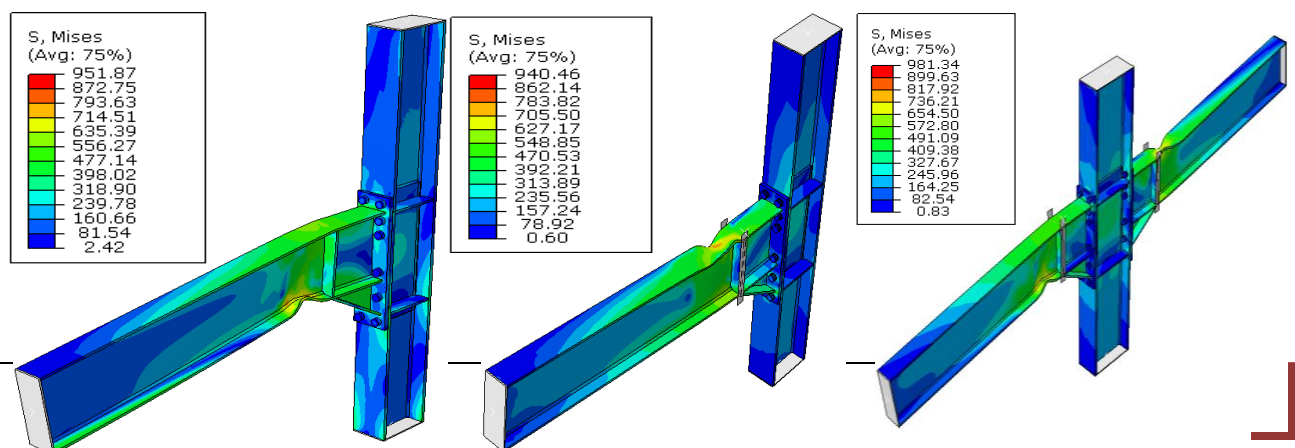
(a)   (b)   (c)

Figure 5.4.4.12.von Mises stresses in models EH3-TS-30-M-S(a), EH3-TS-30-M-H(b) and EH3-XB-30-M(c)

(a)   (b)   (c)

Figure 5.4.4.13. Equivalent plastic strain in models EH3-TS-30-M-S(a), EH3-TS-30-M-H(b) and EH3-XB-30-M(c)

(a)   (b)   (c)

Figure 5.4.4.14.von Mises stresses close up view in models EH3-TS-30-M-S(a), EH3-TS-30-M-H(b) and EH3-XB-30-M(c)

European Erasmus Mundus Master
Sustainable Constructions under natural hazards and catastrophic events
520121-1-2011-1-CZ-ERA MUNDUS-EMMC

ЈUЈᒪОЈ
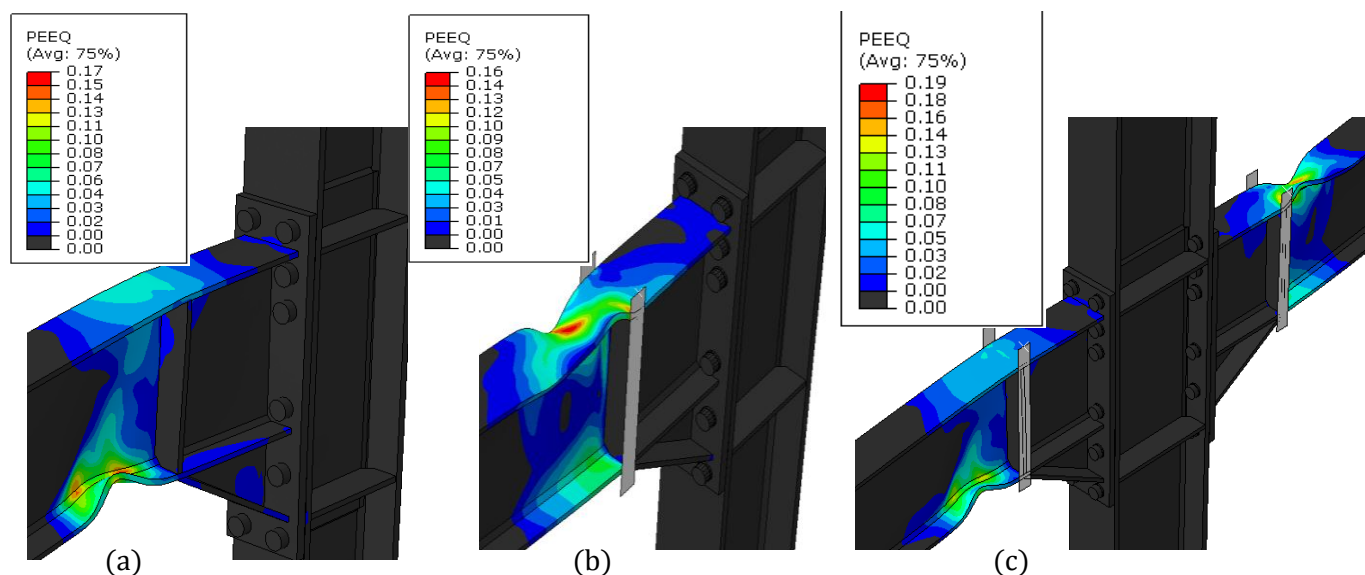
Figure 5.4.4.15. Equivalent plastic strain close up view in models EH3-TS-30-M-S(a), EH3-TS-30-M-H(b) and EH3-XB-30-M(c)

Table 5.4.4.1. von Mises stresses in models EH1-TS-30-M(IPE360-HEB280), EH1-XB-30-M(IPE360-HEB340), EH2-TS-30-M(IPE450-HEB340), EH2-XB-30-M(IPE450-HEB500), EH3-TS-30-M(IPE600-HEB500), EH3-XB-30-M(IPE600-HEB650).

		von Mises stresses (N/mm²)					
		Group 1	Group 3	Group 1	Group 3	Group 1	Group 3
		EH1-TS-30-M	EH1-XB-30-M	EH2-TS-30-M	EH2-XB-30-M	EH3-TS-30-M	EH3-XB-30-M
Beam	S	633.9	667.8	649.5	690.2	765.1	731.0
	H	624.5	649.3	693.9	691.8	731.4	765.1
Haunch	S	527.3	524.0	518.5	689.2	611.8	571.4
	H	487.1	499.0	506.3	568.4	598.1	595.2
Endplate	S	444.6	445.7	444.5	474.8	428.9	418.9
	H	444.9	446.9	429.7	432.4	433.9	443.0
Bolt	S	947.6		952.3		919.3	
	H	958.6	986.4	912.3	942.2	940.5	981.3
Column	S	443.9		442.9		441.5	
	H	443.4	446.3	438.9	440.9	436.1	438.3

Table 5.4.4.2. Equivalent plastic strain in models EH1-TS-30-M(IPE360-HEB280), EH1-XB-30-M(IPE360-HEB340), EH2-TS-30-M(IPE450-HEB340), EH2-XB-30-M(IPE450-HEB500), EH3-TS-30-M(IPE600-HEB500), EH3-XB-30-M(IPE600-HEB650).

		Equivalent plastic strain (PEEQ)					
		Group 1	Group 3	Group 1	Group 3	Group 1	Group 3
		EH1-TS-30-M	EH1-XB-30-M	EH2-TS-30-M	EH2-XB-30-M	EH3-TS-30-M	EH3-XB-30-M
Beam	S	0.073	0.091	0.082	0.106	0.202	0.150
	H	0.073	0.080	0.110	0.108	0.155	0.192
Haunch	S	0.037	0.036	0.034	0.121	0.064	0.050
	H	0.027	0.029	0.031	0.09	0.058	0.058
Endplate	S	0.009	0.008	0.011	0.026	0.004	0.008
	H	0.008	0.009	0.007	0.008	0.006	0.007
Bolt	S	0.006		0.004		0.004	
	H	0.009	0.025	0.008	0.002	0.010	0.012
Column	S	0.009		0.008		0.005	
	H	0.010	0.010	0.006	0.003	0.006	0.008

Table 5.4.4.3. Shear check for column web plate.

	$V_{wp,ED}/V_{wp,RD}$		
	EH1	EH2	EH3
T-joint	0.32	0.34	0.33
X-joint	0.9	0.79	0.88

5.4.5 Influence of beam clear span-t0-depth ratio (EH3-TS-30 M): 3, 5,7 ,9

The objective of this study is to assess the effect of beam clear span to depth ratio in joints. For numerical analysis one model was chosen from group1; EH3-TS-30-M(IPE600-HEB500). Beam length was taken according to the beam clear span to depth ratio of 3, 5, 7 and 9. Only downward displacement was applied corresponds to a magnitude of 0.1rad rotation on the tip of the beam in all models. Expected material properties (f_y= 1.25*355= 443.75MPa) was defined for all parts in the joint except bolts. For bolts (f_y=940MPa) was used. Figure 5.4.5.1 and Figure 5.4.5.2 show the moment-rotation capacity. From the curves we can see that moment capacity of joint is higher for ratio 3 and lower with ratio 9. Strength degradation takes place for all cases. From Figure 5.4.5.5 and Figure 5.4.5.6, we can see that beam went to failure due to shear in web for span to depth ratio 3. Here the elastic stiffness is not equal.
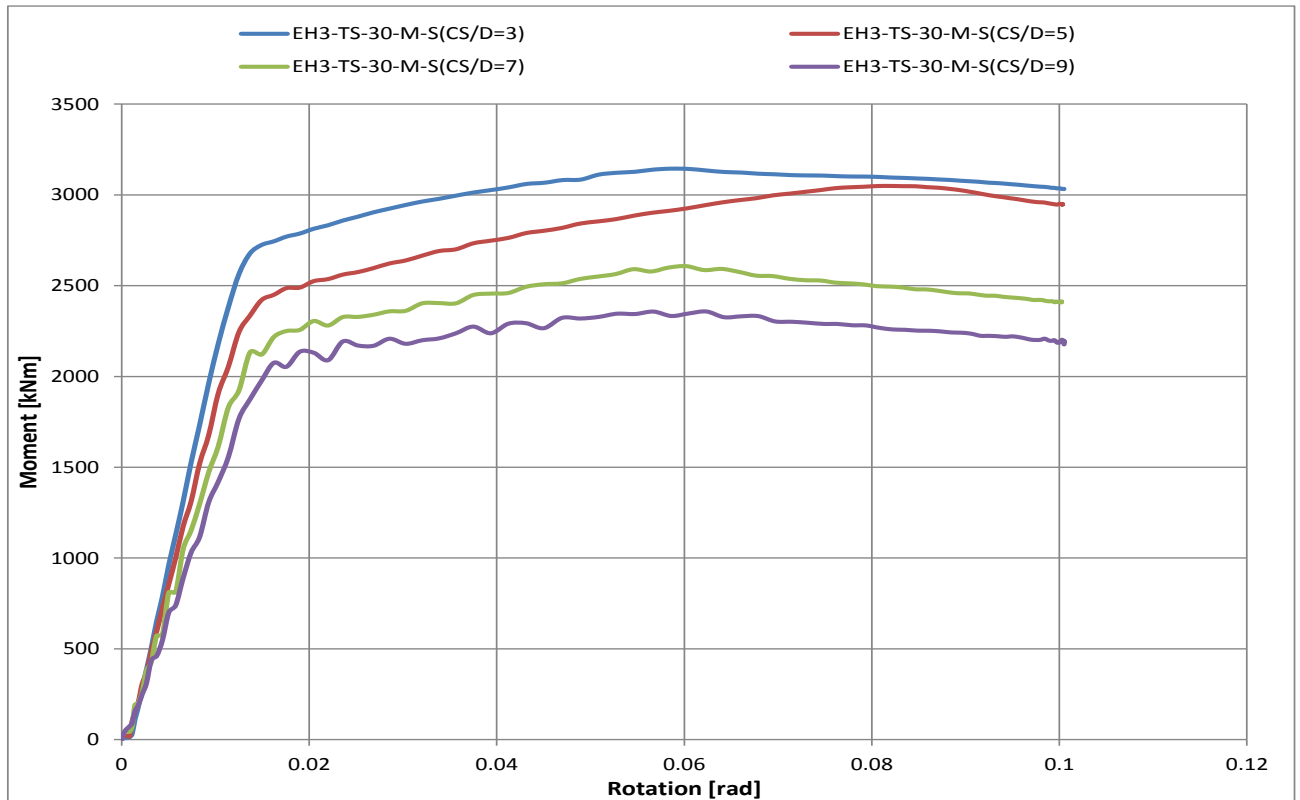
Figure 5.4.5.1.Comparision of moment–rotation among models EH3-TS-30-M-S(CS/D=3), EH3-TS-30-M-S(CS/D=5), EH3-TS-30-M-S(CS/D=7), EH3-TS-30-M-S(CS/D=9).
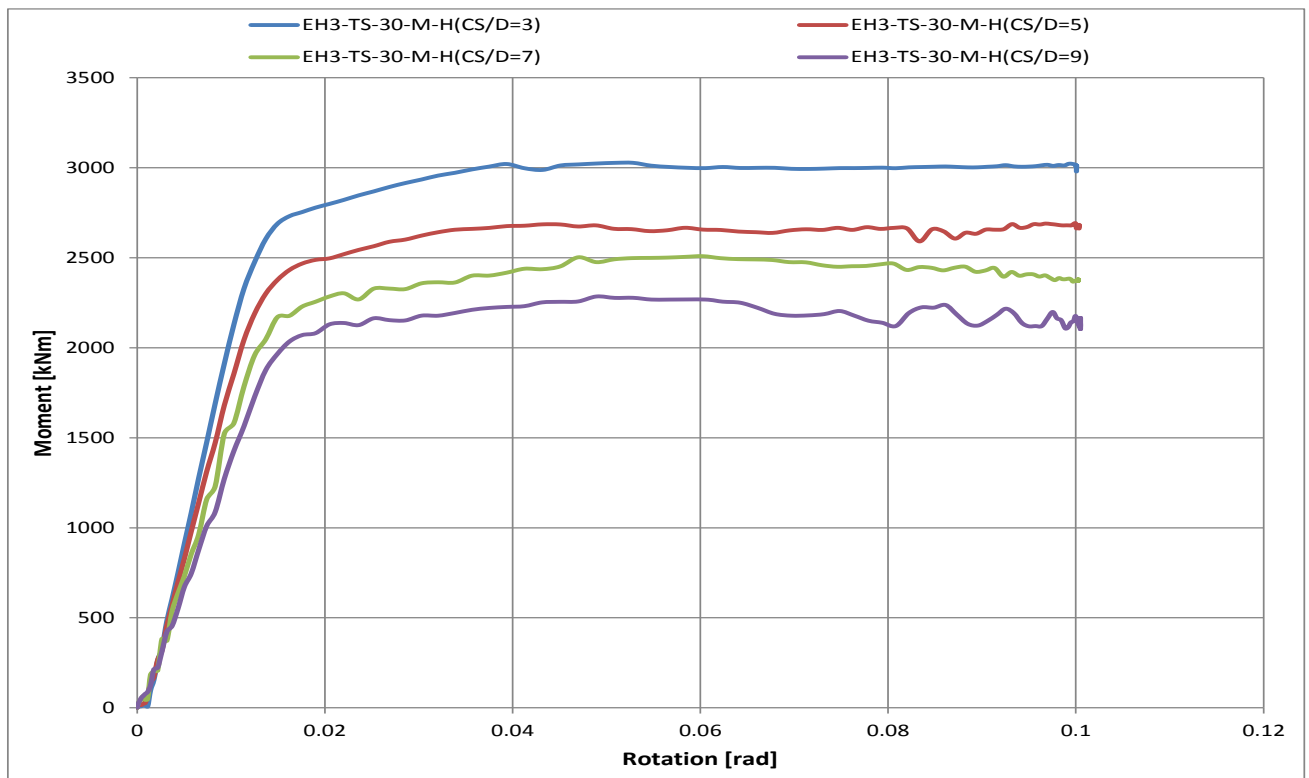
Figure 5.4.5.2.Comparision of moment–rotation among models EH3-TS-30-M-H(CS/D=3), EH3-TS-30-M-H(CS/D=5), EH3-TS-30-M-H(CS/D=7), EH3-TS-30-M-H(CS/D=9).

European Erasmus Mundus Master
Sustainable Constructions under natural hazards and catastrophic events
520121-1-2011-1-CZ-ERA MUNDUS-EMMC

ςυγςος

Figure 5.4.5.3 presents the von Mises stresses in models span-depth ratio 3(a), span-depth ratio 5(b).and span-depth ratio 7(c). It can be observed that beam flanges and web are exceeding the yield stress near the haunch end and inside the haunch for ratio 3 & 5. **Figure 5.4.5.9** and **Figure 5.4.5.10** show von Mises stresses and equivalent plastic strain close up view in those models. Where we can clearly see that plastic hinges have formed in top flange of beam inside the haunch and very close to haunch end for depth ratio 7. As we know that assumption for design procedure was to consider plastic hinge formation at the end of the haunch. But we have found from the analysis that plastic hinges have occurred inside haunch which must be avoided.

Due to safety reason, it is not desire to have plastic strain in the non-dissipative parts. Eventually from the analysis we have seen that some portion of the haunch, endplate, column and bolts have plastic strain. Joint performance is not adequate for depth ratio 3 and 5. With depth ratio 7, it might be safe but very close to safety limit. In overall beam clear span to depth ratio 9 gives better performance. **Table 5.4.5.1** and **Table 5.4.5.2** present maximum von Mises stresses and equivalent plastic strain for all the parts in joint.

Models: EH3-TS-30-M-S(IPE600-HEB500)

Span to depth ratio 3 | Span to depth ratio 5 | Span to depth ratio 7

(a) (b) (c)
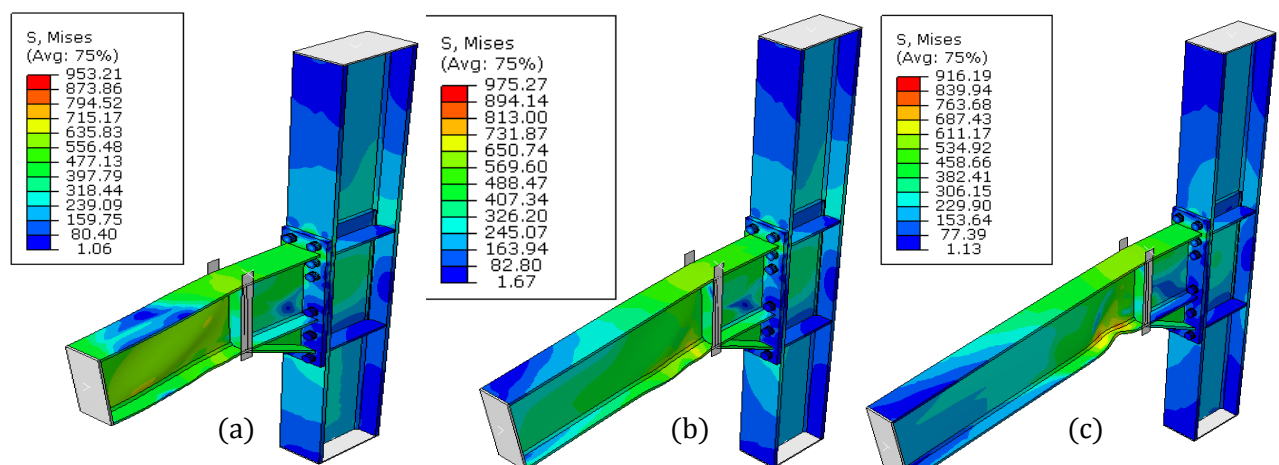
Figure 5.4.5.3.von Mises stresses in models EH3-TS-30-M-S(a), EH3-TS-30-M-S(b), EH3-TS-30-M-S(c)

European Erasmus Mundus Master
Sustainable Constructions under natural hazards and catastrophic events
520121-1-2011-1-CZ-ERA MUNDUS-EMMC

ꓝ山ꓩᴄ口ꓩ
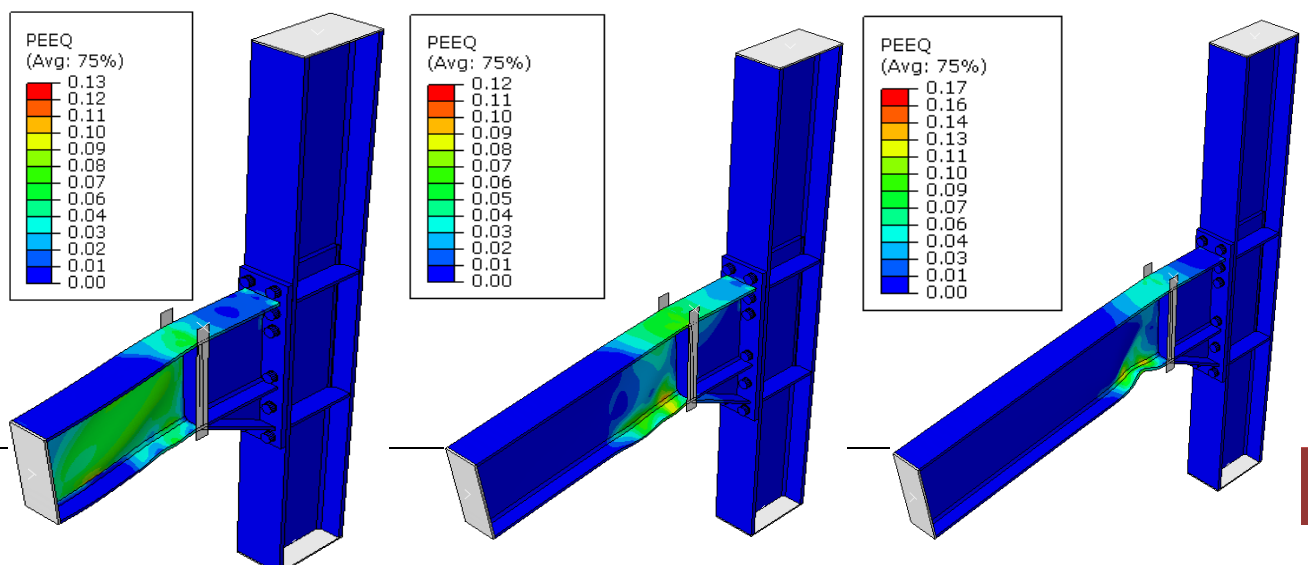
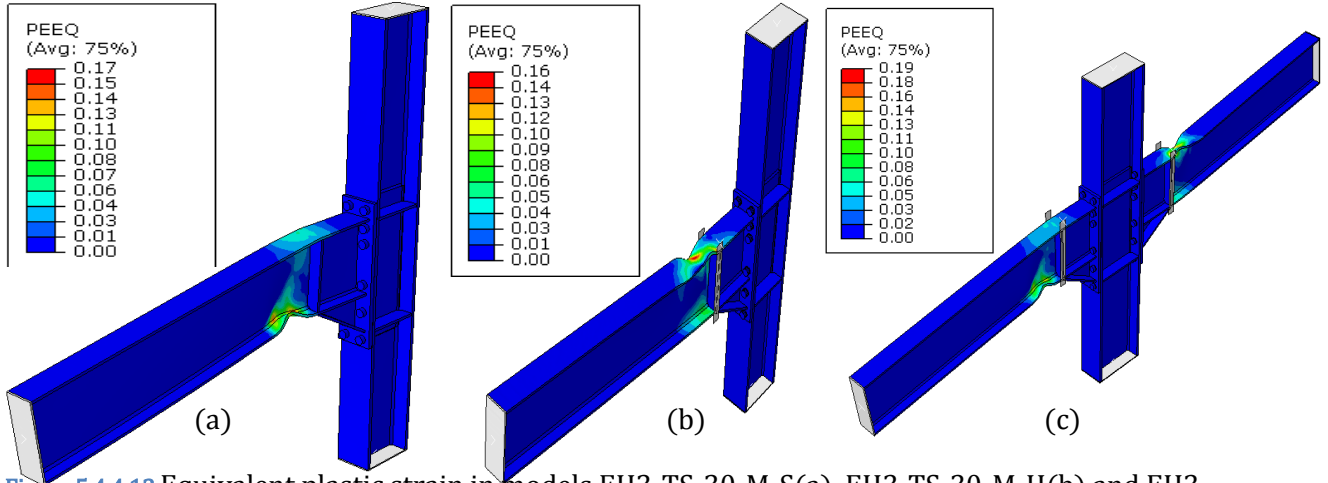(a)   (b)   (c)

Figure 5.4.5.4. Equivalent plastic strain in models EH3-TS-30-M-S(a), EH3-TS-30-M-S(b), EH3-TS-30-M-S(c)
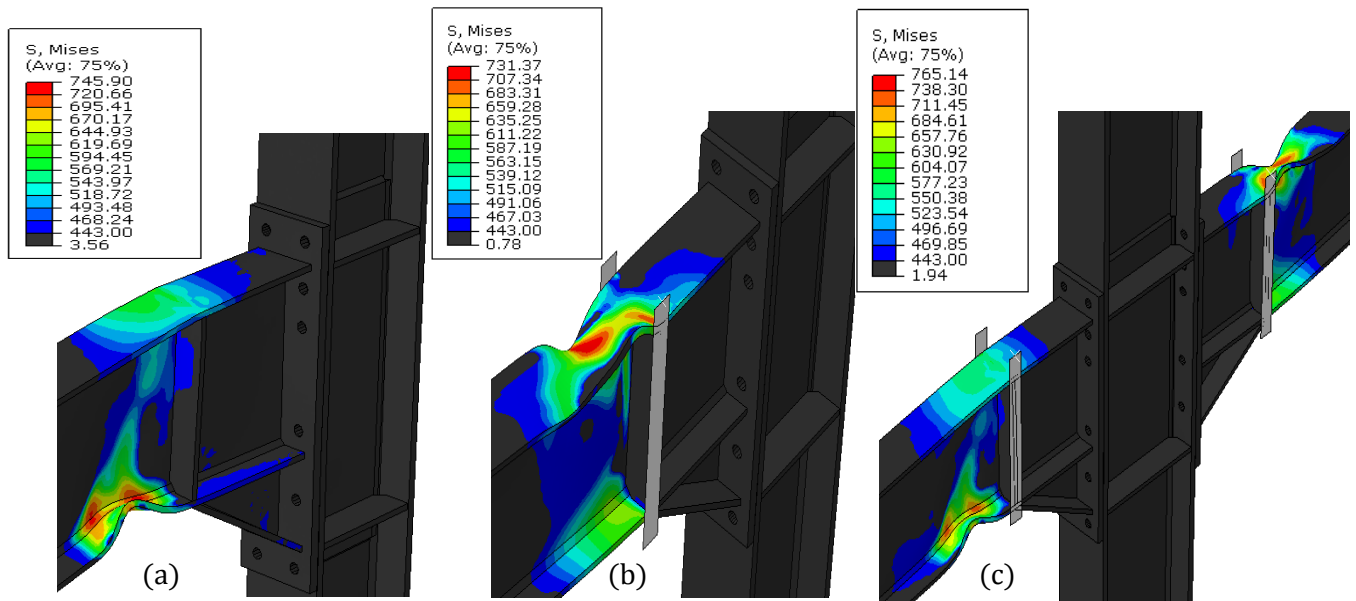

(a)   (b)   (c)
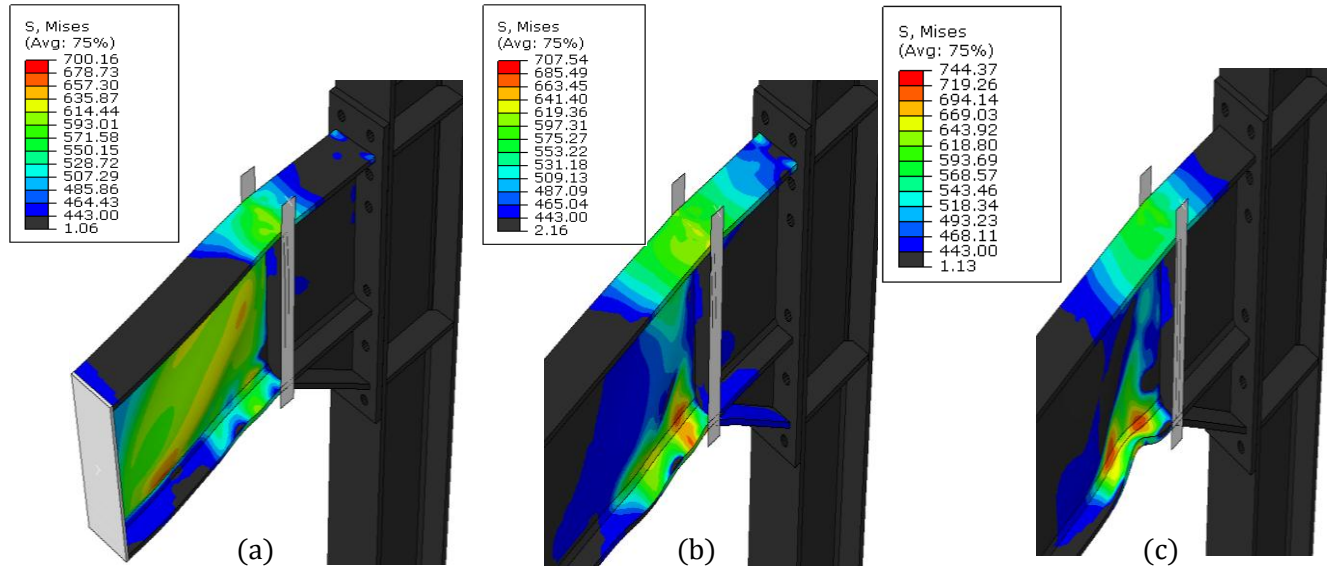
Figure 5.4.5.5. von Mises stresses close up view in models EH3-TS-30-M-S(a), EH3-TS-30-M-S(b), EH3-TS-30-M-S(c)

(a)   (b)   (c)
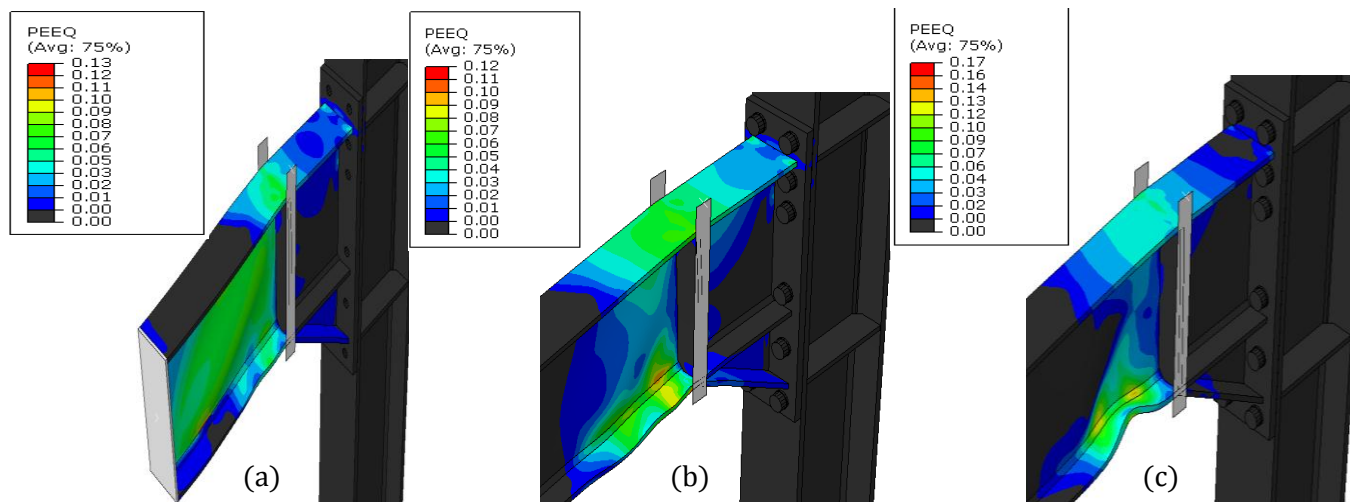
Figure 5.4.5.6. Equivalent plastic strain close up view in models EH3-TS-30-M-S(a), EH3-TS-30-M-S(b), EH3-TS-30-M-S(c)

European Erasmus Mundus Master
Sustainable Constructions under natural hazards and catastrophic events
520121-1-2011-1-CZ-ERA MUNDUS-EMMC

Models: EH3-TS-30-M-H(IPE600-HEB500)

Span to depth ratio 3 Span to depth ratio 5 Span to depth ratio 7

(a) (b) (c)
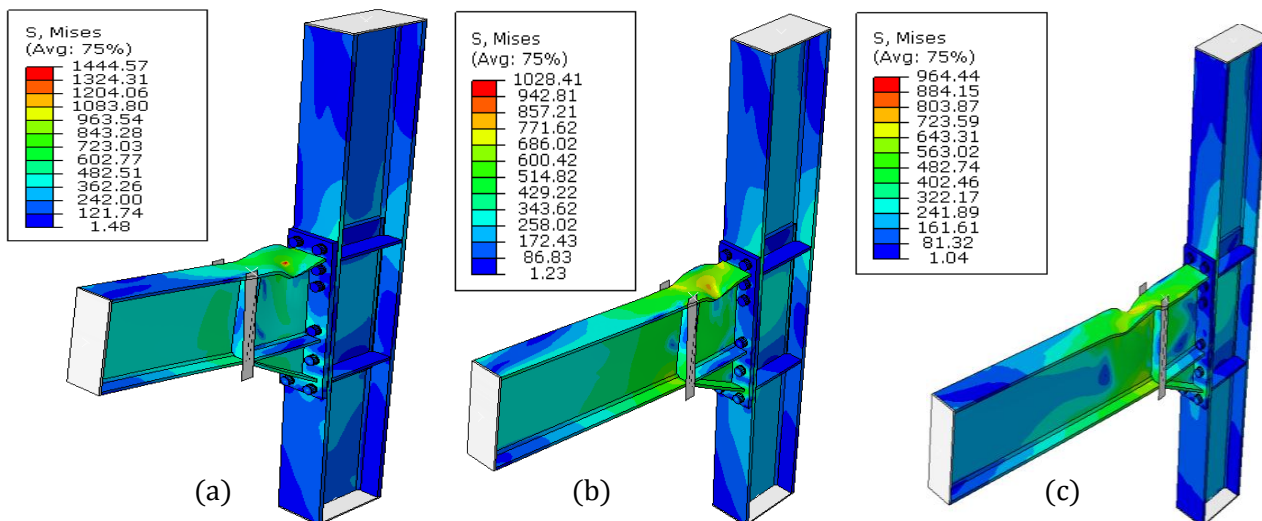
Figure 5.4.5.7.von Mises stresses in models EH3-TS-30-M-H(a), EH3-TS-30-M-H(b), EH3-TS-30-M-H(c)

(a) (b) (c)
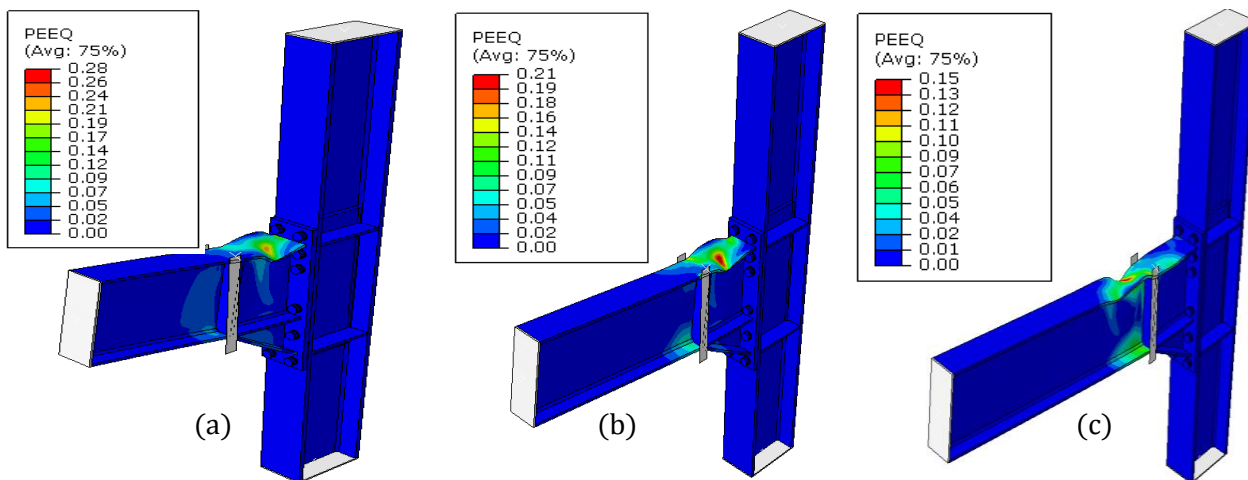
Figure 5.4.5.8. Equivalent plastic strain in models EH3-TS-30-M-H(a), EH3-TS-30-M-H(b), EH3-TS-30-M-H(c)
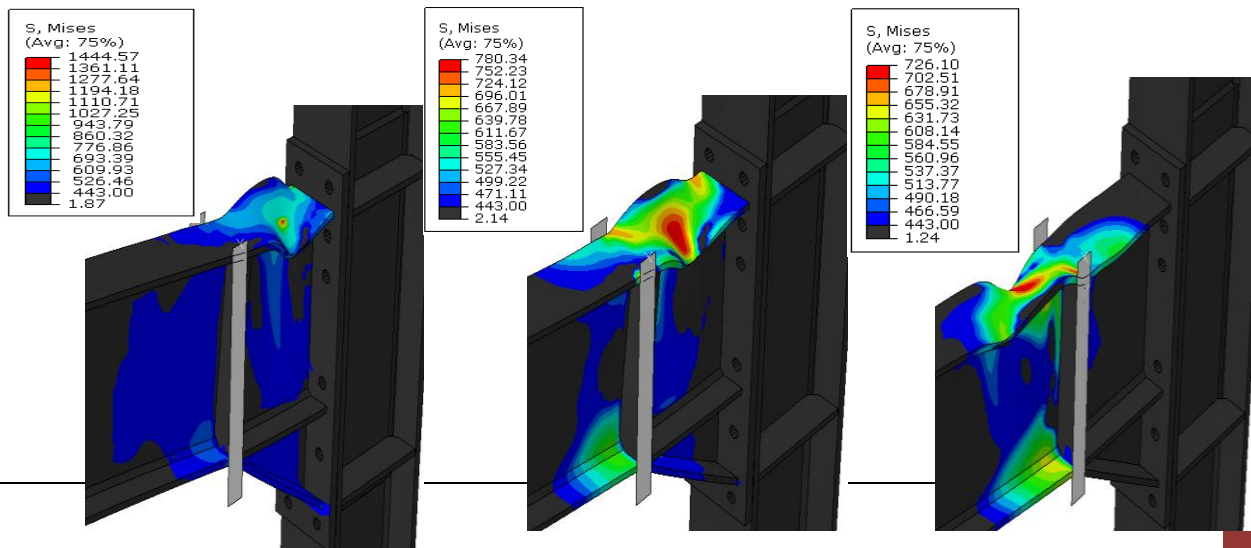
(a)   (b)   (c)

Figure 5.4.5.9.von Mises stresses close up view in models EH3-TS-30-M-H(a), EH3-TS-30-M-H(b), EH3-TS-30-M-H(c)

(a)   (b)   (c)
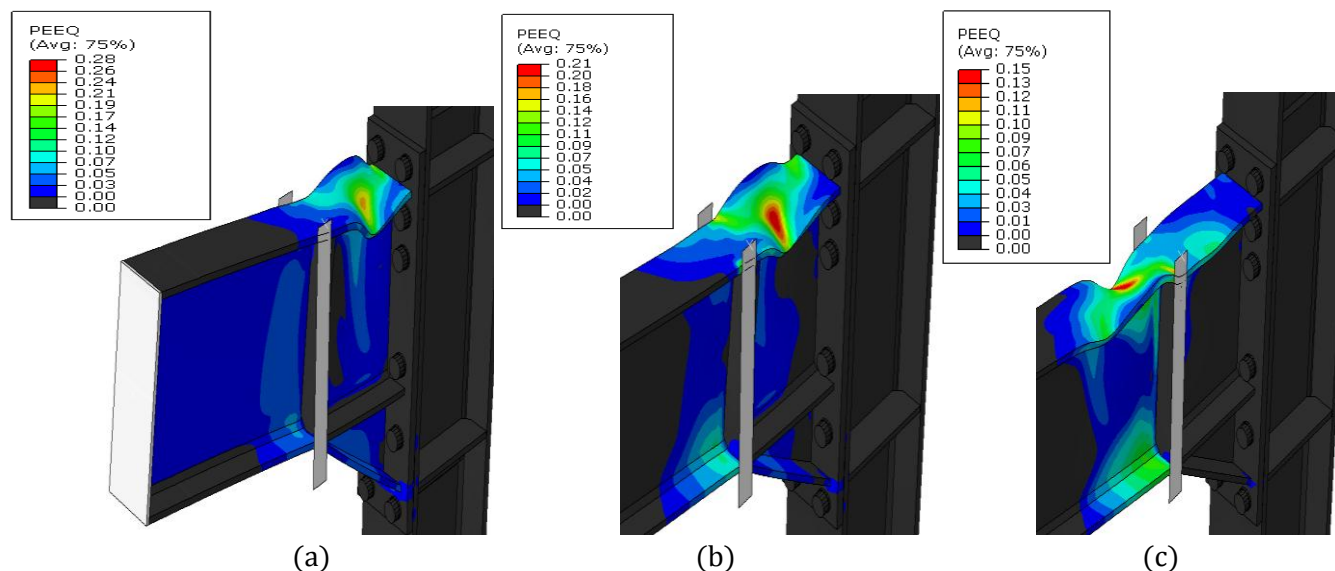
Figure 5.4.5.10. Equivalent plastic strain close up view in models EH3-TS-30-M-H(a), EH3-TS-30-M-H(b), EH3-TS-30-M-H(c)

Table 5.4.5.1.von Mises stresses in models EH3-TS-30-M(CS/D=3), EH3-TS-30-M(CS/D=5), EH3-TS-30-M(CS/D=7), EH3-TS-30-M(CS/D=9).

		von Mises stresses (N/mm^2)			
		Group 1			
		EH3-TS-30-M(IPE600-HEB500)			
		CS/D=3	CS/D=5	CS/D=7	CS/D=9
Beam	S	700.2	707.5	744.4	732.6
	H	1444.6	780.3	726.1	731.4
Haunch	S	542.5	625.8	586.1	596.2
	H	628.6	637.8	618.4	598.1
Endplate	S	438.3	441.9	423.8	429.9
	H	510.8	454.8	437.4	433.9
Bolt	S	953.2	975.3	916.2	903.8
	H	1090.9	1028.4	964.4	940.5
Column	S	440.1	443.3	431.7	430.9
	H	453.6	443.5	435.3	436.1

Table 5.4.5.2.Equivalent plastic strain in models EH3-TS-30-M(CS/D=3), EH3-TS-30-M(CS/D=5), EH3-TS-30-M(CS/D=7), EH3-TS-30-M(CS/D=9).

		Equivalent plastic strain (PEEQ)			
		Group 1			
		EH3-TS-30-M(IPE600-HEB500)			
		CS/D=3	CS/D=5	CS/D=7	CS/D=9
Beam	S	0.132	0.121	0.172	0.155
	H	0.284	0.213	0.146	0.155
Haunch	S	0.044	0.070	0.055	0.058
	H	0.073	0.075	0.069	0.058
Endplate	S	0.025	0.025	0.014	0.009
	H	0.037	0.021	0.010	0.006
Bolt	S	0.020	0.020	0.007	0.004
	H	0.063	0.031	0.015	0.010
Column	S	0.026	0.019	0.009	0.006
	H	0.022	0.012	0.008	0.006

5.4.6 Influence of lateral restraints (EH3-TS-30-M-S)

The objective of this study is to assess the influence of lateral restraints in joints. For numerical analysis one model was chosen from group1; EH3-TS-30-M(IPE600-HEB500). Four cases were chosen assess the influence of lateral restraints. 1. No restraint no slab. 2. Restraint no slab. 3. Lateral restraint at top flange of beam. 4. Lateral and torsional restraint at top flange of beam. Only downward displacement was applied corresponds to a magnitude of 0.1rad rotation on the tip of the beam in all models. Expected material properties (f_y= 1.25*355= 443.75MPa) was defined for all parts in the joint except bolts. For bolts (f_y=940MPa) was used. Figure 5.4.6.1 shows the moment-rotation capacity. From the curves we can see that moment capacity of joint is higher with lateral restraint no slab. Strength degradation takes place for all cases. Here the elastic stiffness is equal.
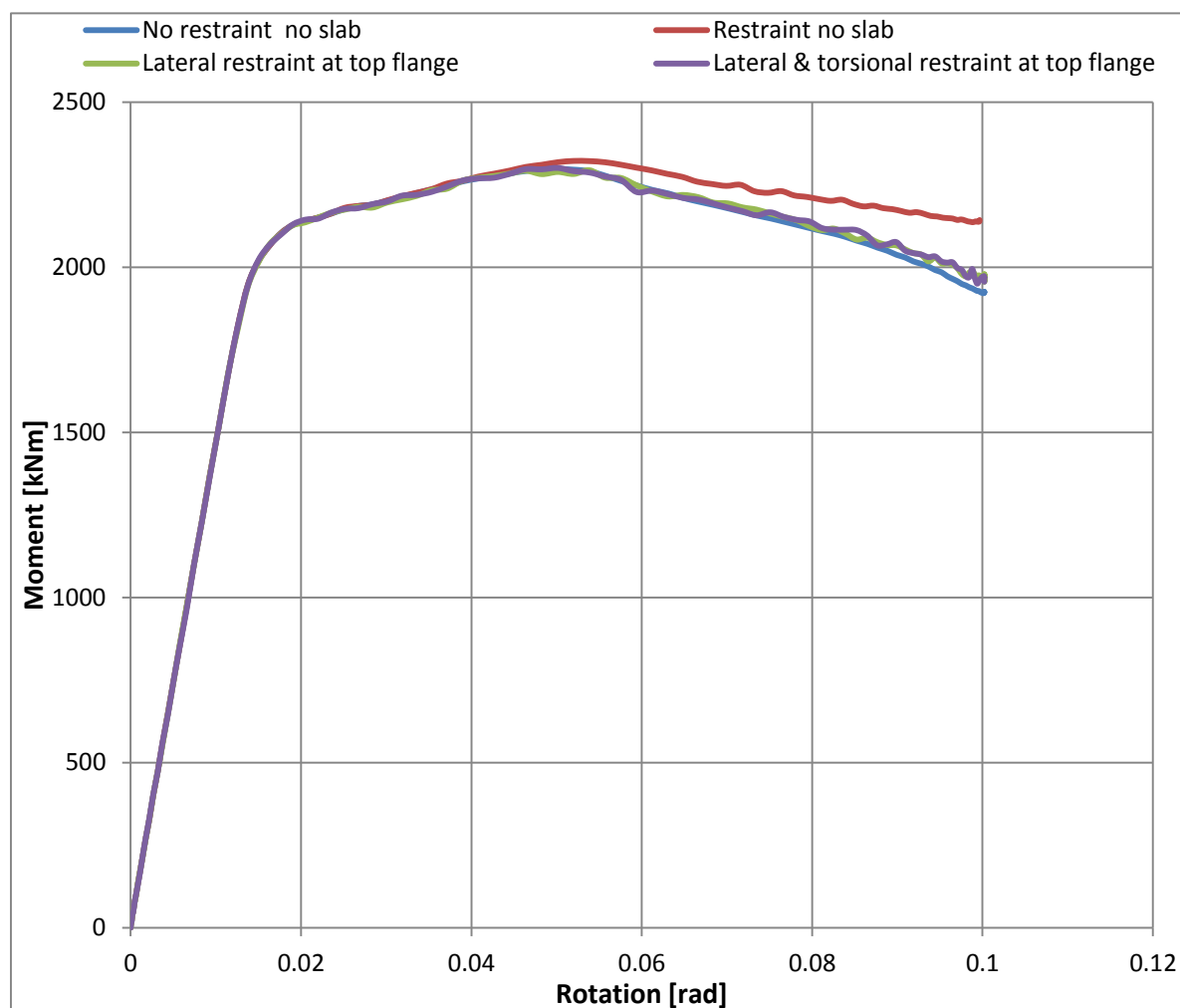
Figure 5.4.6.1.Comparision of moment–rotation among models (No restraint no slab), (Restraint no slab), (Lateral restraint at top flange), (Lateral & torsional restraint at top flange).

For model (No restraint no slab), the von Mises stresses and equivalent plastic strain are mentioned in section 5.4.2. Figure 5.4.6.2.presents the von Mises stresses in models EH3-TS-30-M-S(a), EH3-TS-30-M-S(b), EH3-TS-30-M-S(c). It can be observed that beam flanges and web are exceeding the yield stress near the haunch end. Figure 5.4.6.4and Figure 5.4.6.5 show von Mises stresses and equivalent plastic strain close up view in those models. We can see that plastic strain in the top flange is close to column face and in bottom flange bit away from column face due to downward displacement. The assumption in design procedure was to consider plastic hinge formation at the end of the haunch. But we have found from the analysis that plastic hinges have occurred at a distance from haunch end: 261mm ($0.43h_b$), 261mm($0.43h_b$), 246mm($0.41h_b$), 246mm($0.41h_b$) for models (No restraint no slab), (Restraint no slab), (Lateral restraint at top flange), (Lateral & torsional restraint at top flange).

Due to safety reason, it is not desire to have plastic strain in the non-dissipative parts. Eventually from the analysis we have seen that some portion of the haunch, endplate, column and bolts have plastic strain. Lateral restraint has small influence on joints.

European Erasmus Mundus Master
Sustainable Constructions under natural hazards and catastrophic events
520121-1-2011-1-CZ-ERA MUNDUS-EMMC

surcos

Table 5.4.6.1 and **Table 5.4.6.2** present maximum von Mises stresses and equivalent plastic strain for all the parts in joint.

Models: EH3-TS-30-M-S(IPE600-HEB500)

No restraint no slab   Lateral restraint at top flange   Lateral & torsional restraint at top flange

(a)   (b)   (c)

Figure 5.4.6.2. von Mises stresses in models EH3-TS-30-M-S(a), EH3-TS-30-M-S(b), EH3-TS-30-M-S(c)

(a)   (b)   (c)

Figure 5.4.6.3. Equivalent plastic strain in models EH3-TS-30-M-S(a), EH3-TS-30-M-S(b), EH3-TS-30-M-S(c)

European Erasmus Mundus Master
Sustainable Constructions under natural hazards and catastrophic events
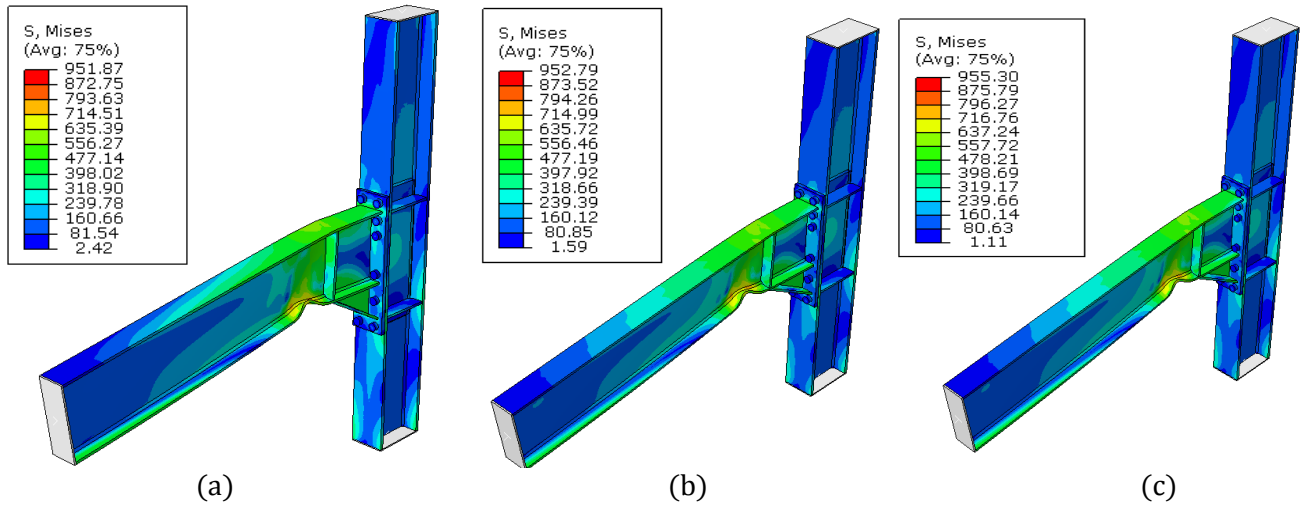**520121-1-2011-1-CZ-ERA MUNDUS-EMMC**

surcos

Figure 5.4.6.4. von Mises stresses close up view in models EH3-TS-30-M-S(a), EH3-TS-30-M-S(b), EH3-TS-30-M-S(c)
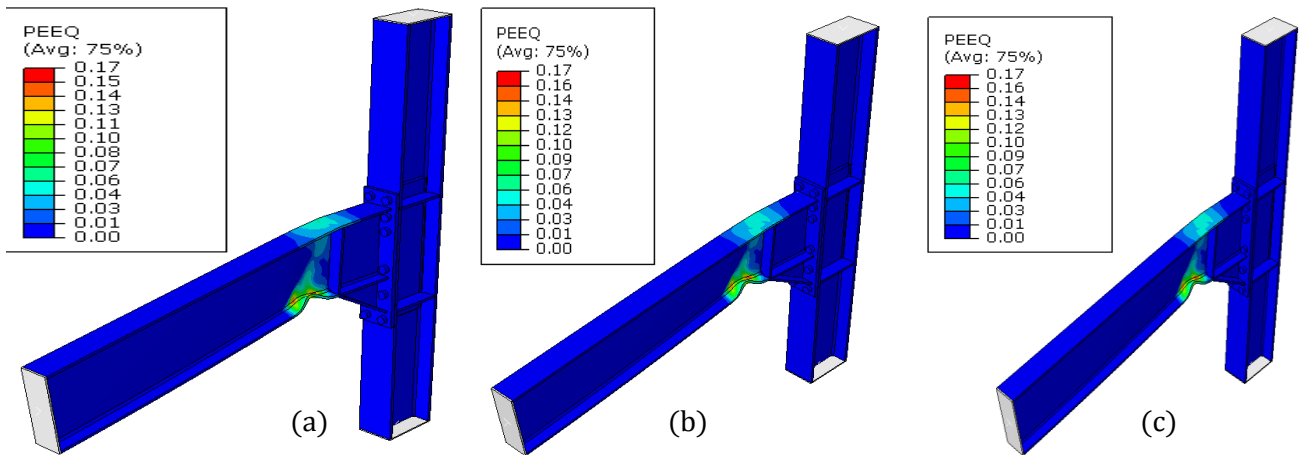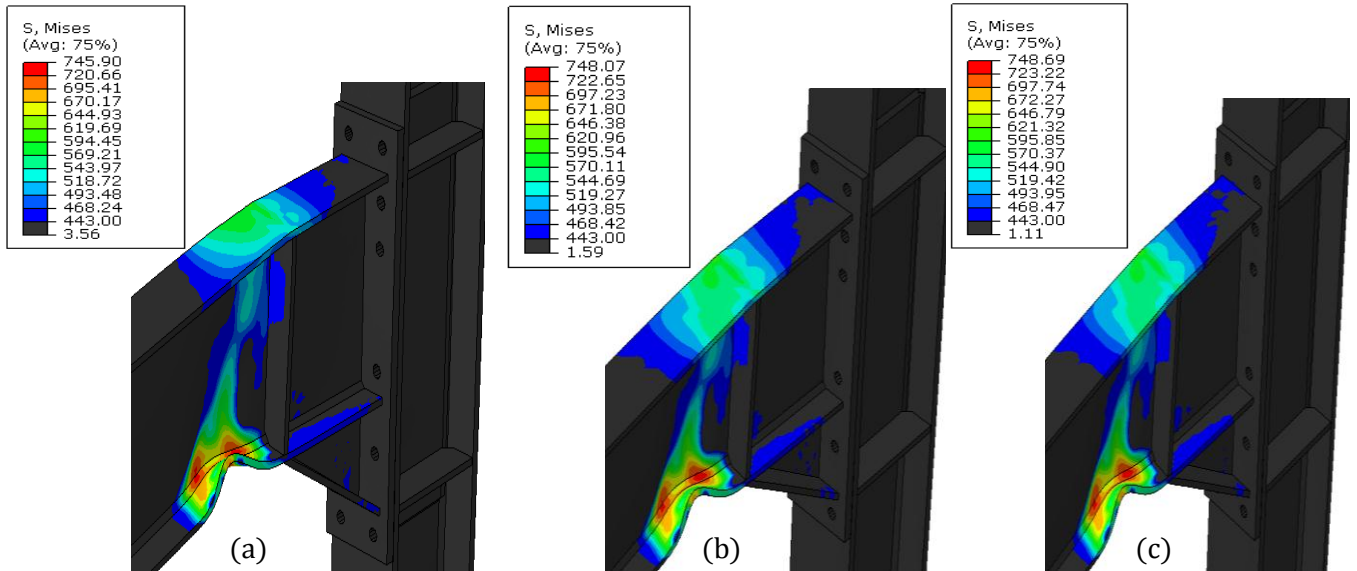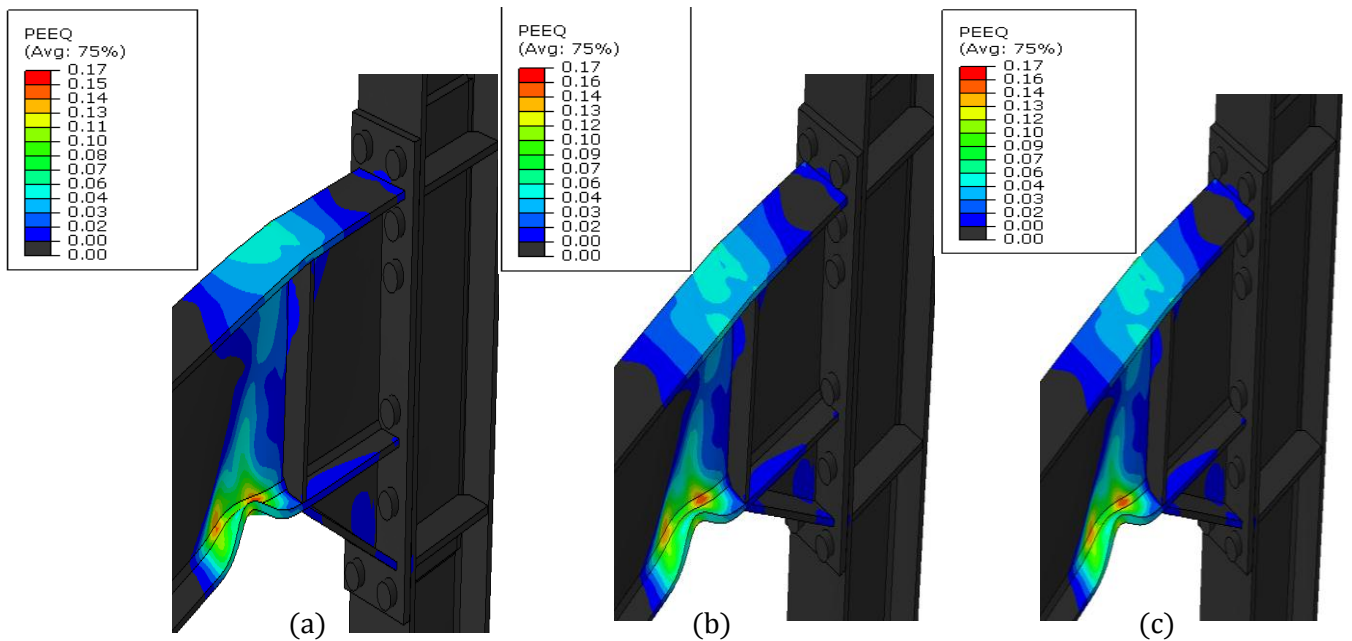

Figure 5.4.6.5. Equivalent plastic strain close up view in models EH3-TS-30-M-S(a), EH3-TS-30-M-S(b), EH3-TS-30-M-S(c)

Table 5.4.6.1.von Mises stresses in models (No restraint no slab), (Restraint no slab), (Lateral restraint at top flange), (Lateral & torsional restraint at top flange).

	von Mises stresses (N/mm²)			
	Group 1			
	EH3-TS-30-M-S(IPE600-HEB500)			
	no restraint no slab	restraint no slab	Lateral restraint at top flange	Lateral & torsional restraint at top flange
Beam	745.9	765.1	748.1	748.7
Haunch	653.2	611.8	659.8	662.0
Endplate	445.1	428.9	444.1	444.6
Bolt	951.9	919.3	952.8	955.3
Column	445.5	441.5	444.0	444.7

Table 5.4.6.2.Equivalent plastic strain in models (No restraint no slab), (Restraint no slab), (Lateral restraint at top flange), (Lateral & torsional restraint at top flange).

	Equivalent plastic strain (PEEQ)			
	Group 1			
	EH3-TS-30-M-S(IPE600-HEB500)			
	No restraint no slab	Restraint no slab	Lateral restraint at top flange	Lateral & Torsional restraint at top flange
Beam	0.167	0.202	0.173	0.173
Haunch	0.082	0.064	0.087	0.087
Endplate	0.006	0.004	0.004	0.004
Bolt	0.004	0.004	0.004	0.004
Column	0.006	0.005	0.005	0.005

5.4.7   Influence of cyclic loading (EH3-TS-30 C)

The objective of this section is to assess the influence of the loading history on the deformation capacity of joints for model EH3-TS-30-C(IPE600-HEB500). The analysis was performed using alternative loading protocol ECCS 45 and AISC 341. Both upward and downward displacement were applied corresponds to first cycle on the tip of the beam. Expected material properties (f_y= 443.75MPa) was set for all the parts in the joints. For bolts (f_y=940MPa) was used. Figure 5.4.7.1 shows the moment-rotation capacity for the model in case of ECCS and AISC loading scheme. From Figure 5.4.7.4, we

can clearly distinct moment-rotation capacity between AISC and ECCS loading protocol. From the curve, we can see that ECCS scheme has less steps with high magnitude .Besides, AISC goes with more steps with low magnitude. It's obvious that AISC cyclic loading protocol can provide more information after the analysis. On the other hand, if we consider the computational time during the analysis AISC load protocol requires two times longer time than ECCS load protocol.

Figure 5.4.7.2 shows the construction of cyclic envelope curve for AISC scheme. Figure 5.4.7.8 represents von Mises stresses in models EH3-TS-30-M-C (a) and EH3-TS-30-M-C(b) correspond to two loading systems. We can see plastic hinges are formed near to the haunch The design procedure was assumed that plastic hinge forms at the end of the haunch. From the numerical analysis we have found that plastic hinges have occurred at a distance from the haunch end of 119mm ($0,2h_b$) for AISC scheme also 119mm ($0.2h_b$) for ECCS scheme. Figure 5.4.7.10 and Figure 5.4.7.11 depicts the von Mises stresses and equivalent plastic strain close up view in those two systems.

Table 5.4.7.1 and Table 5.4.7.2 present maximum von Mises stresses and equivalent plastic strain for all the parts in joint.
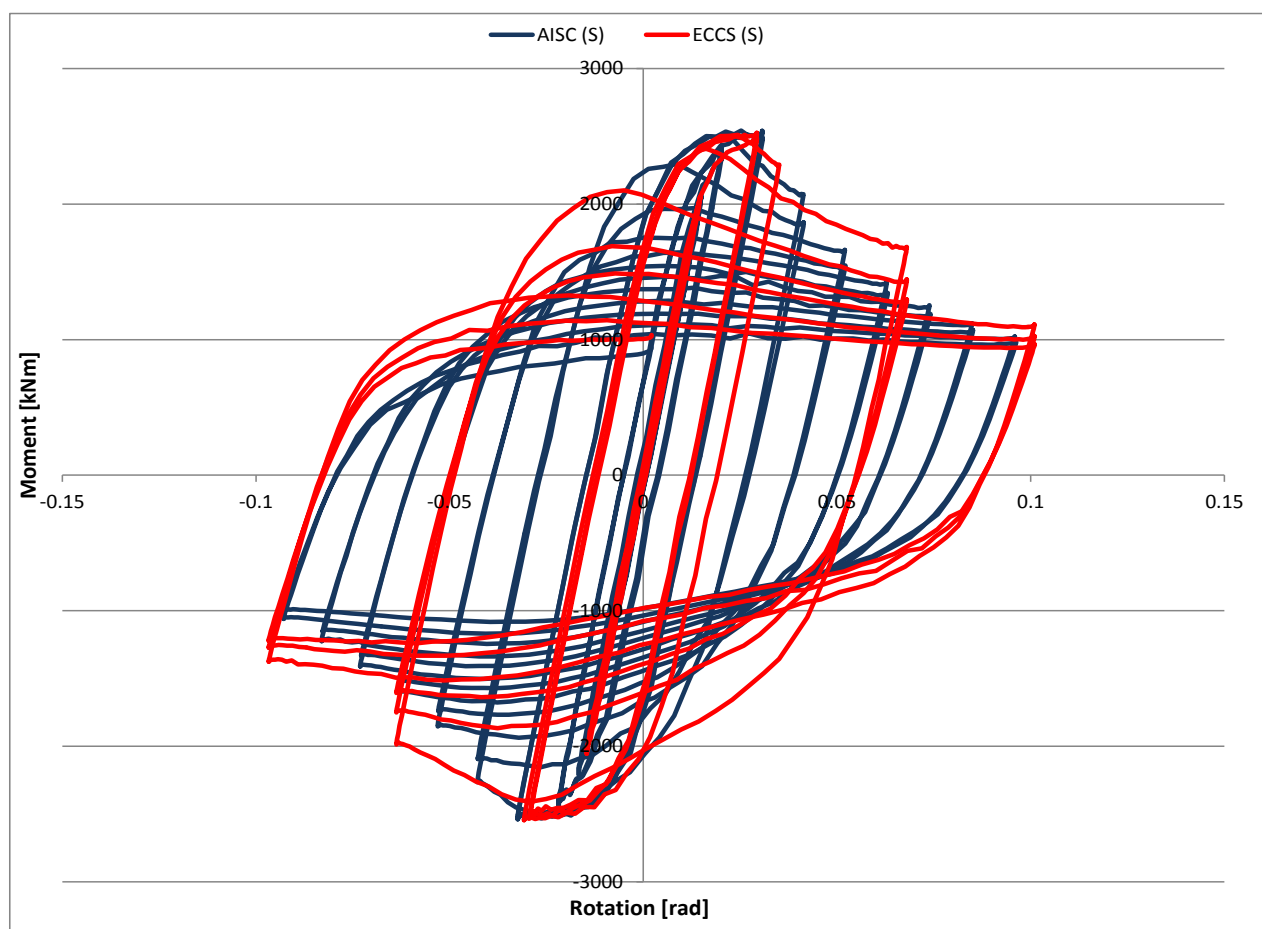

Figure 5.4.7.1.Comparison moment-rotation between cyclic loading protocol AISC (S) and ECCS (S).

Construction of the Cyclic Envelope Curve:

The cyclic envelope curve should be constructed in accordance with the following requirements:

- The curve for should be constructed separately for positive and negative directions of loading.
- At each level of deformation, up to the peak load experienced in the test, the load value of the cyclic envelope curve should be taken as the greater of: (1) the maximum value of load for all cycles at that level of deformation; or (2) the value of load described by a series of straight lines that connect points of peak load at subsequent deformation amplitudes.
- After the peak load has been reached, the envelope curve should be defined using only (1) above for the following two cases:
  - If there is more than 20% difference in peak loads at subsequent deformation amplitudes.
  - If the cyclic response curve has a negative stiffness (i.e., strength is lost in a single cycle of loading).
- The value of the cyclic envelope curve should drop to zero load at the maximum deformation executed in the test.
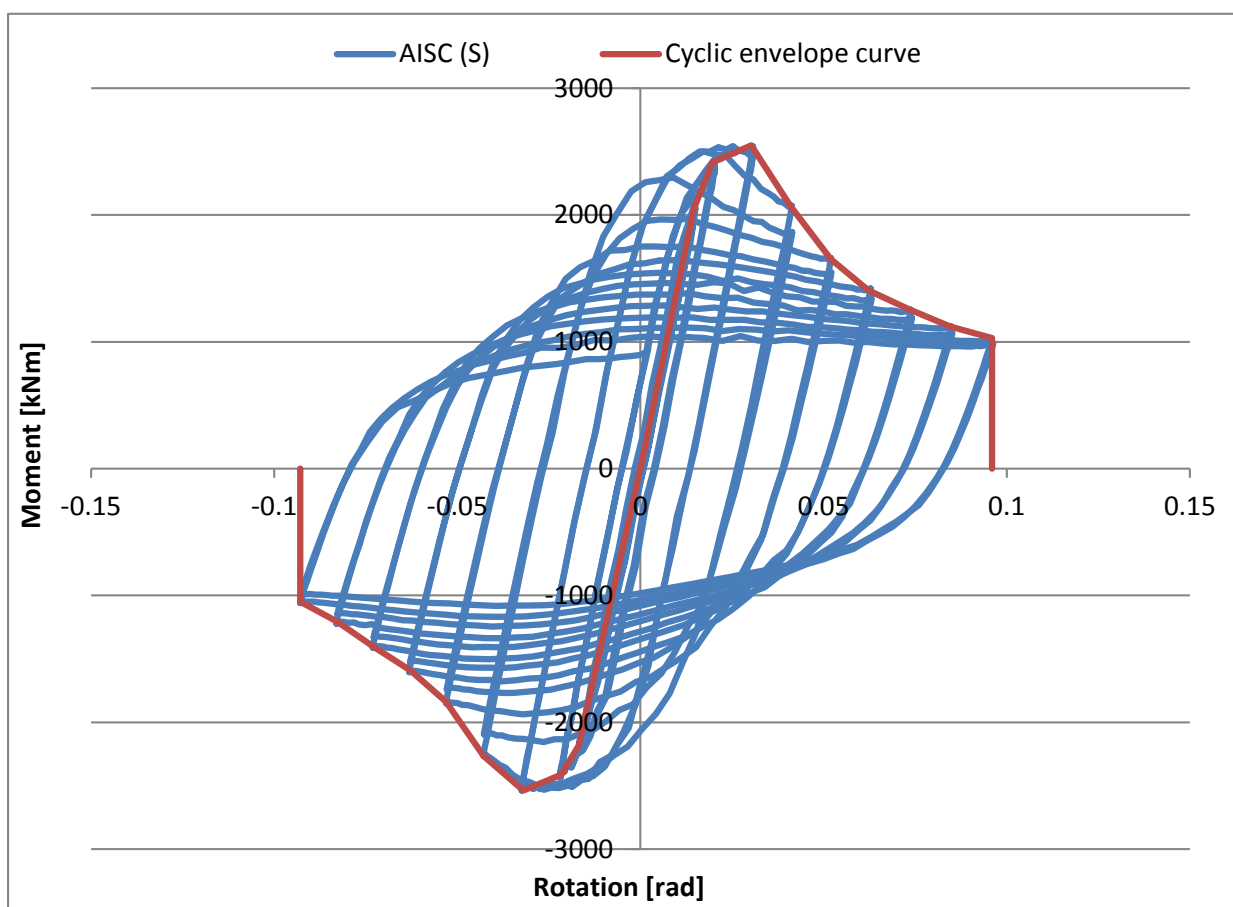

Figure 5.4.7.2. Construction of cyclic envelope curve for AISC (S).

European Erasmus Mundus Master
Sustainable Constructions under natural hazards and catastrophic events
520121-1-2011-1-CZ-ERA MUNDUS-EMMC

sursos

Figure 5.4.7.3. Construction of cyclic envelope curve for ECCS (S).

Figure 5.4.7.4. Comparison moment-rotation between cyclic loading protocol AISC (S) and ECCS (S) by envelope.

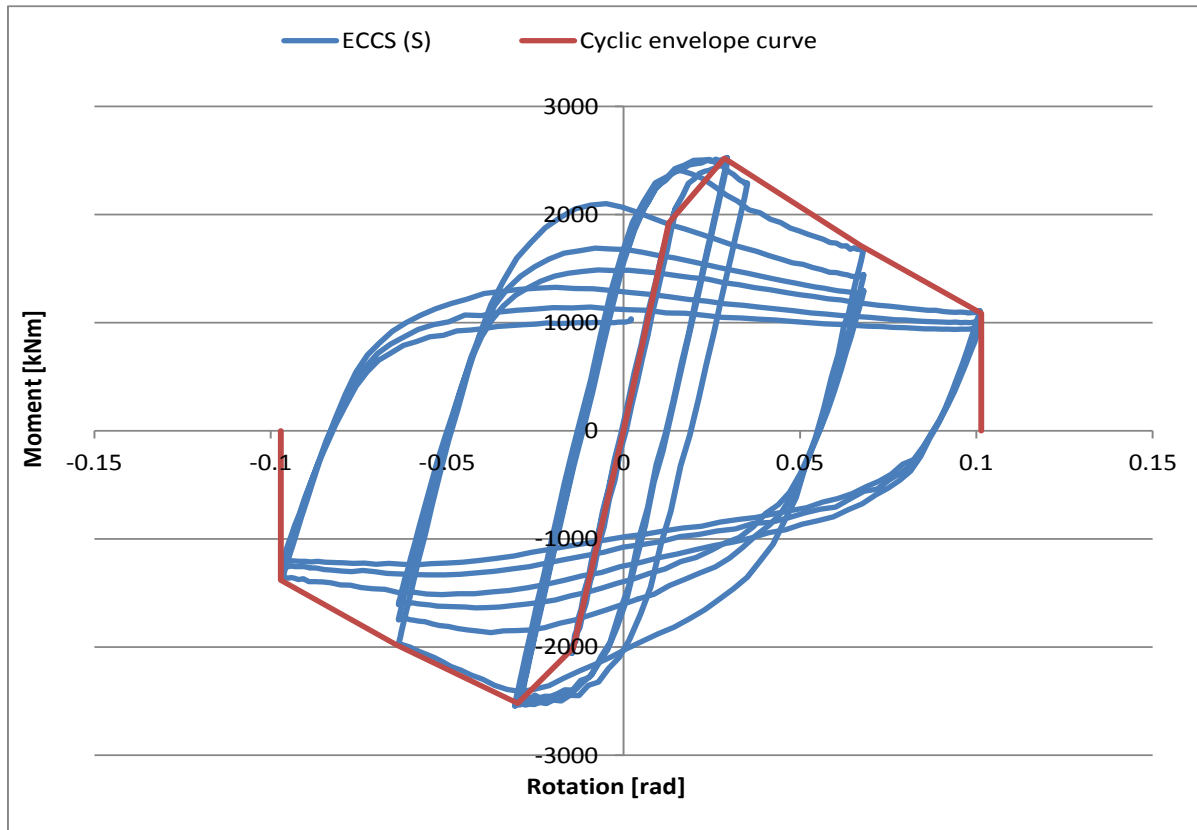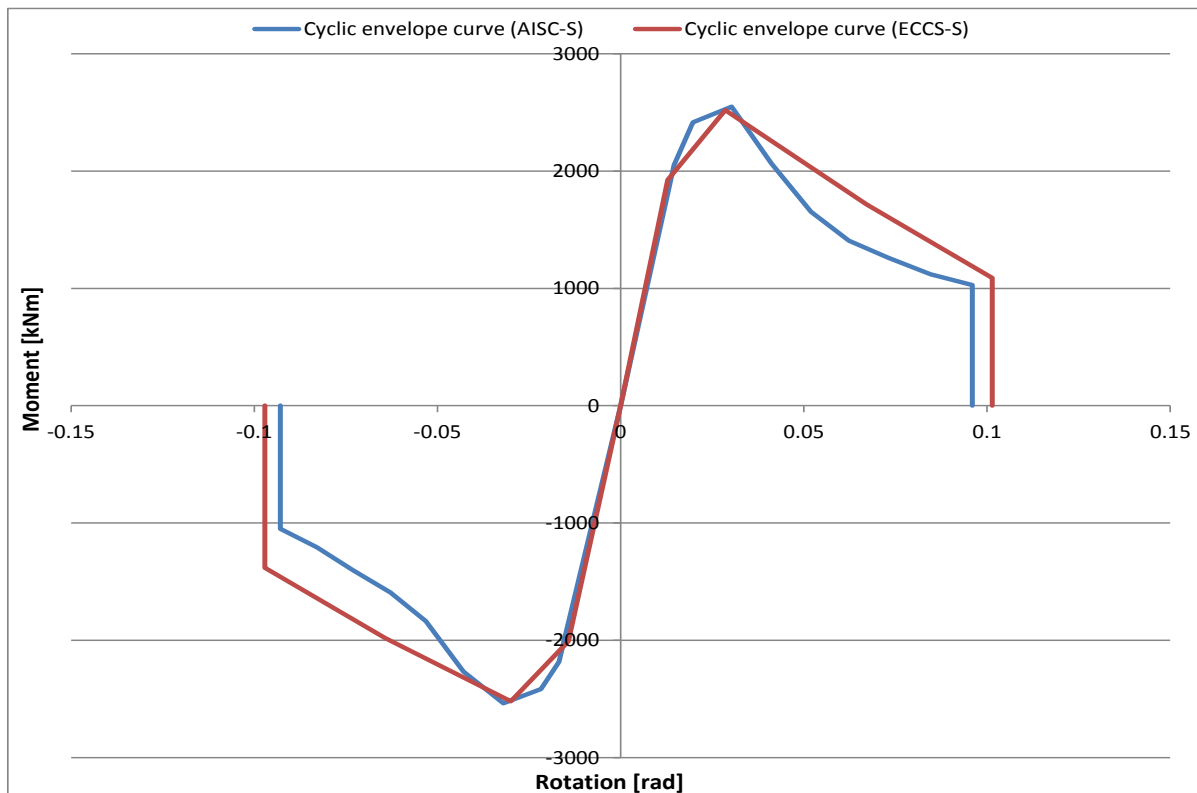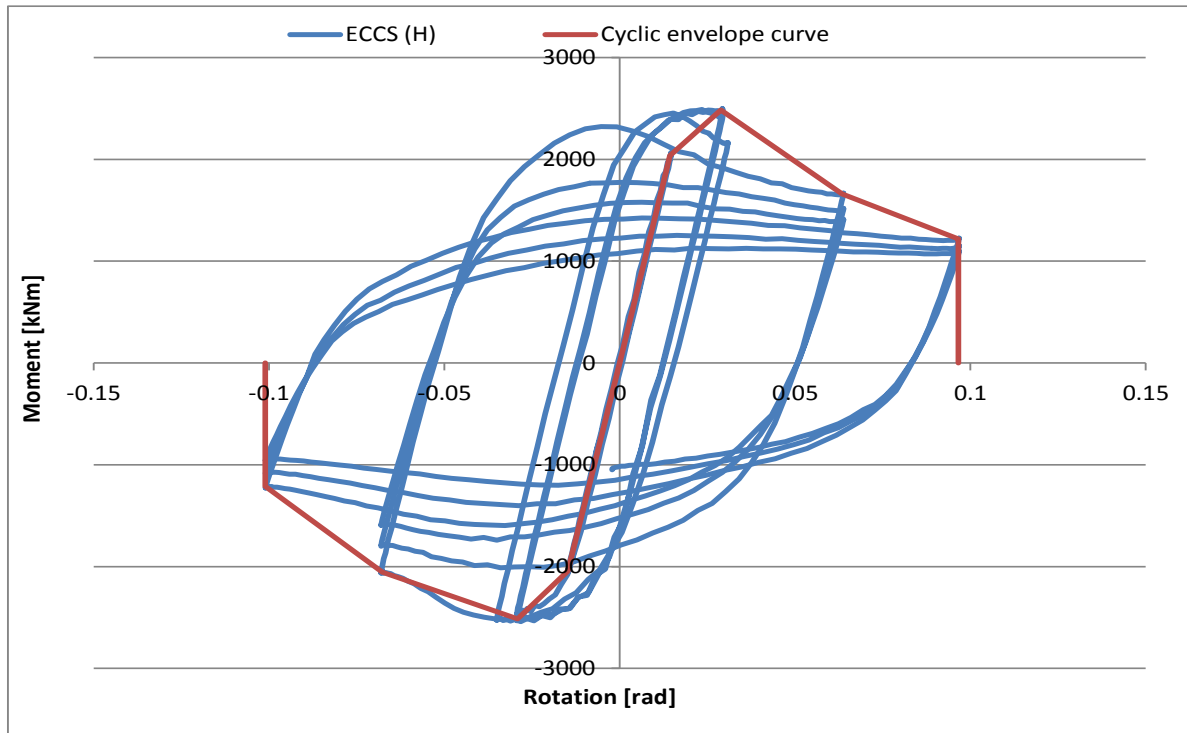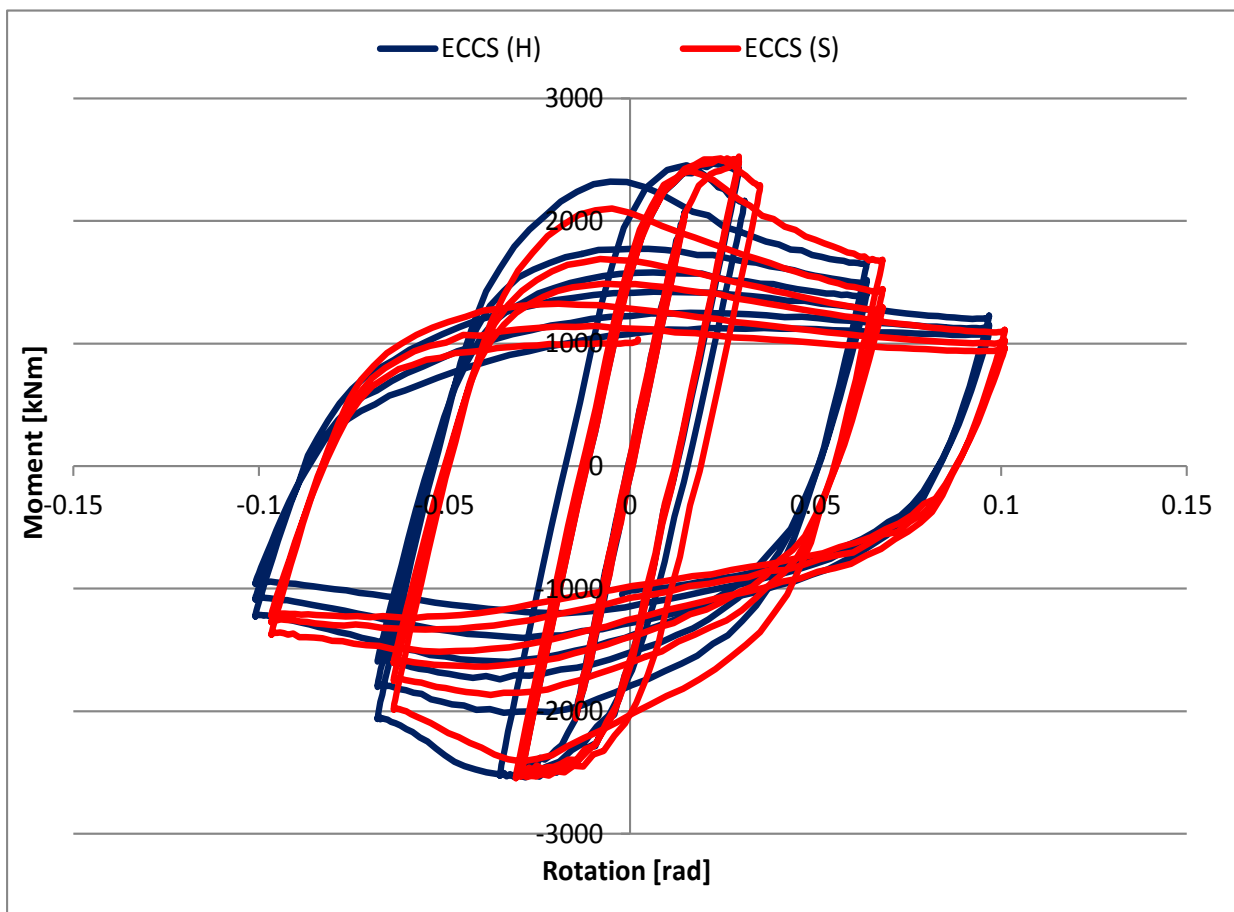**Figure 5.4.7.5.** Construction of cyclic envelope curve for ECCS (H).

Figure 5.4.7.6. Comparison moment-rotation between cyclic loading protocol ECCS (S) and ECCS (H).

European Erasmus Mundus Master
Sustainable Constructions under natural hazards and catastrophic events
520121-1-2011-1-CZ-ERA MUNDUS-EMMC
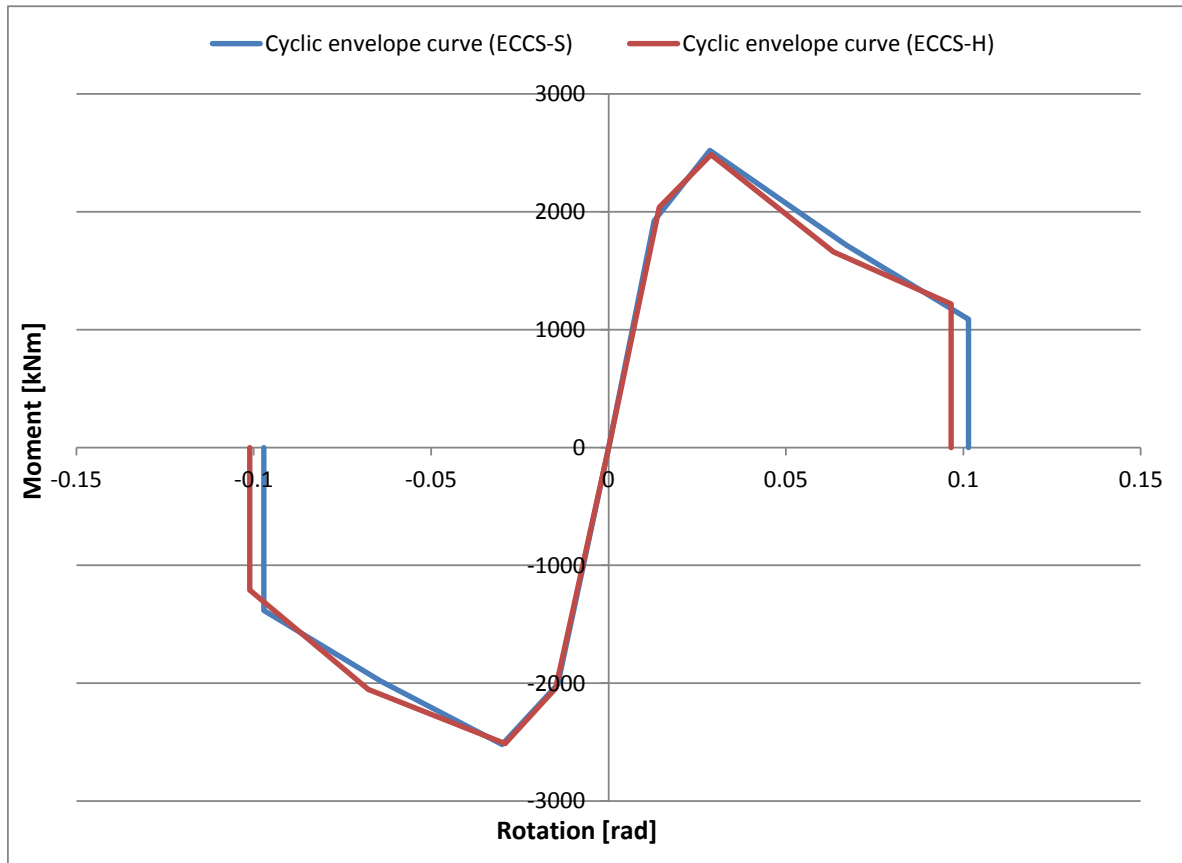
ɹuɹcoɹ

Figure 5.4.7.7. Comparison moment-rotation between cyclic loading protocol ECCS (S) and ECCS (H) by envelope.

Models: EH3-TS-30-C-S(IPE600-HEB500)

Load Protocol ECCS 45   Load Protocol AISC 341

(a)   (b)
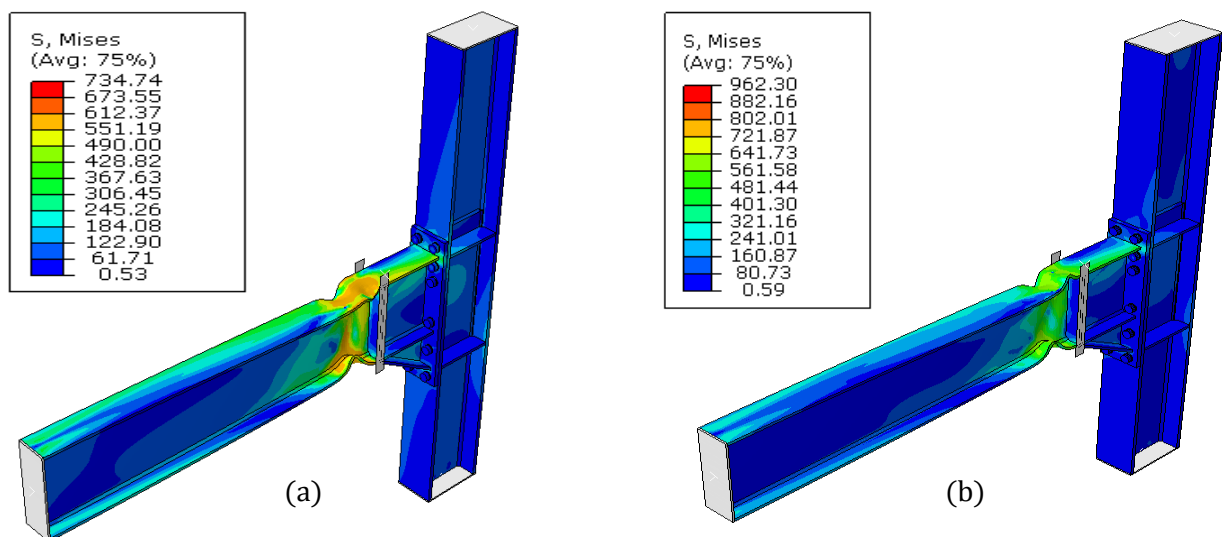
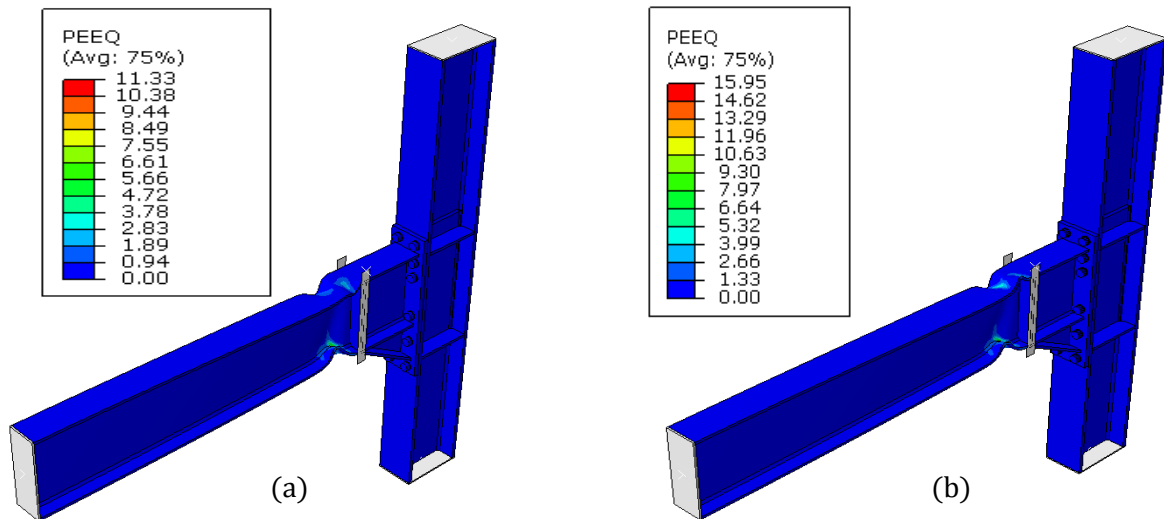**Figure 5.4.7.8.** von Mises stresses in models EH3-TS-30-C-S(a) and EH3-TS-30-C-S(b)

Figure 5.4.7.9.Equivalent plastic strain in models EH3-TS-30-C-S(a) and EH3-TS-30-C-S(b)

Figure 5.4.7.10.von Mises stresses close up view in models EH3-TS-30-C-S(a) and EH3-TS-30-C-S(b)

European Erasmus Mundus Master
Sustainable Constructions under natural hazards and catastrophic events
520121-1-2011-1-CZ-ERA MUNDUS-EMMC

surcos

(a)

(b)

Figure 5.4.7.11. Equivalent plastic strain close up view in models EH3-TS-30-C-S(a) and EH3-TS-30-C-S(b)
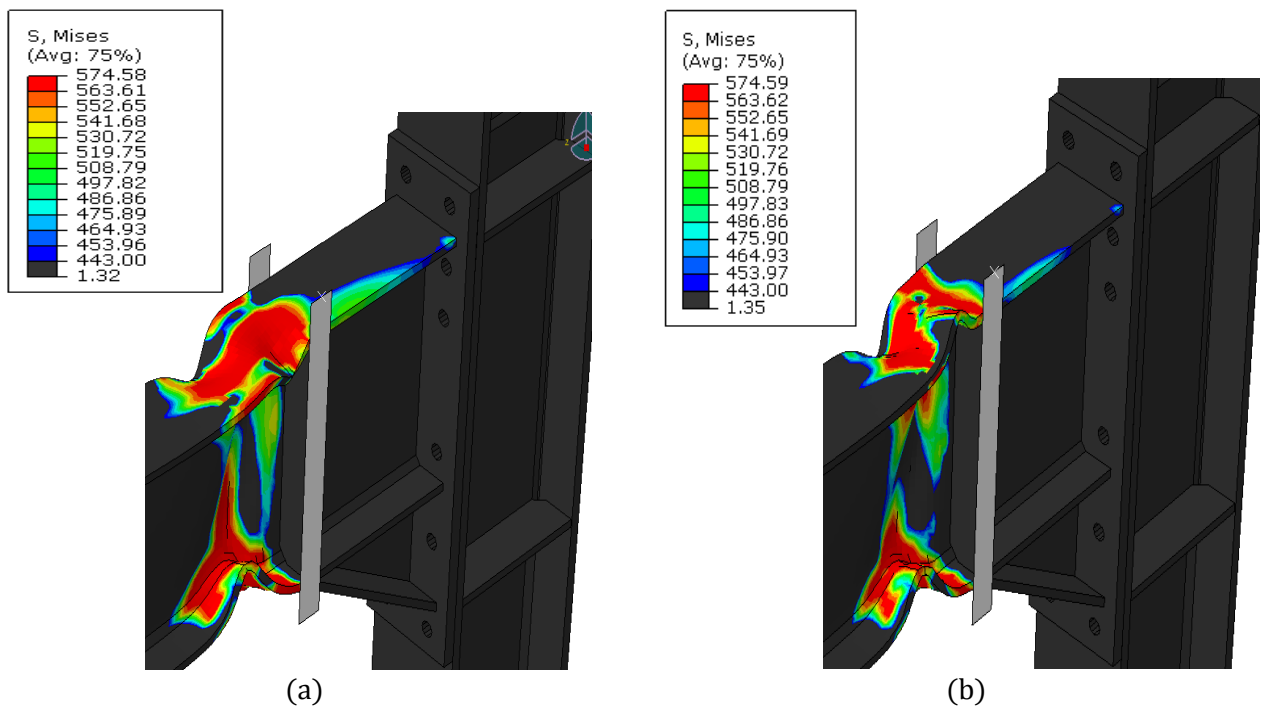

(a)

(b)
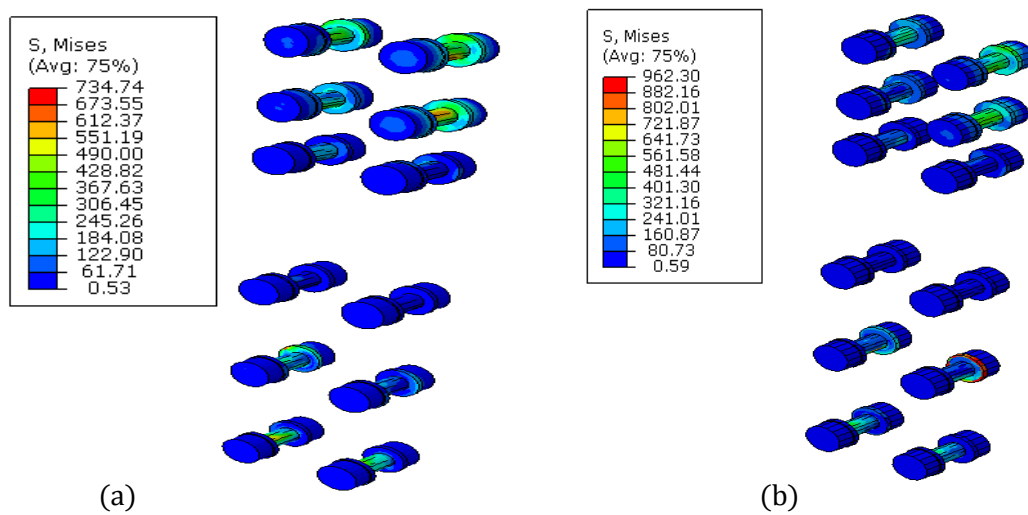
Figure 5.4.7.12. von Mises stress of bolts in models EH3-TS-30-C-S(a) and EH3-TS-30-C-S(b)

(a)

(b)

Figure 5.4.7.13. Equivalent plastic strain of bolts in models EH3-TS-30-C-S(a) and EH3-TS-30-C-S(b)

Models: EH3-TS-30-C-H(IPE600-HEB500)

Load Protocol ECCS

Figure 5.4.7.14.von Mises stresses and equivalent plastic strain in models EH3-TS-30-C-H(a) and EH3-TS-30-C-H(b)

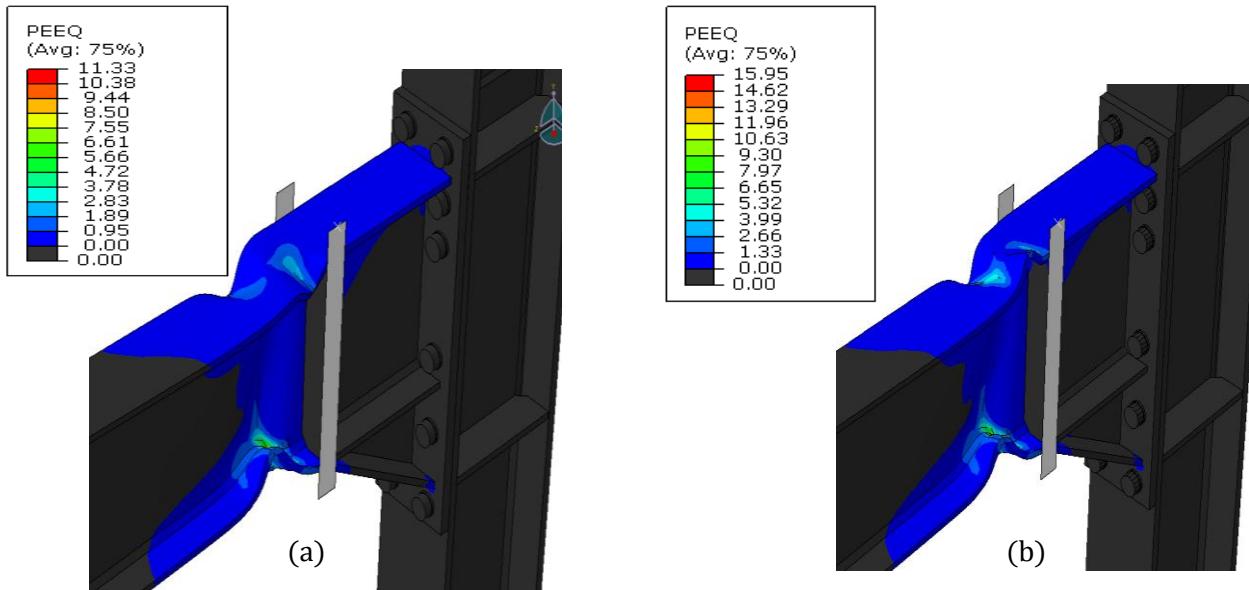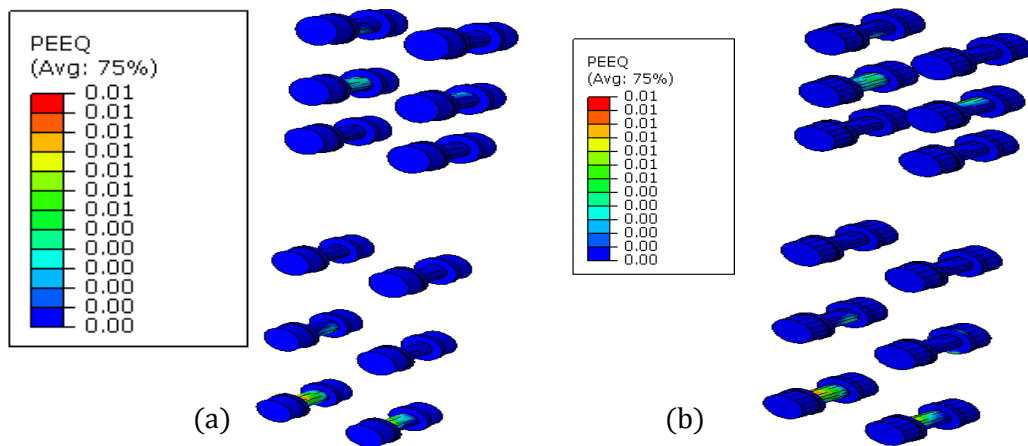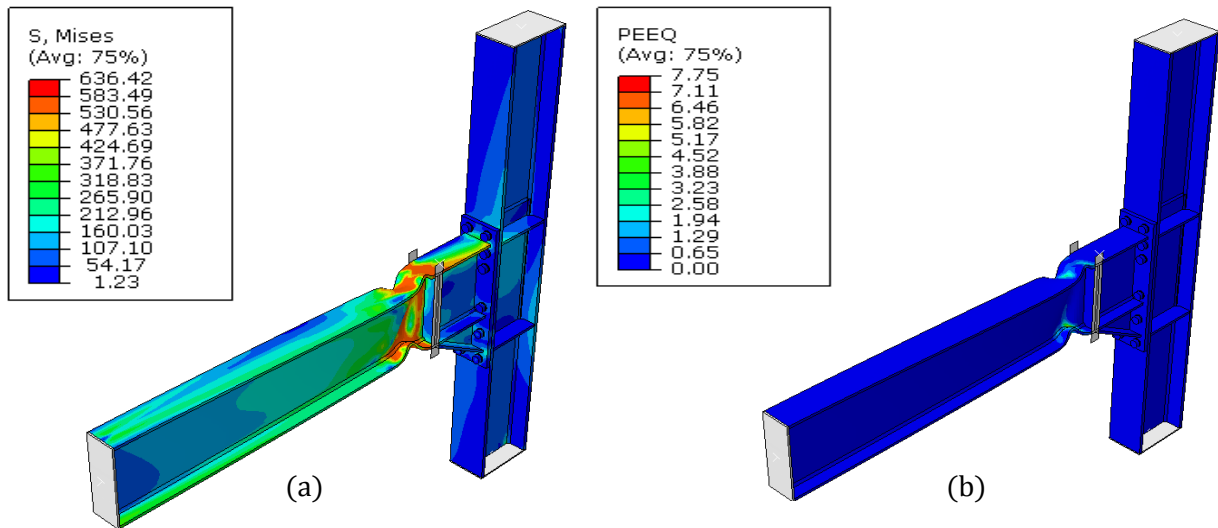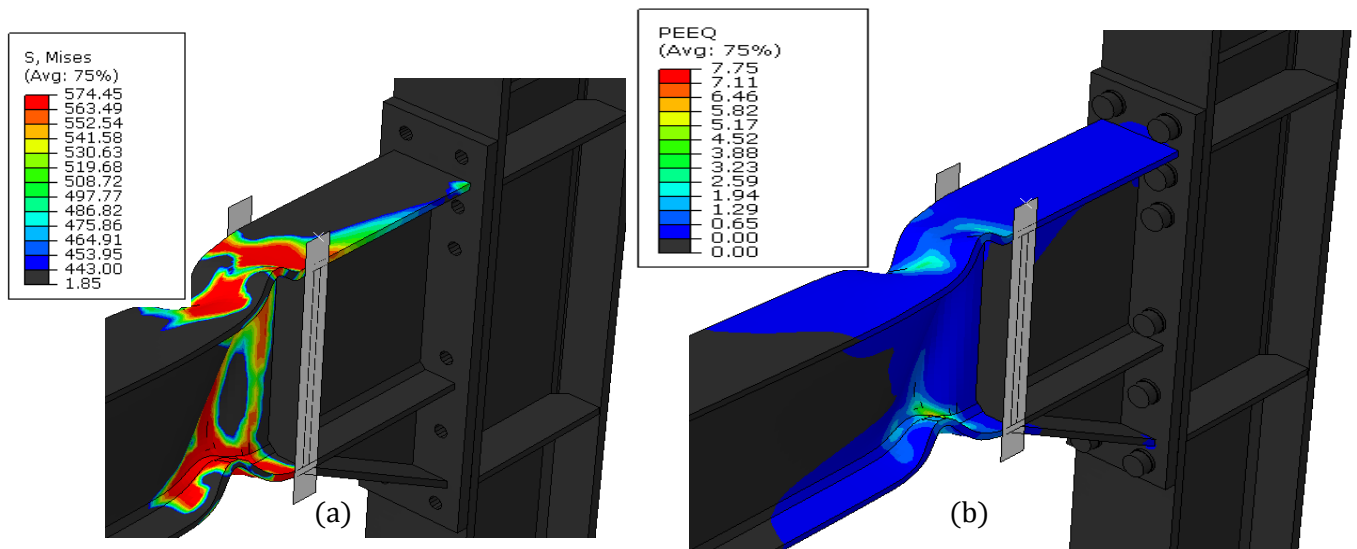Figure 5.4.7.15.von Mises stresses and equivalent plastic strain close up view in models EH3-TS-30-C-H(a) and EH3-TS-30-C-H(b)

Table 5.4.7.1. von Mises stresses in models EH3-TS-30-C-S for loading protocol AISC 341 and ECCS 45.

	von Mises stresses (N/mm²)	
	Group 1	
	EH3-TS-30-C-S(IPE600-HEB500)	
	Protocol AISC 341	Protocol ECCS 45
Beam	574.6	574.6
Haunch	504.2	574.5
Endplate	352.7	353.9
Bolt	962.3	734.7
Column	376.9	431.8

Table 5.4.7.2. Equivalent plastic strain in models EH3-TS-30-C-S for loading protocol AISC 341 and ECCS 45.

	PEEQ	
	Group 1	
	EH3-TS-30-C-S(IPE600-HEB500)	
	Protocol AISC 341	Protocol ECCS 45
Beam	15.946	11.326
Haunch	1.639	1.221
Endplate	0.023	0.017
Bolt	0.011	0.012
Column	0.048	0.032

Table 5.4.7.3. Equivalent plastic strain and von Mises stresses in models EH3-TS-30-C-H for loading ECCS 45.

	Protocol ECCS 45	
	EH3-TS-30-C-H(IPE600-HEB500)	
	PEEQ	VMS (N/mm2)
Beam	7.755	574.4
Haunch	0.612	574.0
Endplate	0.016	382.9
Bolt	0.011	636.4
Column	0.032	392.3

6 Conclusions

The main aim of this dissertation work is to investigate the behaviour of bolted beam to column joints with haunches under monotonic and cyclic load. To attain this purpose, a finite element solver named ABAQUS has been used. A parametric study has been performed to assess the influence of different parameters on joints behaviour. Some important outcomes from this work:

During verification of the design procedure, it has been seen that plastic hinges have formed away from the haunch end. Some plastic strain has also occurred inside the haunch with limited magnitude. The angle (30 and 45 degree) of the haunch does not bring any significant difference in joint performance.

On the other hand, beam size has showed three possible effects on joint. Firstly, larger beam size (IPE600) has attained larger strain and larger strength degradation. Secondly, Medium size beam (IPE450) has not showed any strength degradation during downward displacement but upward displacement has brought strength degradation. Thirdly, smaller beam size (IPE360) has not showed strength degradation in any cases.

Panel zone strength has not affected much the response of joints. Although column web panel for T joints were very strong due to stiffness requirement and for the X joints, the column web panel was balanced.

Beam clear span to depth ratio has an important influence in joint behaviour. For very short beam (ratio 3), the failure was governed by shear in the beam web. Plastic hinges have been occurred inside the haunch for very short (ratio 3) and short (ratio 5) beam. AISC recommendation is that beam span to depth ratio should be equal or greater than 7 which provide appropriate behaviour.

The lateral restraints of the beam have not influenced the joints performance.

ECCS cyclic loading protocol attains a given joint rotation in fewer cycles whereas AISC protocol goes with smooth step. The cyclic envelope curves have not much affected though. The positive and negative direction of first loading has not affected much.

7   References

[1] "Experimental assessment of the behaviour of bolted T-stub connections made up of welded plates", Ana M. Gira˜o Coelho a, Frans S.K. Bijlaard b,, Nol Gresnigt b, Luı´s Simo˜es da Silva.

[2] "European pre-qualified steel joints (EQUALJOINTS), RFSR-CT-2013-00021".

[3] "Eurocode 3: Design of steel structures - Part 1-8: Design of joints".

[4] "Eurocode 8, Part 1: General rules, seismic actions and rules for buildings".

[5] "Quantification of Building Seismic Performance Factors: Component Equivalency Methodology: FEMA P-795 / June 2011".

[6] "Abaqus 6.11 Analysis User's Manual".

[7] ESDEP (The European Steel Design Education Programme) "http://www.haiyangshiyou.com/esdep/master/wg17/l0200.htm"